

**DEVELOPMENT AND CHARACTERIZATION OF ULTRA HIGH  
MOLECULAR WEIGHT POLYETHYLENE (UHMWPE) BASED  
HYBRID NANOCOMPOSITE COATING FOR BEARING  
APPLICATIONS UNDER DRY AND WATER LUBRICATION**

BY  
**MUHAMMAD UMAR AZAM**

A Thesis Presented to the  
DEANSHIP OF GRADUATE STUDIES

**KING FAHD UNIVERSITY OF PETROLEUM & MINERALS**  
DHAHRAN, SAUDI ARABIA

In Partial Fulfillment of the  
Requirements for the Degree of

**MASTER OF SCIENCE**  
In  
**MATERIALS SCIENCE & ENGINEERING**

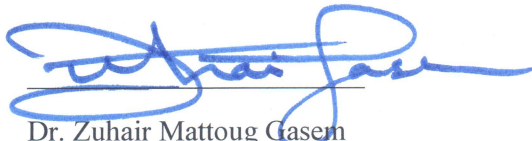
**May 2017**

KING FAHD UNIVERSITY OF PETROLEUM & MINERALS

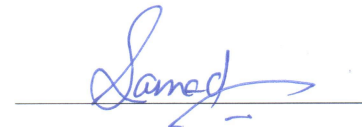
DHAHRAN- 31261, SAUDI ARABIA

DEANSHIP OF GRADUATE STUDIES

This thesis, written by **MUHAMMAD UMAR AZAM** under the direction of his thesis advisor and approved by his thesis committee, has been presented and accepted by the Dean of Graduate Studies, in partial fulfillment of the requirements for the degree of **MASTER OF SCIENCE IN MATERIALS SCIENCE & ENGINEERING.**



Dr. Zuhair Mattoug Gasem  
Department Chairman



Dr. Mohammed Abdul Samad  
(Advisor)



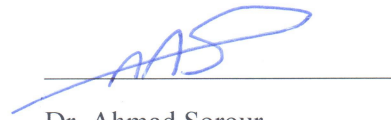
Dr. Salam A. Zummo  
Dean of Graduate Studies



Dr. Tahar Laoui  
(Member)

21/8/17

Date



Dr. Ahmad Sorour  
(Member)

\_\_\_\_\_

© Muhammad Umar Azam

2017

Dedicated to my parents for their continuous support and prayers for my success

## **ACKNOWLEDGMENTS**

First, I would like to Allah Almighty Who fulfilled my dream by giving me chance to secure admission with scholarship for Master degree in Materials science and Engineering at KFUPM and finally successful completion of my degree then my parents who supported me and prayed for my success.

I am highly thankful to my advisor Dr. Mohammed Abdul Samad who guided me actively during all my research work due to which I learned the way of learning and doing research. I really appreciate my committee members for their kind support and valuable suggestions during my work.

I would like to thank all of my friends and colleagues Annas, Zahid, Ismailya, Abdul Akeem, Moath and Sheriff for their kind support. I really appreciate my roommate Hamza Ahmed Mir for his kind behavior and support during all my stay at KFUPM.

I am thankful to Dr. Abbas Hakeem, Dr. Zain and Mr. Latif who provided me the lab facilities to complete my work.

Finally, I am thankful to King Abdulaziz City for Science and Technology (KACST) Research Unit, KFUPM for their financial support for this project through grant No.12-ADV3036-04.

# Table of Contents

<b>ACKNOWLEDGMENTS .....</b>	<b>iv</b>
<b>LIST OF FIGURES.....</b>	<b>x</b>
<b>LIST OF TABLES.....</b>	<b>xvi</b>
<b>LIST OF ABBREVIATIONS .....</b>	<b>xvii</b>
<b>ABSTRACT.....</b>	<b>xviii</b>
<b>ملخص الرسالة.....</b>	<b>xx</b>
<b>CHAPTER 1 INTRODUCTION .....</b>	<b>1</b>
1.1 Background .....	1
1.2 Motivation and Justification .....	2
1.3 Objectives .....	4
1.4 Project phases.....	5
1.5 Research Methodology in the present work.....	7
1.6 Organization of thesis .....	8
<b>CHAPTER 2 LITERATURE REVIEW .....</b>	<b>9</b>
2.1 Importance of Tribology .....	9
2.2 Different strategies to protect mechanical components .....	10
2.3 Introduction of polymers in tribological applications.....	12
2.4 Polymer and polymer based nanocomposite coatings .....	18
2.5 Ultra-high Molecular Weight Polyethylene (UHMWPE) .....	21
2.5.1 Properties of UHMWPE .....	22

2.5.2	Limitations of UHMWPE .....	24
2.5.3	UHMWPE coatings .....	24
2.5.4	UHMWPE nanocomposites coatings.....	25
2.5.5	Tribology of UHMWPE under lubricated conditions.....	26
2.6	Nanoclay (NC) .....	32
2.7	Carbon nanotubes (CNTs) .....	34
2.8	Hybrid nanocomposite coatings.....	38
2.9	Summary .....	39
<b>CHAPTER 3 Experimental Work.....</b>		<b>41</b>
3.1	Materials .....	41
3.1.1	UHMWPE powder.....	41
3.1.2	Nano Clay .....	42
3.1.3	Carbon Nanotubes.....	42
3.1.4	Silicon carbide (SiC) abrasives .....	43
3.2	Preparation of nanocomposite powders for coating.....	43
3.3	Substrate preparation before coating .....	44
3.3.1	Grinding .....	44
3.3.2	Ultrasonic cleaning and drying .....	45
3.3.3	Plasma treatment.....	46
3.4	Coating procedure .....	47
3.5	Characterization techniques .....	48
3.5.1	X-ray diffraction (XRD) .....	48
3.5.2	Raman spectroscopy .....	49

3.5.3	Dispersion analysis .....	49
3.5.4	Thickness measurements .....	49
3.5.5	Hardness measurements.....	50
3.5.6	Tribological testing .....	50
3.5.7	Wear morphology analysis and surface characterization.....	52
<b>CHAPTER 4 RESULTS AND DISCUSSION.....</b>		<b>53</b>
4.1	Development and characterization of C15A/UHMWPE nanocomposite coatings .....	53
4.1.1	Structural analysis by XRD .....	54
4.1.2	Dispersion analysis .....	55
4.1.3	Thickness measurement results.....	58
4.1.4	Surface characterization of the coatings .....	59
4.1.5	Hardness measurement results.....	60
4.1.6	Tribological results .....	61
4.1.7	Effect of linear sliding speed on tribological performance of 1.5 wt% C15A/UHMWPE nanocomposite coating .....	66
4.1.8	Accelerated wear life testing.....	68
4.1.9	Summary .....	70
4.2	Development and characterization of CNTs/UHMWPE nanocomposite coatings .....	71
4.2.1	XRD analysis of pristine and CNT-nanocomposite powders .....	72
4.2.2	Raman spectroscopy of pristine and CNT-nanocomposite powders .....	73
4.2.3	Evaluation of the coatings for dispersion of CNTs and thickness measurement..	74
4.2.4	Surface characterization of the coatings .....	76



4.2.5	Hardness evaluation of pristine and CNT-nanocomposite coatings .....	77
4.2.6	Tribological performance of the CNT-nanocomposite coatings under dry conditions .....	78
4.2.7	Summary .....	83
4.3	Development and characterization of CNTs/C15A/UHMWPE Hybrid nanocomposite coatings .....	84
4.3.1	XRD analysis of pristine and Hybrid nanocomposite powders .....	85
4.3.2	Raman spectroscopy of pristine and Hybrid nanocomposite powders .....	86
4.3.3	Evaluation of the coatings for dispersion of nanofillers and thickness measurements.....	87
4.3.4	Surface characterization of the coatings .....	89
4.3.5	Hardness evaluation of pristine and Hybrid nanocomposite coatings .....	90
4.3.6	Tribological performance of the pristine and Hybrid nanocomposite coatings under dry conditions .....	91
4.3.7	Effect of linear sliding speed on tribological performance of Sample-E (1.5CNT/1.5 C15A/UHMWPE) hybrid coating .....	97
4.3.8	Summary .....	100
4.3.9	Summary of Phase 1 showing the performance of the coatings under dry conditions.....	100
4.4	Tribological characterization of the hybrid nanocomposite and the optimized CNT nanocomposite coatings under water lubrication.....	103
4.4.1	Evaluation of tribological performance of the coatings under water lubrication. ....	104
4.4.2	Summary .....	110
4.5	Tribological characterization of Hybrid nanocomposite coating under water lubrication in the presence of abrasive particles .....	111
4.5.1	Effect of abrasives on tribological performance of Hybrid nanocomposite coating.....	111

4.5.2	Summary .....	114
<b>CHAPTER 5 CONCLUSIONS AND RECOMMEDATIONS .....</b>		<b>115</b>
5.1	Conclusions.....	115
5.2	Recommendations.....	120
<b>References .....</b>		<b>121</b>
<b>Vitae .....</b>		<b>130</b>

## List of Figures

Figure 1.1 Research Methodology followed in the present study .....	8
Figure 2.1 Different factors having an effect on tribological properties of polymers [33] .....	13
Figure 2.2 Coefficient of friction variation verses applied load (a) and wear scar diameter (WSD) (b) of GO/PEEK composite films [36] .....	14
Figure 2.3 Comparison of wear rates of UHMWPE (UH) and CNT nanocomposite (NC) verses UV exposure time [38] .....	15
Figure 2.4 Comparison of BAF of UHMWPE and PET under different environments [39] .....	16
Figure 2.5 Comparison of BF of UHMWPE and PET under different environments [39] .....	16
Figure 2.6 Schematic diagram showing embedment of abrasive particles [44] .....	18
Figure 2.7 Chemical structures (a) monomer (b) polymer .....	22
Figure 2.8 Comparison of wear rate of different polymers [3] .....	23
Figure 2.9 Comparison of Impact resistance of different polymers [3] .....	24
Figure 2.10 Comparison of wear rates by adding different concentrations of GO in GO-UHMWPE nanocomposites under lubricated conditions (a) deionized water (b) normal saline solution [70] .....	27
Figure 2.11 Variation in COF of UHMWPE under different conditions [72] .....	28
Figure 2.12 Variation in wear rate of UHMWPE under different conditions [72] .....	29
Figure 2.14 Average coefficient of friction results over the test period of 20 h [73] .....	29
Figure 2.15 Specific wear rate of verses water contact angle [73] .....	30
Figure 2.16 Comparison of specific wear rate for pristine UHMWPE and UHMWPE nanocomposites with varying clay contents before and after water absorption [74] .....	31

Figure 2.17 Comparison of average COF for pristine UHMWPE and UHMWPE nanocomposites with varying clay contents before and after water absorption [74] .....	31
Figure 2.18 (a) Structure of 2:1 phyllosilicates (b) Different structures based on mixing of polymer chains with layered silicates [76, 80] .....	33
Figure 2.19 Structures of SWNT and MWNT.....	34
Figure 2.20 Application of CNTs in tribology [88].....	35
Figure 2.21 Weight loss with respect to CNT contents after wear test [91] .....	36
Figure 2.22 COF with respect to CNT contents after wear test [91] .....	37
Figure 2.23 Variation of (a) Electrical conductivity (b) Tensile strength (c) Thermal conductivity with addition of CNTs and effect of dispersion [92] .....	38
Figure 3.1 SEM image of UHMWPE powder .....	41
Figure 3.2 SEM image of C15A nanoclay .....	42
Figure 3.3 SEM image of CNTs .....	42
Figure 3.4 SEM image of SiC abrasives .....	43
Figure 3.5 Nanocomposite powder preparation setup (a) Probe sonication of filler material (b) Mixing of filler and polymer matrix by magnetic stirring (c) Drying of nanocomposite powder .....	44
Figure 3.6 Grinding machine .....	45
Figure 3.7 Ultrasonic cleaner.....	45
Figure 3.8 (a) Schematic diagram of plasma treatment showing the carbon cleaning effect and the oxidation effect (b) Harrick plasma equipment .....	47
Figure 3.9 Electrostatic spray gun .....	48
Figure 3.10 Tribometer used in current study.....	51
Figure 3.11 Lubrication assembly setup used in tribometer for current study .....	51
Figure 4.1 XRD patterns of pristine UHMWPE, C15A organoclay and C15A reinforced UHMWPE nanocomposites with different loadings of clay .....	55
Figure 4.2 FE-SEM images of C15A/UHMWPE nanocomposite coatings with different loadings of C15A.....	57
Figure 4.3 SEM-EDS elemental map images of C15A/UHMWPE nanocomposite powders with different loadings of C15A for carbon (C) and Silicon (Si).....	58

Figure 4.4 Cross sectional images of pristine UHMWPE and C15A/UHMWPE nanocomposite coatings for thickness measurements .....	59
Figure 4.5 Surface roughness (Ra) of Pristine UHMWPE and C15A/UHMWPE nanocomposite coatings with different loadings of nanoclay .....	60
Figure 4.6 Comparison of the hardness of C15A/UHMWPE nanocomposite coatings with different loadings of C15A.....	61
Figure 4.7 Comparison of average coefficient of friction of pristine and nanoclay/UHMWPE nanocomposite coatings .....	63
Figure 4.8 Typical frictional graphs (left), photographs of wear tracks (middle) and counterface ball (right) of pristine UHMWPE coatings after the wear tests performed at normal load of 5, 7 and 9 N and a linear sliding speed of 0.1m/s.....	64
Figure 4.9 Comparison of average wear life of pristine UHMWPE and C15A/UHMWPE nanocomposite coatings at normal load of 9 N and a linear sliding speed of 0.1 m/s.....	64
Figure 4.10 Typical frictional graphs of pristine UHMWPE and C15A/UHMWPE nanocomposite coatings along with FE-SEM images (middle) and EDS spectrums (right) after wear tests performed at normal load of 9 N and a linear sliding speed of 0.1 m/s for 10,000 cycles. Inset: Counterface ball images after cleaning with acetone.. .....	65
Figure 4.11 Typical frictional graph of 1.5 wt% C15A/UHMWPE nanocomposite coating along with FE-SEM image of wear track and EDS spectrum after wear test conducted at 12 N and a linear sliding speed of 0.1 m/s .....	66
Figure 4.12 Typical frictional graphs of 1.5 wt% C15A/UHMWPE nanocomposite coatings (a) to (c), FE-SEM images of wear tracks (d) to (f), 3D optical profile images of wear tracks (g) to (f) and profile depths of wear tracks (j) to (l) after wear tests conducted at a normal load of 9 N at linear sliding speeds of 0.1, 0.2, 0.3 m/s .....	68
Figure 4.13 Typical frictional graph of 1.5 wt% C15A/UHMWPE nanocomposite coating for a wear test conducted at a normal load of 9 N and a linear sliding speed of 0.1 m/s for 100,000 cycles. Inset (Left): 3D optical	

image of the wear track. Inset (Right): Comparison of 2D-Optical wear profiles of wear tracks after wear test conducted at normal load of 9 N and a linear speed of 0.1 m/s for 25,000 and 100,000 cycles.....	69
Figure 4.14 XRD patterns of CNT-nanocomposites.....	72
Figure 4.15 Raman spectra for CNT-nanocomposites.....	74
Figure 4.16 FE-SEM images of CNT-nanocomposite coatings .....	75
Figure 4.17 FE-SEM images of the cross-section of pristine and CNT-nanocomposite coatings.....	76
Figure 4.18 Surface roughness (Ra) of CNTs/UHMWPE nanocomposite coatings with different loadings of CNTs.....	77
Figure 4.19 Effect of different loading of CNTs on hardness of the coatings.....	78
Figure 4.20 Comparison of average wear life of CNT-nanocomposite coatings for 10,000 cycles at a normal load of 12 N .....	79
Figure 4.21 Typical frictional graphs of CNT-nanocomposite coatings for 10,000 cycles at a normal load of 12 N. Inset (left): Photographs of wear tracks on samples. Inset (right): Optical images of counterface at 10x (captured after cleaning with acetone) at the end of sliding test .....	80
Figure 4.22 Comparison of average coefficient of friction of pristine and CNT/UHMWPE nanocomposite coatings.....	81
Figure 4.23 Comparison of average wear life of Sample-B (1.5CNT/UHMWPE) at normal loads of 12 and 15 N for 100,000 cycles.....	82
Figure 4.24 FE-SEM images of wear tracks of Sample-B (a & b) after sliding tests conducted at normal loads of 12 and 15 N for 100,000 cycles. Inset (middle): EDS analysis at wear track. Inset (right): 2D-Optical wear profiles of wear tracks .....	83
Figure 4.25 XRD patterns of Hybrid nanocomposite powders.....	86
Figure 4.26 Raman spectra for Hybrid nanocomposite powders.....	87
Figure 4.27 FE-SEM images of Hybrid nanocomposite coatings .....	88
Figure 4.28 FE-SEM images of the cross-section of pristine and Hybrid nanocomposites coatings .....	89

Figure 4.29 Surface roughness (Ra) of Hybrid nanocomposite coatings with different loadings of nanofillers .....	90
Figure 4.30 Effect of different loadings of CNTs/C15A on hardness of coatings .....	91
Figure 4.31 Comparison of average wear life of Hybrid nanocomposite coatings for 10,000 cycles at a normal load of 12N.....	92
Figure 4.32 Typical frictional graphs of Hybrid nanocomposite coatings for 10,000 cycles at a normal load of 12 N. Inset (left): Photographs of wear tracks on samples. Inset (right): Optical images of counterface at 10x (captured after cleaning with acetone) at the end of sliding test .....	93
Figure 4.33 Comparison of average coefficient of friction of pristine and CNT/C15A/UHMWPE hybrid nanocomposite coatings .....	94
Figure 4.34 Comparison of average wear life of Sample- E (1.5CNT/1.5C15A /UHMWPE) at normal loads of 12 and 15 N for 100,000 cycles .....	95
Figure 4.35 FE-SEM images of wear tracks of Sample-E (a & b) after sliding tests conducted at normal loads of 12 and 15 N for 100,000 cycles. Inset (middle): EDS analysis at wear track. Inset (right): 2D-Optical wear profiles of wear tracks .....	96
Figure 4.36 Comparison of wear track profile depths (Z) of Sample-E and Sample-B (optimized coatings) after wear test conducted at a normal load of 12 N and linear speed of 0.1 m/s for 100,000 cycles .....	97
Figure 4.37 Comparison of average wear life of Sample- E (1.5CNT/1.5C15A/UHMWPE) at normal loads of 12N for 25,000 cycles at three different sliding velocities .....	98
Figure 4.38 Photographs of wear tracks of sample along with their corresponding 3D-optical profile images (middle) and wear track profile depths (Z) (lower) at a normal load of 12 N for 25,000 cycles at three different velocities. Inset: cleaned counterface ball images after the wear tests .....	99
Figure 4.39 Comparison of the hardness of the coatings.....	101
Figure 4.40 Comparison of the average COF of the coatings.....	101
Figure 4.41 Comparison of the average wear life of coatings at a normal load of 12 N and a sliding speed of 0.1 m/s for 100,000 cycles.....	102

Figure 4.42 Comparison of the average wear life of Hybrid nanocomposite coatings at normal loads of 12 N and a linear speed of 0.1 m/s for 150,000 cycles under water lubrication. Inset: Photographs of wear tracks on samples. ....	105
Figure 4.43 Comparison of the average wear life of Sample (B and E) at normal loads of 12 N for 300,000 cycles under water lubrication. Inset: Photographs of wear tracks on samples. ....	106
Figure 4.44 FE-SEM images of wear track of Sample-E at lower and higher magnifications after sliding tests conducted at normal load of 12 N for 300,000 cycles. Inset: EDS analysis and 2D-Optical wear profiles of the wear track .....	107
Figure 4.45 Comparisons of 2D-Optical wear profiles of wear track of Sample-E after sliding tests conducted under water lubrication for 150,000 and 300,000 cycles at normal load of 12 N .....	108
Figure 4.46 Comparison of COF of Sample-E after sliding test under dry and water lubrication.....	109
Figure 4.47 Comparison of hardness of 1.5CNTs/1.5C15A/UHMWPE hybrid nanocomposite coating (Sample-E) before and after conducting the sliding test under water lubrication for 300,000 cycles.....	110
Figure 4.48 Comparison of typical frictional graphs of 1.5 wt% CNT/1.5 wt% C15A/UHMWPE Hybrid nanocomposite coating (a) & (b), FE-SEM images of wear tracks at lower (120 x) and higher (400 x) magnifications (c) & (d), 3D optical profile images of wear tracks (e) & (f) and profile depths of wear tracks (g) & (h) after wear tests performed at normal load of 12 N and linear sliding speeds of 0.1 m/s under water lubricated conditions with/ without the presence of abrasive particles, Counterface ball images (i) & (j) after cleaning with acetone. Insets in (a) & (b) show the wear track on coated sample. ....	113
Figure 4.49 Schematic diagram of abrasive particles embedded in softer polymer coating.....	114



## **List of Tables**

Table 2.1 Mechanical Properties of UHMWPE [60] .....	23
Table 2.2 Comparison of some mechanical properties of CNTs with various materials [4]...	35
Table 4.1 Classification and designation of samples in section 4.2 .....	71
Table 4.2 Classification and designation of samples in section 4.3 .....	85

## **LIST OF ABBREVIATIONS**

<b>UHMWPE</b>	:	Ultra-high molecular weight polyethylene
<b>MWCNTs</b>	:	Multi-walled carbon nanotubes
<b>Z</b>	:	Wear track profile depth
<b>DI</b>	:	Deionized
<b>XRD</b>	:	X-ray diffraction
<b>NC</b>	:	Nanoclay
<b>PVD</b>	:	Physical vapor deposition

## **ABSTRACT**

Full Name : Muhammad Umar Azam  
Thesis Title : Development and characterization of Ultra High Molecular Weight Polyethylene (UHMWPE) based hybrid nanocomposite coating for bearing applications under dry and water lubrication  
Major Field : Materials Science and Engineering  
Date of Degree : [May 2017]

In the recent past, polymer coatings have been extensively developed as an alternative lubrication strategy in demanding tribological applications. These components may be operated under dry conditions or under aqueous environments. So water (with/ without abrasives) may be entrained into these sliding components either accidentally, deliberately or as a contaminant which may lead to the deterioration of the properties of the polymer coatings. Hence, the evaluation of the tribological performance of these coatings under aqueous environment becomes significant.

Among polymers, ultra-high molecular polyethylene (UHMWPE) has a great combination of properties such as low coefficient of friction (COF), high abrasion resistance, high impact resistance and durability. In spite of these excellent properties, UHMWPE still demands modifications to enhance its load bearing capacity, tribological and thermal properties. Hence the main objective of this work is to develop a novel hybrid nanocomposite coating of UHMWPE reinforced with carbon nanotubes (CNTs) and nanoclay (C15A) for bearing applications under dry and water lubricated conditions.

Initially, nanocomposite and hybrid nanocomposite coatings reinforced with different loadings of nanoclay/CNTs or combination of both were optimized under dry conditions.

Finally the optimized nanocomposite and hybrid nanocomposite coatings with various combinations of the nanofillers were evaluated for better tribological performance under water lubrication with/ without abrasive particles.

Ball-on-disk wear tests using a 440C stainless steel ball as the counterface were conducted on the coatings under dry and water lubricated conditions to evaluate their tribological performance. X-ray diffraction, raman spectroscopy, scanning electron microscopy and optical profilometry techniques were used to characterize the coatings in terms of dispersion of the nanofillers, morphology and wear mechanisms respectively. Results showed that the UHMWPE hybrid nanocomposite coating reinforced with 1.5 wt% of CNTs and 1.5 wt% of C15A nanoclay performed best under dry and water lubrication conditions at a normal load of 12 N and a linear speed of 0.1 m/s showing a significant improvement in wear resistance as compared to all other coatings evaluated in this study.

Moreover, the tribological performance of the hybrid nanocomposite coating (1.5 wt% CNT/ 1.5 wt% C15A/UHMWPE) with/ without the presence of abrasives was also evaluated at a normal load of 12 N and sliding speed of 0.1 m/s. It was observed that the hybrid nanocomposite coating survived in both the cases without failure. However, the wear track profile depth of the hybrid nanocomposite coating was less (80  $\mu\text{m}$ ) in case of the sliding test with abrasives as compared to that in the absence of abrasives where in the wear track profile depth was found to be 104  $\mu\text{m}$ , suggesting of a reduction in wear rate in the presence of abrasives. This is mainly attributed to the embedment of the abrasive particles in the softer polymer matrix which help in providing with an enhanced anchoring effect of the polymer chains leading to an improvement in the resistance to their easy pull-out. However, the counterface ball in the presence of abrasives showed severe wear.

## ملخص الرسالة

الاسم الكامل : محمد عمر عزام

عنوان الرسالة : تطوير و توصيف الطلاء الهجينى النانوي لمادة البوليمر (UHMWPE) لتطبيقات المحملات الجافة والمائية

التخصص : هندسة علم المواد

تاريخ الدرجة العلمية : مايو 2017

تم تطوير طلاء البوليمر على نطاق واسع في الماضي القريب على نطاق واسع كبديل للتشحيم في التطبيقات التريبولوجية في البيئات الجافة والرطبة ، و لذلك يمكن أن يكون الماء - مع أو بدون الكاشطات - محصورة في هذه المكونات الانزلاقية إما عن طريق الخطأ أو العمد أو كملوث يؤدي إلى تدهور خصائص طلاء البوليمر وبالتالي فإن تقييم الأداء التريبولوجي ملحا في البيئة المائية.

يعتبر البوليمر (UHMWPE) من بين البوليمرات التي لها مزيج من الخصائص مثل: انخفاض معامل الاحتكاك والمقاومة العالية والمتانة ، وبالرغم من خصائصها الممتازة لازال هناك حاجة لتعزيز قدرة تحملها وخصائصها التريبولوجية و الحرارية ولهذا فالهدف الرئيسي من هذه الدراسة لتطوير الطلاء الهجينى النانوي لمادة البوليمر (UHMWPE) المعزز بأنابيب الكربون النانوية (CNTs) و النانوكلاي (C15A) لتطبيقات المحملات الجافة والمائية.

مبدئياً تم تحسين الطلاء الهجينى النانوي لمادة البوليمر (UHMWPE) بنسب مختلفة من بأنابيب الكربون النانوية (CNTs) و النانوكلاي (C15A) أو خليط منهما معاً في الظروف الجافة ثم تقييم الطلاء مع تركيبات مختلفة من النانوفيلر لتعطي أداء تريبولوجي رطب أفضل مع أو بدون جسيمات كاشطة.

و قد أجريت اختبارات التآكل باستخدام كرة فولاذية (440C) في بيئات جافة و مائية لتقييم ادائها التريبولوجي باستخدام الأشعة السينية و طيف رامان و المجهر الالكتروني و التقنيات البصرية لتوصيف تشتت النانوفيلر في الطلاء و التشكل و ميكانيكيات التآكل. حيث أظهرت النتائج النهائية ان الطلاء الهجينى النانوي لمادة البوليمر (UHMWPE) المعزز بنسبة ( 1.5 wt% ) من (CNTs) و بنسبة ( 1.5 wt% ) من (C15A) يعطي الأداء الأفضل في الظروف الجافة والمائية في حمولة ( 12N ) و سرعة خطية ( 0.1 m/s ) و أظهرت تحسناً كبيراً في ممانعة التآكل بالمقارنة مع الطلاءات الأخرى المستخدمة في هذه الدراسة.

تم تقييم الأداء التريبولوجي للطلاء النانوي مع أو بدون استخدام الكاشطات بإستخدام ثقل (12N) وسرعة (0.1m/s) ولوحظ مقاومة الطلاء بدون فشل، ولوحظ أن عمق التآكل للمركب النانوي بإستخدام الكاشطات أقل من 80 مايكرومتر مقارنة بعمق 104 مايكرومتر مع عدم إستخدامها وذلك بسبب الكاشطات التي تعزز المقاومة وتحد من التآكل مع أنها تزيد من تآكل الكرة.

# CHAPTER 1

## INTRODUCTION

### 1.1 Background

Friction and wear are major concerns in practically all tribological applications. At present, about one third of energy resources are being wasted due to involvement of friction directly or indirectly [1]. Therefore, it is significantly important to consider the causes of friction and wear to develop a strategy which can minimize the losses due to friction and wear.

In the recent past, polymer coatings are being used as an alternative lubrication strategy in various tribological applications due to their low cost, good tribological properties, environment friendliness and ability to be coated by using simple techniques. Polymethylmethacrylate (PMMA), polyurethane (PU), polytetrafluoroethylene (PTFE), polyamide (PA), polyetheretherketone (PEEK) and ultra-high molecular weight polyethylene (UHMWPE) are some of the most common polymers which have been used to develop coatings. However, limitations such as low strength and low thermal stability have hindered the use of these polymer coatings to their full potential.

With the advent of materials such as carbon nanotubes (CNTs), graphene, nanoclays etc. which can be used as reinforcements, a new class of materials called the polymer nanocomposites have been developed in bulk and in the form of coatings with enhanced mechanical, thermal and tribological properties. Nanocomposites are a novel class of

materials in which any one of the constituent materials has at least one of the dimensions less than 100 nm. They have the advantage of exhibiting excellent properties as compared to conventional composites due to the very high surface to volume ratio and very high aspect ratio of the nanofillers used as reinforcements. Hence, these polymer nanocomposites in the form of bulk or coatings are fast replacing metals and metallic/ceramic coatings in various demanding tribological applications including different types of bearings, bearing cages, biomedical implants, cams, valves, vacuum pumps, seals, automobile brake pads etc. under dry sliding and lubricated conditions because of their enhanced mechanical, thermal and tribological properties [2].

## **1.2 Motivation and Justification**

However, there is still a lot of scope to further improve the properties of these polymer nanocomposites and their coatings so that they can be used in varying environments. The polymer or polymer nanocomposite coatings can be exposed to different environments during their operational life. For example, the coated components may be operated under dry conditions or under aqueous environments. So there is a likely chance that water (with/without abrasives) may be entrained into these sliding components either accidentally, deliberately or as a contaminant which may lead to the deterioration of the properties of the polymer coatings due to swelling by water absorption. Hence, there is an urgent need to further enhance the properties of these coatings so that they will be able to function and protect the sliding components against wear and tear, irrespective of the environment they are exposed to.

Thus we were motivated to explore a novel approach of developing a hybrid nanocomposite coating to solve this problem. A hybrid nanocomposite or a hybrid nanocomposite coating is a new emerging approach of reinforcing any parent matrix with two or more nanofillers to mainly take advantage of the individual properties of each of the nanofiller into one product.

Hence based on this concept, we set about selecting the best polymer matrix and the nanofillers which would help in developing a polymer coating that would protect the sliding components under dry as well as aqueous environments (with/without abrasives). For this purpose, it is very essential that the developed hybrid nanocomposite coating should have a low coefficient of friction (COF), high wear resistance, high load bearing capacity and high resistance to water absorption.

UHMWPE is one of the most suitable polymer among all other polymers which can be used for coating purposes in tribological applications because of its unique properties such as COF, high abrasion resistance, self-lubricity, high durability and high impact resistance. However, it has some limitations such as low thermal properties, load bearing capacity and low Young's modulus [3]. Various researchers have modified these properties by reinforcing it with different nanofillers.

CNTs are the allotropes of carbon and one of the most effective nanofiller used as a reinforcement in different polymer matrices to improve their load bearing capacity, due to their unique properties such as high tensile strength, extraordinary thermal conductivity, large aspect ratio, high electrical conductivity and low thermal expansion coefficient [4]. Such a combination of these properties makes them a pioneer among the different



nanofillers. Various researchers have modified the tribological, mechanical and thermal properties of polymer matrices, by reinforcing them with CNTs [5, 6] under dry and base oil lubricated sliding conditions.

Nanoclays also known as layered silicates another class of nanofillers which are very effectively used to enhance the barrier properties such as resistance to water absorption because of their unique platelet like structure which provides a tortuous path for the diffusion of gas or liquid molecules. In recent years, a lot of research in polymer layered silicates nanocomposite coatings has been carried out. From the literature review, it is found that various researchers enhanced barrier properties of epoxy coating [7], mechanical properties of epoxy coating [8], tribological properties of polyester coating [9], anti-corrosion and thermal properties of polystyrene-acrylonitrile coating [10] by reinforcing them with nanoclay.

### **1.3 Objectives**

Hence in view of the above justification, we defined the main objective of our study to be as follows: *To develop and characterize the tribological performance of a novel hybrid nanocomposite coating of UHMWPE reinforced with carbon nanotubes (CNTs) and nanoclay (C15A) under dry and water lubricated (with/without abrasives) conditions for mechanical bearing applications.* CNTs shall be added to improve the load bearing capacity of the coating and nanoclay will be added to improve the resistance to water absorption along with mechanical properties.

## **1.4 Project phases**

To achieve the above mentioned objective, the overall project is divided into *two major phases* as described below. In the first phase, optimization of nanofillers' loadings was carried out through tribological characterization under dry conditions. In second phase, optimized coatings were evaluated for tribological performance under water lubrication with/without abrasive particles.

### **Phase 1 - Development and characterization of nanocomposite and hybrid nanocomposite coatings under dry conditions**

Phase 1 is further divided into three sections where different combination of nanofillers are optimized as described below.

#### **1) Development and characterization of nanoclay/UHMWPE nanocomposite coatings**

In this phase, UHMWPE nanocomposite coatings reinforced with nanoclay were developed and characterized in terms of tribological performance under dry conditions by optimizing the loading of nanoclay. Following tasks were performed in this phase such as selection of a proper coating process, optimization of the coating parameters, development/deposition of nanocomposite coatings with different loadings (0.5, 1.5, 3 wt%) of nanoclay, structural and mechanical characterization of coatings and tribological characterization of the coatings.

## **2) Development and characterization of CNTs/UHMWPE nanocomposite coatings**

In this phase, UHMWPE nanocomposite coatings reinforced with carbon nanotubes (CNTs) were developed and characterized in terms of tribological performance under dry conditions by optimizing the loading of CNTs. Following tasks were performed in this phase such as development/deposition of nanocomposite coatings with different loadings (0.5, 1.5, 3 wt%) of CNTs, structural and mechanical characterization of coatings and tribological characterization of coatings

## **3) Development and characterization of nanoclay/CNTs/UHMWPE Hybrid nanocomposite coatings**

In this phase, different combinations of hybrid nanocomposite coatings were developed and characterized in terms of tribological performance under dry conditions by optimizing the loading of CNTs. Following tasks were performed in this phase such as development/deposition of hybrid nanocomposite coatings with different loadings (0.5, 1.5, 3 wt%) of CNTs while keeping the optimum loading of nanoclay constant as obtained from section 1, tribological characterization of coatings, structural and mechanical characterization of coatings

## **Phase 2 - Tribological characterization of the hybrid nanocomposite coatings under water lubrication with/without abrasives**

In this phase, tribological characterization of the hybrid nanocomposite coatings under water lubrication was evaluated. Later the tribological performance of the optimized hybrid nanocomposite coating was evaluated under water lubrication in the presence of abrasives.

Following tasks were performed in this phase such as development/deposition of hybrid nanocomposite coatings with different loadings (0.5, 1.5, 3 wt%) of CNTs while keeping the optimum loading of nanoclay constant as obtained from phase 1, structural and mechanical characterization of coatings, tribological characterization of coatings under water lubrication and then tribological characterization of the best coating under water lubrication with the presence of abrasive particles such as silicon carbide (SiC).

## **1.5 Research Methodology in the present work**

Figure 1.1 shows the research methodology which was adopted during our research to meet all the objectives as stated above. Electrostatic powder spray system was used for deposition of coatings on metallic substrate. Initially tribological performance of pristine UHMWPE was evaluated under dry conditions. Then different fillers (nanoclay and CNTs) and their combinations, prepared by sonication followed by magnetic stirring, were used to reinforce the polymer matrix for better tribological properties under dry conditions. Finally, optimized coatings were evaluated for tribological performance under water lubrication in the presence/ absence of abrasive particles. Along with the tribological characterization, other characterization techniques were also used to characterize the coatings in terms of dispersion of the nanofillers, morphology and wear mechanisms etc.

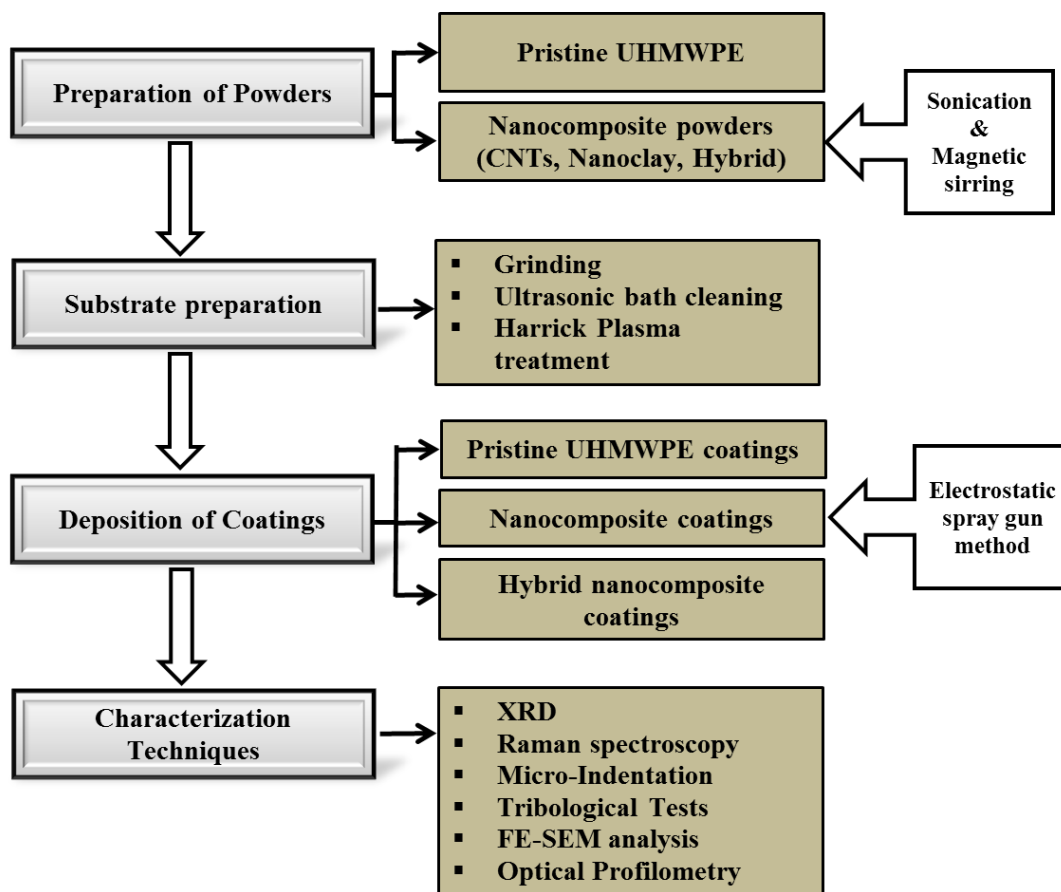


Figure 1.1 Research Methodology followed in the present study

## 1.6 Organization of thesis

In this thesis, Chapter 1 is related to introduction part of the work. In chapter 2, an extensive literature review is presented on various lubrication strategies being used, tribological applications of polymers under different environments, developments regarding polymer nanocomposite coatings particularly UHMWPE based nanocomposite coatings in the perspective of the current research work. In chapter 3, the experimental methods/procedures used in this study are described. Chapter 4 presents the experimental results and discussion related to all the project phases. Chapter 5 presents all the conclusions obtained from the work and suggests a few recommendations for future.

## **CHAPTER 2**

### **LITERATURE REVIEW**

#### **2.1 Importance of Tribology**

Science of interacting surfaces in their relative motion is known as Tribology. It is a multi-disciplinary field. It deals with phenomenon of friction, wear and lubrication to reduce energy losses as well as increase the operational life of component in a system. It plays an important role in modern machinery that involves sliding and rolling surfaces. Friction and wear are major concerns in practically all modern mechanical machines. A few examples are internal combustion and aircraft engines, automobiles, gears, cams, bearing, and seals. In a survey in 1966, it was estimated that about 4% of GNP of United States was wasted due to neglect the role of Tribology. At present, about one third of energy resources are wasted due to involvement of friction directly or indirectly [1]. So, it is significant to consider the causes of friction and wear. The aim of research and development in tribology is to minimize losses due to friction and wear as much as possible. Today tremendous research is going on to achieve this aim and tremendous achievements have been achieved. People are using different fillers to make composites to get better tribological properties. But research to improve further is still necessary.

## 2.2 Different strategies to protect mechanical components

The usage of various protective coatings and modified lubricants for the protection of contacting surfaces is the current strategy of lubrication in mechanical systems [11]. Diamond-like carbon (DLC) coatings, metal carbides coatings (CrC, TiC, WC), molybdenum disulphide (MoS<sub>2</sub>) coatings and PVD coatings (ZrN, TiAlN, CrAlN, ZrC, W–C:H, WC/C, TiO<sub>2</sub>, Al<sub>2</sub>O<sub>3</sub>) are mostly used protective coatings in industry [12–16]. Although these coatings are useful in providing high wear resistance but there are some limitations associated with them such as high thermal stresses in the coating, high friction, incompatibility with the lubricant, poor adhesion with the substrates and sensitive to the environment [17, 18]. There is also a concern regarding worn debris particles from hard coating because that can damage the entire tribological system adversely.

Recently a lot of research has been done to develop efficient lubricant and understand the lubrication mechanism [18] in order to resolve all issues associated with these protective coatings mentioned above. Different lubricants such as mineral oils with most appropriate additives such as molybdenum dialkyl dithiocarbamate (MoDTC) and zinc dialkyl dithiophosphate (ZDDP) are being used to enhance the lubricant's performance. The additives basically form tribofilms on contacting surface by reacting with it which is helpful in order to avoid wear especially in case of boundary lubrication [19]. In spite of lot of developments in field of lubricants and additives, there are some environmental and health issues [20, 21] which have to be overcome by changing the lubrication strategies. For this purpose, such kind of lubrication strategy is needed in which there is less or no involvement of these harmful additives.

Polymers have made their worth in different tribological applications to enhance wear lives of many components due to their low density, anticorrosion properties, low cost and ease of coating methods [22]. Moreover, their importance becomes more prominent in the areas where the fluids cannot be endured because of their contamination with the product such as corrosive environments. When the polymeric materials are rubbing in tribological contacts it is very useful and often the lubrication is not necessary because they are self-lubricated.

Different researchers [23–25] have explored a new approach in which they used water as an environment friendly lubricant in combination with polymer coating and studied the tribological behavior of polymers in the aqueous environments and found that water could play a significant role in reduction of COF and absorb the heat generated due to friction. In aqueous conditions, there are various factors such as the surface wettability, interaction of the polymer with water which significantly affect the properties of polymers in term of tribology. The drawbacks of using water as a lubricant are

- Water can deteriorate the properties of polymers because polymers are swelled after absorbing water and due to this their hardness and strength is reduced [26,27].
- Water has very less viscosity as compared to other oil lubricants that's why it can be evaporated very easily with small increase of temperature produced by two sliding surfaces as compared to that of oil lubricants.
- It is well established that formation of adherent transfer film on counterface reduce wear rate of polymers. It is found in literature that presence of water affects the formation of transfer layer on the counterface material [27–29].



- Water may cause corrosion of counterface or substrate if it is being exposed to water after failure of protecting polymer coatings.

So water can either behave as a lubricant or as a contaminant when it is in contact with the machine elements based on different applications and interaction of water with polymers [30]. A lot of research has been conducted by using different nanofillers to minimize these drawbacks so that water can be used as environment friendly lubricant or it can not deteriorate the properties of polymers when it is in contact with polymeric coated sliding components.

### **2.3 Introduction of polymers in tribological applications**

The tribology of polymers is not same as that of metals, ceramic materials and their derivatives because of difference in chemical and physical structures. The polymers have very low surface free energy [31]. Polymers show viscoelastic properties due to which they are being affected in a different ways in terms of tribological behaviors. The effect of different tribo-system parameters on wear of polymer is even stronger than that for metals [32]. Following Figure 2.1 shows different factors that have an effect on tribological behaviors of polymers.

The ability of the polymers to be easily modified in coatings as well as in bulk form gives them uniqueness. Therefore they are mostly used as a matrix to develop many composites. The figure 3 below is representing different factors that have an impact on tribological properties of polymers.

Different researchers have studied the tribological behavior of different polymers and their composites under different environments and conditions for specific applications. Based on various wear mechanisms, environments and conditions they obtained different results which are being highlighted below.

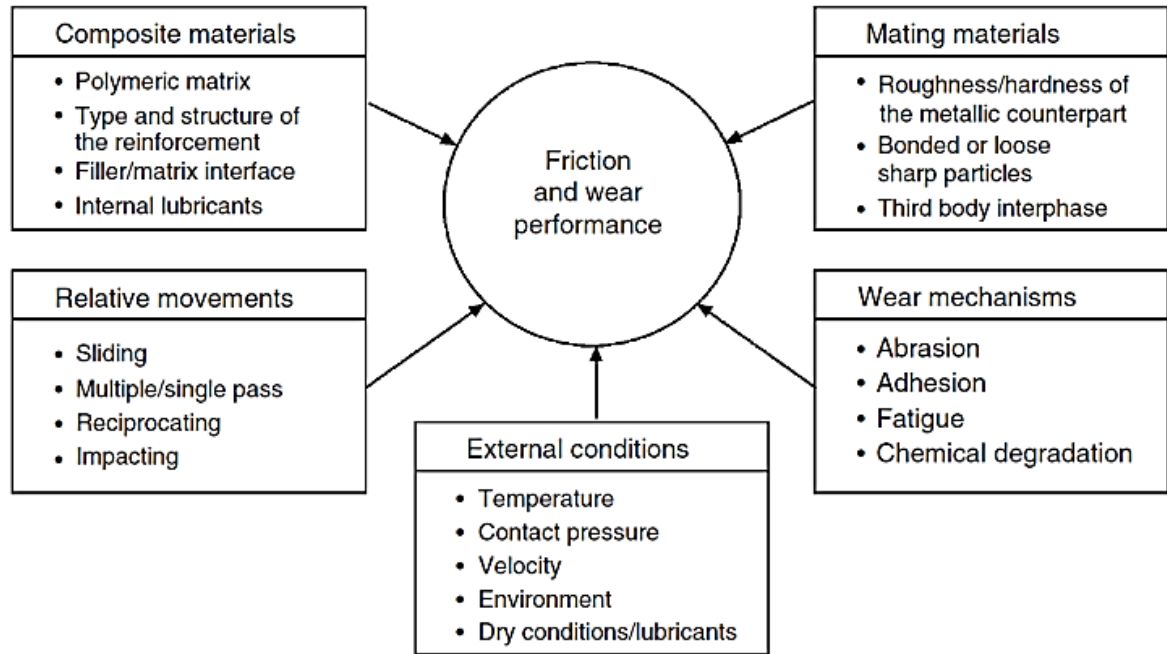


**Figure 2.1** Different factors having an effect on tribological properties of polymers [33]

C. G. Clarke et al. [34] in their studies, evaluated the tribological behaviors of five different polymers (UHMWPE, PETP, P (A-I)/GR, POM and PA6/MoS<sub>2</sub>) under water lubrication for applications of bearing surfaces between the body of a hydraulic drill and tool holder. They proved that all parameters including counterface roughness, sliding velocities and pressure had a great impact on tribological behaviors of these polymers.

Shiwei W et al. [35] evaluated the tribological and mechanical behavior of polyurethane (PU) based composites modified with UHMWPE under water lubrication for water-lubricated bearings applications which are generally used in hydraulic engineering,

metallurgy, mining and other various applications. They found improvement in these properties (as mentioned above) of composite as compared to pristine polymer.

HJ Song et al [36] studied the effect of graphene oxide (GO) nanosheets addition on tribological properties of PEEK film fabricated by cast method in dry, water and paraffin oil lubricated conditions. They found different tribological results under different environment mentioned above. They concluded that GO nanosheets reinforcement decreased the COF and increased the coating life in all three environments but best results were obtained in oil lubricated conditions. Following Figure 2.2 below shows the tribological results of PEEK/GO film in terms of COF and wear behavior measured by resultant wear scar diameter (WSD) at linear speed of  $0.0628 \text{ ms}^{-1}$ .

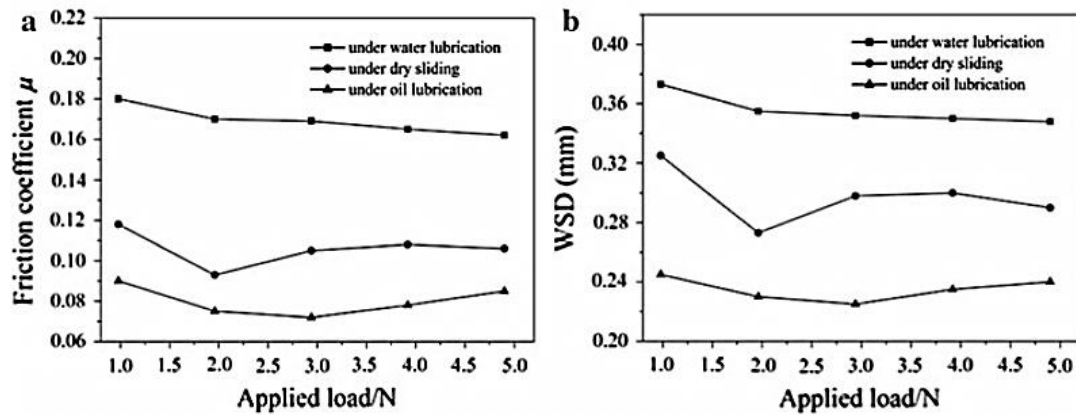


Figure 2.2 Coefficient of friction variation verses applied load (a) and wear scar diameter (WSD) (b) of GO/PEEK composite films [36]

Samad et al [37] developed 0.1 wt% CNTs-UHMWPE nanocomposite by dip coating procedure and evaluated the effects of different counterface materials on the mechanical and tribological behaviors of the nanocomposite coating. Moreover, they studied the effect of UV radiation on the tribological and mechanical properties of these coating. They found

that nanocomposite coatings showed lowest COF when they slid against brass as compared to other counterfaces as mentioned above at normal load of 4N and a linear velocity of 0.41 ms<sup>-1</sup>. At this particular velocity and load, nanocomposite coatings did not fail until 240,000 cycles in all the three counterface material cases. There was no particular effect of UV radiation (exposed for 300 h) on tribological behavior of these nanocomposite coatings.

In another study, N. Campo and A. M. Visco [38] evaluated the effect of UV irradiation on UHMWPE and CNT-UHMWPE nanocomposite. The figure below show the comparison of wear rates results of both cases with respect to UV exposure time. It can be observed from Figure 2.3 that nanocomposite performed better after being exposed to UV radiations as compared to pristine UHMWPE and showed lowest wear resistance at time of 2 hours.

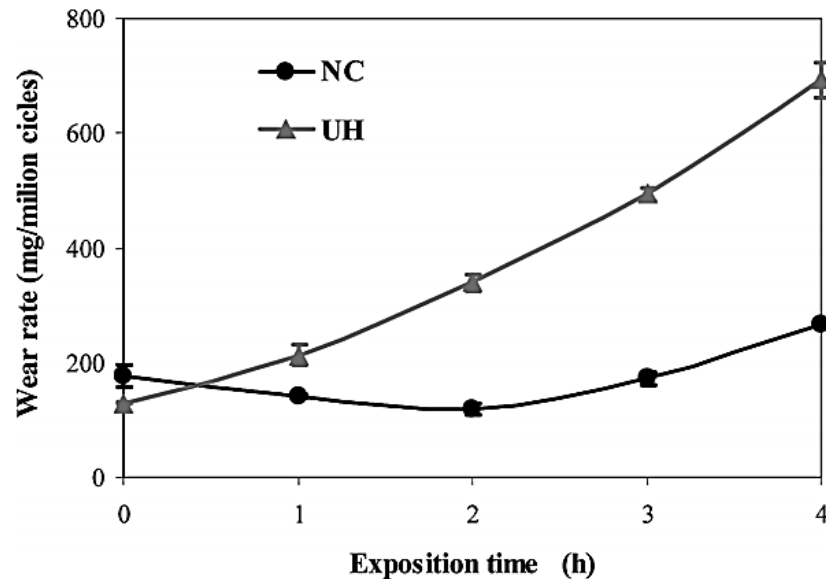


Figure 2.3 Comparison of wear rates of UHMWPE (UH) and CNT nanocomposite (NC) verses UV exposure time [38]

TD. Nguyen et al. [39] reported the tribological behavior of two polymers UHMWPE and PET for journal bearing applications under dry and four different lubricated conditions

which were river water, distilled water, tap water and demineralized water. Wear tests were performed in a special “Stribeck configuration” at contact pressure of 0.3 MPa and different sliding speeds varying from 0 to 1.07 ms<sup>-1</sup> at ambient temperature. They reported break-away friction (BAF) and boundary friction (BF) results of both polymers under all above mentioned conditions. Comparison of these results is presented in Figure 2.4 and Figure 2.5 below.

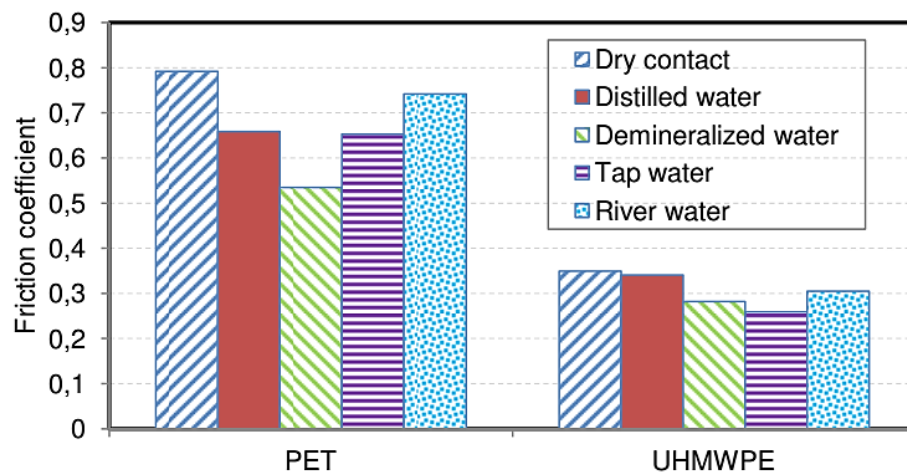


Figure 2.4 Comparison of BAF of UHMWPE and PET under different environments [39]

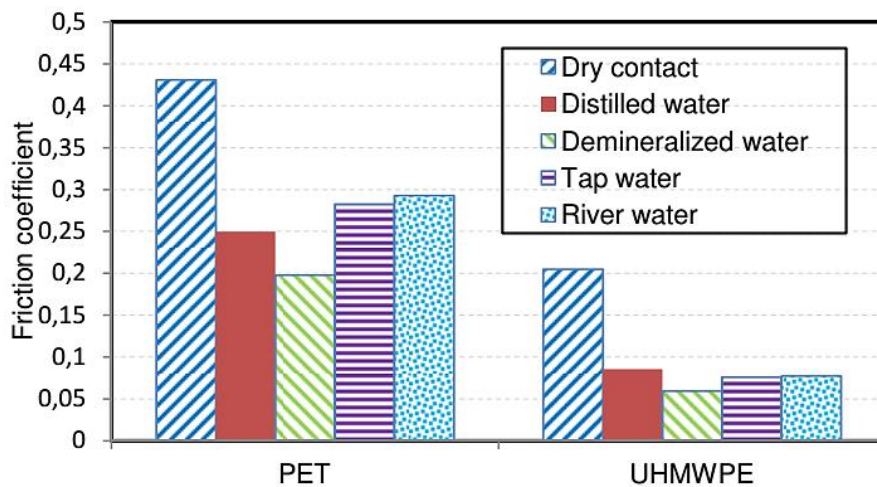


Figure 2.5 Comparison of BF of UHMWPE and PET under different environments [39]

Sliding speed can also play its role differently based on type of environment. For example in dry condition, at higher sliding speed there are chances of rise in temperature at point of contacts between two mating surfaces which can cause softening of polymer. In presence of some lubricants this heat can be dissipated which definitely affect the wear rate differently. Also at different loads tribological behavior of polymers varies due to change in contact pressures and temperature.

H. Meng et al. [40] compared the tribological behavior of CNTs reinforced polyamide 6 (PA6) composites with pristine polymer in dry and water lubricated condition at different loads. They found that CNTs reinforced composites showed less COF and more wear resistance under dry and lubricated conditions as compared to that of pristine PA6 matrix.

The performance of polymers in terms of tribological behavior significantly depends on temperature because it can change the crystallinity of polymer which affects the mechanical as well as tribological properties of polymers. At elevated temperature softening of polymers can be occurred. Samad et al [41] evaluated the effect of temperature on tribological behavior of a CNTs reinforced UHMWPE nanocomposite coating on steel substrates with or without PFPE overcoat under dry as well as base oil lubricated conditions and found variation in the tribological results at different temperatures.

Similar to other factors, the tribological performance of polymers also depends on presence of foreign particles which can be entrained in the particular tribo-system through any source such as sandstorm, dusty condition or rain especially in desert environment These abrasives can either act as third body particles which can abrade the polymer and increase the wear rate [42] or they can be embedded in polymer, resulting in reduced wear rate [43].

Ezzat A. A et al [44] evaluated the abrasive wear of polyethylene coating reinforced with aluminum oxide nanofibers deposited onto the steel substrate in the presence of sand particles. They found decrease in wear rate due to embedment of sand particles in the coating acting as protective wear layer of hard particles. Following Figure 2.6 shows the schematic diagram indicating the embedment of abrasive particles.

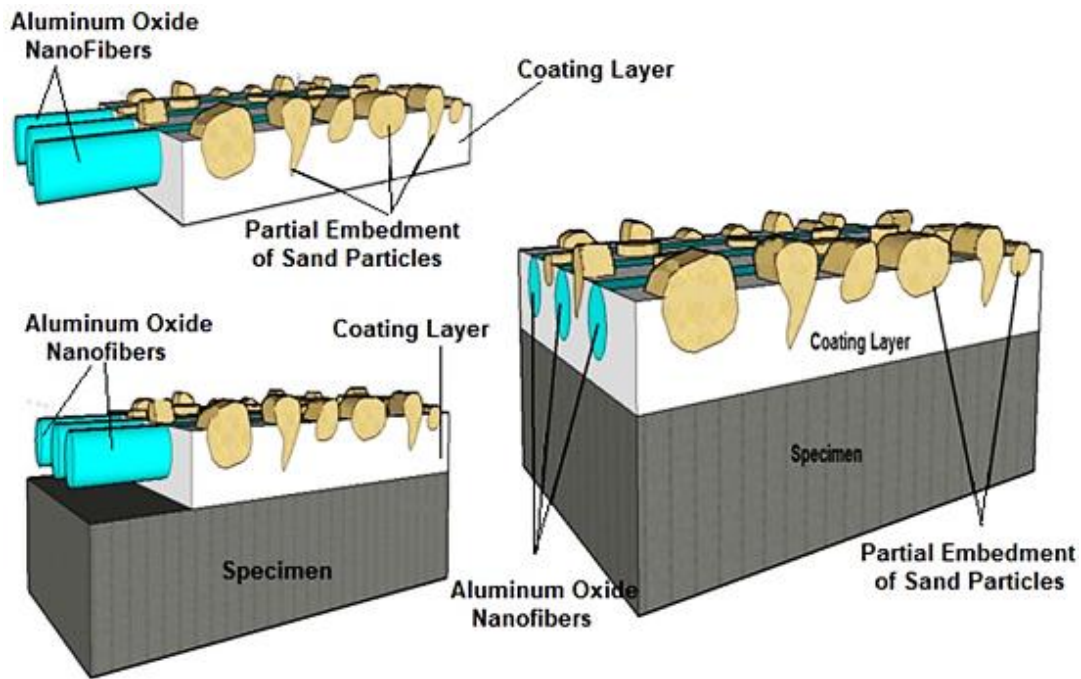


Figure 2.6 Schematic diagram showing embedment of abrasive particles [44]

## 2.4 Polymer and polymer based nanocomposite coatings

It is found from literature review that many polymers coatings have been developed to overcome friction, wear issues as well as for anti-corrosion purposes. Many polymers are being used as barrier coatings to reduce diffusivity of gas/ water molecules such as in packaging industries. Polymethylmethacrylate (PMMA), polyurethane (PU), polytetrafluoroethylene (PTFE), polyamide (PA), polyetheretherketone (PEEK) and ultra-

high molecular weight polyethylene (UHMWPE) are mostly used polymers for coatings for tribological purposes. All these polymers have some specific useful tribological characteristics as well as some limitations which will be discussed below. To modify the tribological properties of these polymer coatings fillers have been used.

PTFE coating has high temperature stability and low COF but shows poor wear resistances which make it unable to be used in mechanical systems because it causes failure of component due to wear [45]. Lee et al [46] have improved the wear resistance of PTFE by adding 2wt% nano-diamond in it. PEEK coating has good chemical resistance, high strength and good tribological properties. McCook et al [47] observed the decrease in the COF of low carbon steel substrate by depositing PTFE-epoxy composite coating on it. The measured COF for this coating was about 0.15 under dry conditions.

Yeh et al [10] improved anti-corrosion properties as well as thermal stability by adding 3% Montmorillonite (MMT) - polystyrene-acrylonitrile coating, prepared by in-situ thermal polymerization process, on cold rolled steel. By adding 10 % SiO<sub>2</sub> nanoparticles by volume in PEEK polymer, Hedayati et al. [48] improved the wear resistance of PEEK coating on plain carbon steel substrate by using electrostatic spray system. A. Golgoon et al [9] enhanced the wear and corrosion resistance of plain carbon steel by depositing 5wt% clay-polyester nanocomposite coating. Bagherzadeh et al [7] compared the water uptake of pure epoxy coating and 1wt% nanoclay-epoxy nanocomposite coating. They observed that water uptake was three times less in case of nanocomposite coating as compared to pure one.



Wang Y et al. [49] evaluated the mechanical and tribological behaviors of pristine polyamide (PA-1010) and SiO<sub>2</sub>-(PA-1010) nanocomposite coatings under dry sliding conditions and at ambient temperature. They found that nanofillers enhanced the crystallinity and mechanical properties of coatings and reduced the wear and friction of polymer coatings effectively. Moreover, optimum results were obtained by adding 1.5 wt. % nano-sized silica particles in polymer matrix.

Bello et al [50] evaluated the tribological properties of polyamide (PA11) coatings. D. Bellisario et al [51] evaluated the impact of the mixing time on the tribological properties of the functionalized montmorillonite (MMT) filled polyester coatings. Optimized results were achieved with low filler contents and mixing times. Kowalczyk et al [8] evaluated the performance of epoxy coatings by adding 2.5% and 5% (by weight) modified MMT. They observed the improvement in hardness, abrasion and scratch strength by addition of this filler. Davood et al. [52] prepared organo-clay filled epoxy coatings by utilizing high-shear mixing and ultrasonication for good dispersion. They used organo-clay content as filler (up to 4 wt%) and found optimized results for 3 wt% filled coatings. Gadow and Scherer [53] improved the tribological behavior of light metal magnesium by producing composite polymer coating (PTFE particles as solid lubricants+ MoS<sub>2</sub> + pure C) in on it using thermal spray process. Recently Subasri et al [54] prepared super hydrophobic coatings by adding nanoclay into silica matrix (hydrophobic) by using sol-gel process. The clay provided super hydrophobicity by offering low surface energy.

Wang ZZ et al. [55] compared the tribological and mechanical performances of pristine polycarbonate film with polycarbonate composite coating reinforced with nano-SiO<sub>2</sub>. Scratch tests and micro/nano-scale indentation showed increase in stiffness and hardness

after reinforcing the matrix with nano-SiO<sub>2</sub>. Moreover, scratch depth and COF in case of composite coating was decreased.

Song HJ et al. [56] enhanced the tribological properties of polyurethane (PU) coatings by adding ZnO whiskers and ZnO nanoparticles into the PU-matrix. They observed adherent transfer film formed at counterface in both cases due to addition of these fillers which reduced the COF and wear rate.

Wang Y et al. [57] found the effect of nanostructured tungsten carbide (WC) particles on tribological and corrosion behaviors of Xylan based nanocomposite coatings. Xylan is commercial name of polymer which has specific composition. They found that scratch resistance and hardness were increased as compared to that of pristine polymer coating with the addition of these nanoparticles due to the dispersion hardening of polymer coatings by these particles. Corrosion resistance of polymer nanocomposite coating was also increased relatively as compared to that of pristine polymer coating.

Wang Y et al. [58] evaluated the tribological behaviors and electrochemical corrosion properties of Al<sub>2</sub>O<sub>3</sub>-polymer nanocomposite coatings. They found improvement in scratch resistance as well as corrosion resistance due to addition of Al<sub>2</sub>O<sub>3</sub> nanoparticles. The improvement in the properties was attributed to the dispersion hardening of polymer coatings by these nanoparticles.

## **2.5 Ultra-high Molecular Weight Polyethylene (UHMWPE)**

UHMWPE is a linear homo-polymer which is made up of hydrogen and carbon. It is thermoplastic polymer and is a type of polyolefin. Polymerization of ethylene (C<sub>2</sub>H<sub>4</sub>) gives

polyethylene having formula  $(C_2H_4)_n$ , where “n” represents degree of polymerization. Figure 2.7 below shows the chemical structures for polyethylene and ethylene. One molecular chain of UHMWPE can have about 200,000 ethylene repeated units and the molecular mass in range of 2-6 million u.

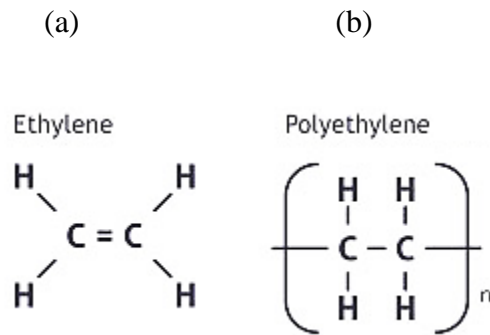


Figure 2.7 Chemical structures (a) monomer (b) polymer

### 2.5.1 Properties of UHMWPE

UHMWPE has such great combination of properties such as very low COF which is ~0.1, highly resistant to abrasion, self-lubricating, high impact resistance and durability which made it outstanding to use it for coating purposes in tribological applications. Table 2.1 below shows some mechanical properties of UHMWPE (in bulk form). Melting point of UHMWPE is in range of 138 – 142 °C but it can retain its excellent dimensional stability at temperatures up to 80-90 °C [3].

Harvey and Sinha [3, 59] compared the wear rate and impact resistance of different polymers as shown in Figure 2.8 and Figure 2.9 below. From these figures, it is found that UHMWPE has excellent wear resistance and impact resistance as compared to other polymers. UHMWPE, in coatings as well as bulk form, has a lot of applications in various

fields where good tribological properties are required such as in bearings gears, impellers, pump housings, biomedical transplants.

Table 2.1 Mechanical Properties of UHMWPE [60]

Mechanical property	Value
Elastic Modulus	0.69 GPa
Poisson's Ratio	0.46
Yield Strength	21.4-27.6 MPa
Tensile Strength	38.6-43.8 MPa
Coefficient of Thermal Expansion	234-360 $10^{-6}/^{\circ}\text{C}$

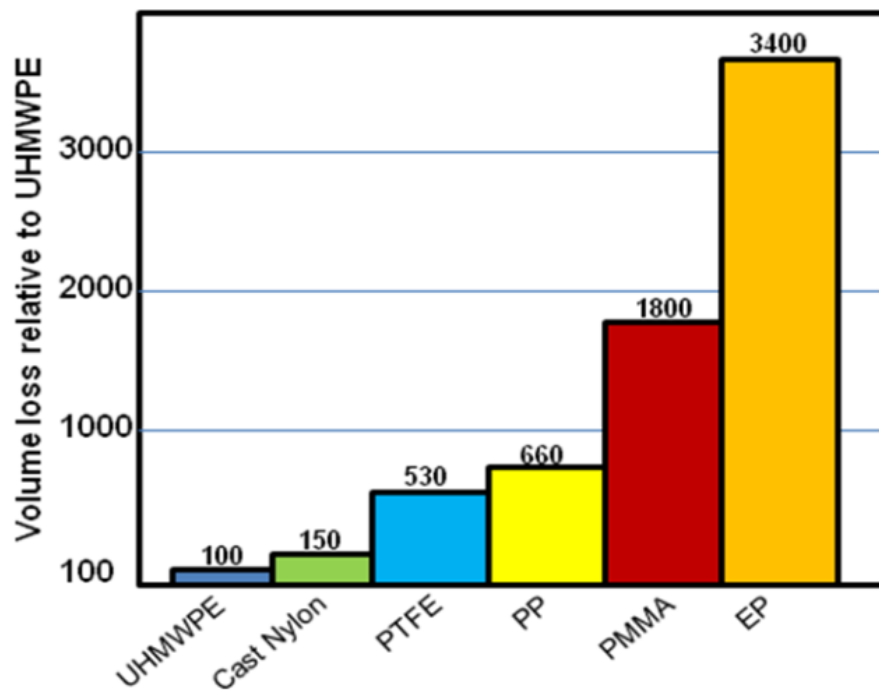


Figure 2.8 Comparison of wear rate of different polymers [3]

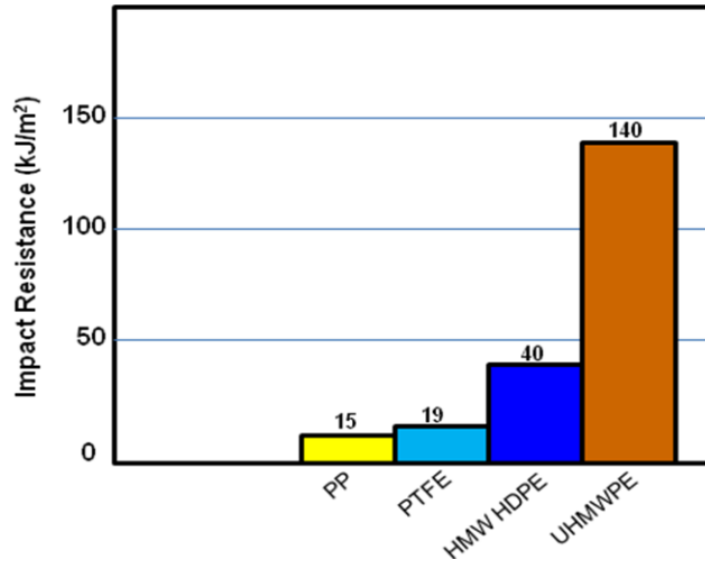


Figure 2.9 Comparison of Impact resistance of different polymers [3]

### 2.5.2 Limitations of UHMWPE

Although UHMWPE has excellent tribological properties as mentioned above but it has some restrictions such as low load bearing capacity, low Young's modulus, its poor adhesion to the substrates [3] and poor processability due to its high viscosity which demands improvements in its properties. Many researchers used different approaches to enhance the adherence of UHMWPE coatings as well as mechanical and tribological properties.

### 2.5.3 UHMWPE coatings

Due to excellent tribological properties of UHMWPE many researcher used it for coatings on different substrates. UHMWPE thin films on bare silicone as well as on modified silicone surfaces have proved UHMWPE a good thin coating material due to its high wear resistance as well as low COF against ceramics and metals [61, 62]. UHMWPE coating has been deposited onto steel and aluminum substrates through dip-coating process to increase their wear life [63, 64].

To modify adhesion between UHMWPE coating and substrate some surface pre-treatments such as chemical treatments (e.g. piranha treatment) or plasma treatment can be applied. It is found in literature that UHMWPE film deposited onto plasma pre-treated Silicone exhibited a wear life of~50000 cycles (twenty five times more) as compared to that of 2000 cycles when it was deposited onto piranha pre-treated Silicone, operated at a rotational speed of 200 rpm & normal load of 1 N [65].

Researchers have improved the load bearing capacity along with tribological properties by using intermediate layer between UHMWPE and substrate. Minn et al. [62] used this idea and enhanced the wear life (5 times) by depositing intermediate DLC coating (50 nm) between Si substrate and UHMWPE coating as compared to coating without intermediate DLC layer. Recently, Samad and Irfan [66] studied the surface modification of Polyether Ether Ketone (PEEK) by depositing thin coating of UHMWPE ( $27 \pm 2 \mu\text{m}$  thickness) by using dip coating process. They found that at load of 7 N with linear speed of 0.1 m/s, this UHMWPE coating was not failed up to 250,000 cycles. COF was reduced from~0.3 to~0.09 and wear life of PEEK was also increased due to this effective modification.

#### **2.5.4 UHMWPE nanocomposites coatings**

One of the ways to define nanomaterials is that materials having a characteristic length scale less than about a hundred nanometers are called nanomaterials. Nanomaterials have different mechanical, electrical, magnetic, thermal, and chemical properties than those of the bulk due to have more surface area (more grain boundaries) and hence having high surface energy. The improvement of these properties depends on well dispersion of these added fillers. One most important development to improve tribological properties of these

polymers is to make nanocomposite coatings by adding nanofillers such as carbon nanotubes (CNTs), graphene, etc.

Samad et al [5] successfully improved the tribological, thermal and mechanical properties of the UHMWPE film by adding CNTs in UHMWPE matrix. Recently Z. X. Tai [67] added 1% graphene oxide nanosheets by weight into UHMWPE which improved micro-hardness as well as wear resistance of UHMWPE coating. Samad and Irfan [68] modified the surface of Polyether Ether Ketone (PEEK) by depositing thin nanocomposite coating of UHMWPE reinforced with different concentrations of CNTs by using dip coating process. Among different wt. % of CNTs, optimum result were obtained at 0.2 wt% of CNTs in 3 wt% UHMWPE matrix. They found that at normal load of 9 N and linear speed of 0.5 m/s, this UHMWPE nanocomposite coating was not failed up to 250,000 cycles. Due to this effective modification, COF was reduced from ~0.3 to ~0.09 and wear life of PEEK was also increased. It is also to be noted that load bearing capacity in case of nanocomposite coatings was increased to 9N which was 7N in their previous study [66] where they modified the PEEK surface with pristine UHMWPE coating.

### **2.5.5 Tribology of UHMWPE under lubricated conditions**

It is well established that tribological behavior of materials is different in different environments. Many researchers evaluated the tribological behavior of UHMWPE composites and coatings under lubricated conditions because of different applications.

Kahyaoglu et al [69] compared the wear rate of UHMWPE (bulk form) at different loads against AISI 304L stainless steel surface under distilled water, salt solution and various

protein lubrication environments. Wear rate was more in distilled water lubrication condition at all loads.

Yingfei et al [70] improved the tribological properties of UHMWPE bulk by adding graphene oxide (varying from 0-1 wt %) in matrix and tested them under deionized water and normal saline solution lubricated conditions. Figure 2.10 below compares the variation of wear rate by adding different concentrations of GO in GO-UHMWPE nanocomposites under lubricated conditions (deionized water and normal saline solution). Xiong Dangsheng [71] reinforced UHMWPE with carbon fiber and investigated the tribological behavior of this reinforced bulk composite under dry as well as distilled water lubrication conditions.

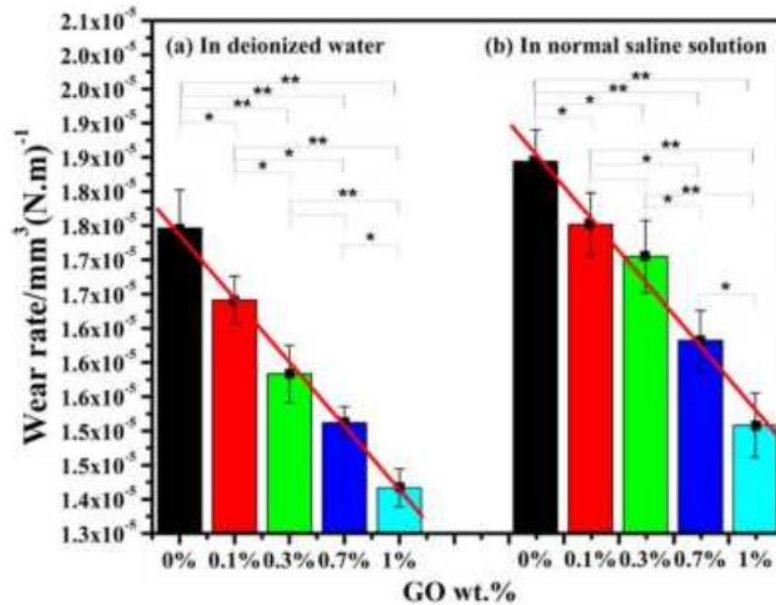


**Figure 2.10 Comparison of wear rates by adding different concentrations of GO in GO-UHMWPE nanocomposites under lubricated conditions (a) deionized water (b) normal saline solution [70]**

Dangsheng Xiong et al [72] evaluated the effect of different lubricated conditions on tribological properties of bulk UHMWPE. In their experiments, pin-on-disk configuration



was used for tribological testing in which pin was made of UHMWPE (flat circular cylinder) and disk was made of  $\text{Al}_2\text{O}_3$ . They evaluated the COF and wear rate of UHMWPE in dry condition as well as under lubrication of distilled water, fresh plasma and saline solution. The tribological testing parameters were  $20 \text{ mm s}^{-1}$  sliding speed and 10 km sliding distance. Figure 2.11 and Figure 2.12 below show the results of COF and wear rate with reference to sliding distance. The variation in results is depended on condition of water absorption by UHMWPE because due to water absorption shear strength of polymer is reduced due to swelling of polymer. The best results regarding wear rate were achieved by plasma lubricated conditions because plasma produced crosslinking of polymer hence reduce the water uptake by polymer. But COF was slightly increased in this case.

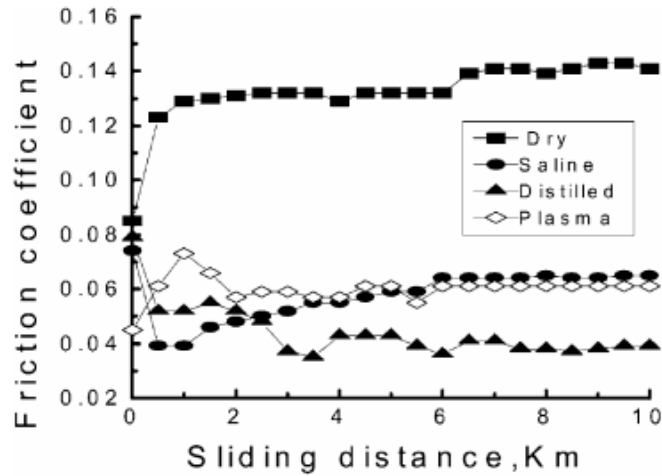


Figure 2.11 Variation in COF of UHMWPE under different conditions [72]

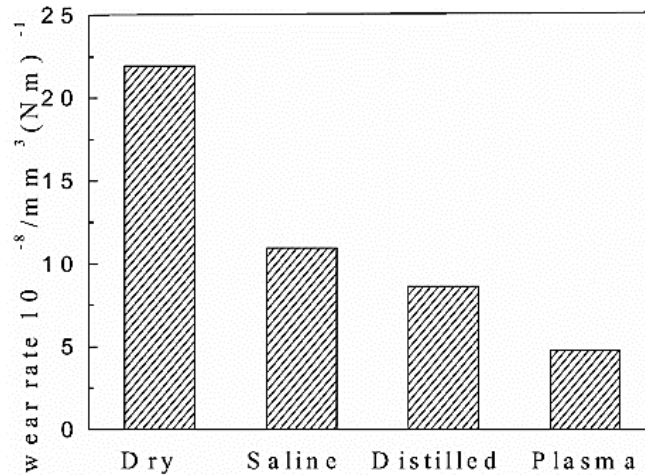


Figure 2.12 Variation in wear rate of UHMWPE under different conditions [72]

A Golchin et al [73] evaluated the tribological behavior of eleven different polymers (in bulk form) under water lubrication by using pin on disk configuration. They found that among all of the polymers UHMWPE showed optimum results in terms of wear resistance, water contact angle and coefficient of friction. These results can be seen in, Figure 2.13 and Figure 2.14 below.

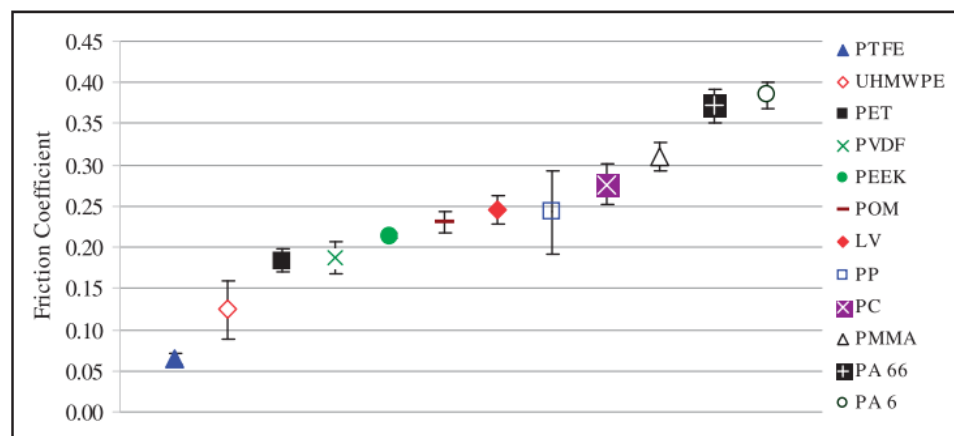


Figure 2.13 Average coefficient of friction results over the test period of 20 h [73]

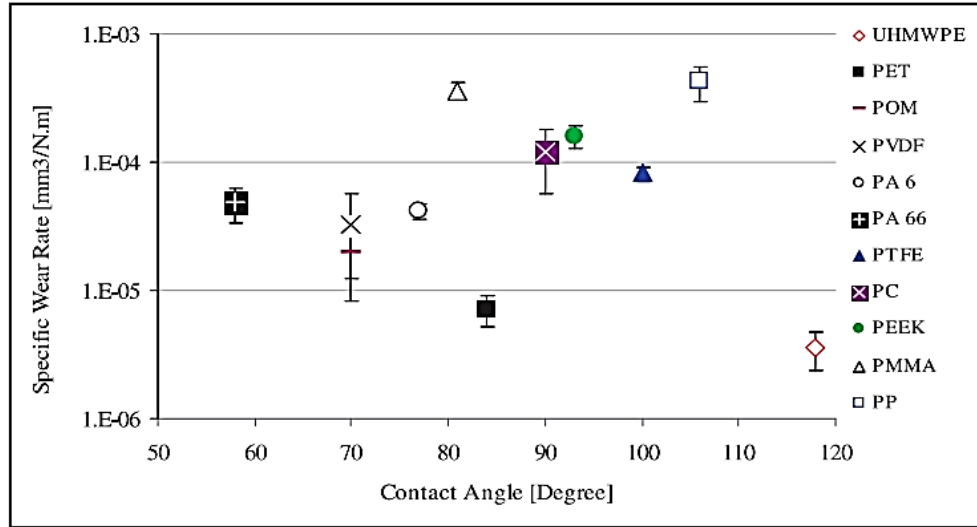


Figure 2.14 Specific wear rate of versus water contact angle [73]

Recently, Samad at el [74] investigated the effect of water uptake on the tribological properties of C15A/UHMWPE nanocomposites (bulk) by varying the concentration of nanoclay. They used ball-on-disk configuration for wear testing of specimens before and after the water uptake at 30 N load with 300 rpm for 5000 cycles. Following figures below compare the results of wear rate and average COF of pristine UHMWPE with UHMWPE nanocomposite having different C15A clay loadings. From Figure 2.15 and Figure 2.16 below it can be noticed that the specific wear rates and average COF of all types of UHMWPE composites are lower than that of pristine UHMWPE before water uptake.

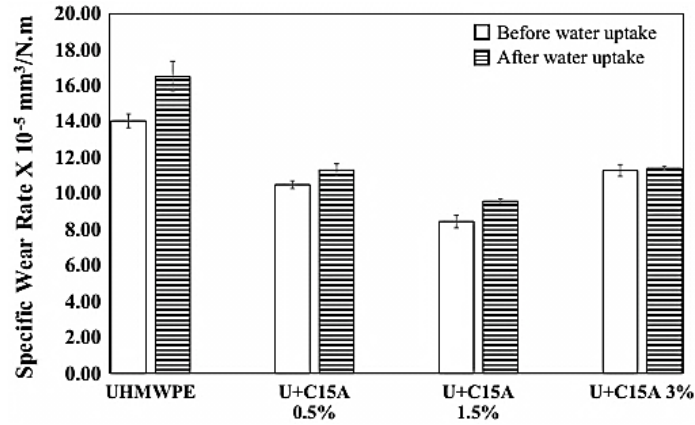


Figure 2.15 Comparison of specific wear rate for pristine UHMWPE and UHMWPE nanocomposites with varying clay contents before and after water absorption [74]

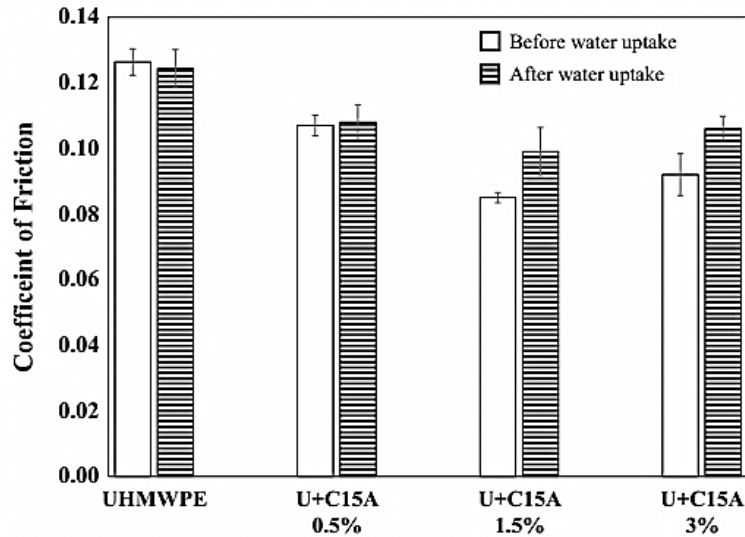


Figure 2.16 Comparison of average COF for pristine UHMWPE and UHMWPE nanocomposites with varying clay contents before and after water absorption [74]

Regarding investigation of UHMWPE coatings under lubricated conditions very limited published work is available. M. A. Samad and S K. Sinha [75] evaluated the CNT-UHMWPE nanocomposites coating on Aluminum substrate under oil lubricated condition.

## 2.6 Nanoclay (NC)

The montmorillonite clays belong to phyllosilicate family (2:1 layered silicates) and they are inorganic materials which occur naturally. The crystal structure of nanoclay consists of two-dimensional layers in which one layer of octahedral ( $\text{AlO}_6$ ) is sandwiched between two layers of tetrahedral ( $\text{SiO}_4$ ). Chemical structure of montmorillonite is  $\text{M}_x (\text{Al}_{4-x}\text{Mg}_x) \text{Si}_8 \text{O}_{20} (\text{OH})_4$  [76]. The thickness of these layers is  $\sim 1$  nm and the dimensions of other sides vary from 30 nm to some microns which depend on the clay's source and its synthesis technique. and have high aspect ratio ( $> 1000$ ) [77–79]. The gap ( $\sim 1$  nm) between silicates interlayers is called “interlayer” or “gallery”. Cations of rare earth metal such as sodium, magnesium and calcium can entrap in these galleries. On the basis of degree of dispersion of these clay platelets in the polymer matrix, different structures can be formed which are intercalated, phase separated and exfoliated as seen in Figure 2.17 below. Clay particles on basis of their composition are hydrophilic and can be converted into organophilic by ion- exchange method in which inorganic cations in gallery are being exchanged with organic cationic molecules so that interaction of clay particles with organic substances becomes easy.

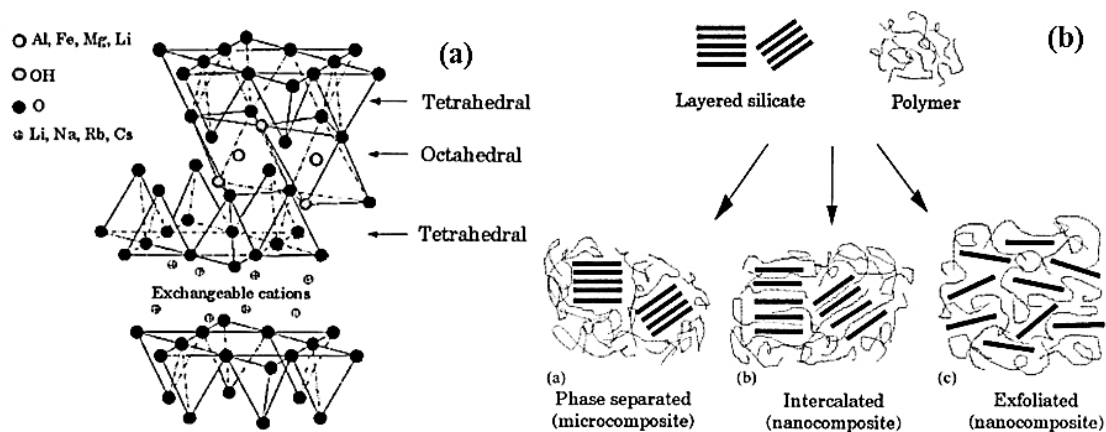


Figure 2.17 (a) Structure of 2:1 phyllosilicates (b) Different structures based on mixing of polymer chains with layered silicates [76, 80]

In recent years, a lot of development in polymer layered silicates nanocomposites has been carried out due to outstanding properties offered by these nanocomposites as compared to pristine polymers. These properties include increased heat resistance and strength [81], high moduli [82], reduction in gas permeability and flammability [83, 84]

Kaloshkin et al. [85] evaluated the tribological and mechanical properties of clay-UHMWPE nanocomposite in which clay was used as reinforcement. Their study showed that modulus of elasticity was increased by increasing clay contents (0 to 30 wt. %) while ductility was decreased. And by increasing clay contents, wear rate was decreased from  $120 \times 10^{-6} \text{ mm}^3/\text{Nm}$  to  $70 \times 10^{-6} \text{ mm}^3/\text{Nm}$ .

Recently, Samad et al. [86] evaluated the tribological behavior of UHMWPE nanocomposites reinforced with different concentrations of C15A organoclay varied from 0.5 wt% to 3 wt%. By adding nanoclay in UHMWPE, they found that the COF and wear rate were decreased. Especially 1.5 wt% of clay in UHMWPE matrix exhibited best results

because of well dispersion of clay platelets in the matrix and adherent transfer film formed on the counterface ball.

Although different researchers have used nanoclay as filler in other different composites and coatings but nobody has used nanoclay as nanofiller in UHMWPE coating up till now.

## 2.7 Carbon nanotubes (CNTs)

They are allotropes of carbon and have cylindrical structures with diameter of few nanometers and length of several millimeters. They are light, flexible, thermally stable, and are chemically inert [87]. They can be multi-walled carbon nanotubes (MWNTs) or single walled carbon nanotubes (SWNTs) multi walled carbon nanotubes (MWNTs) as shown in Figure 2.18 below. MWNTs contain multiple rolled tubes (concentric layers) of graphene.

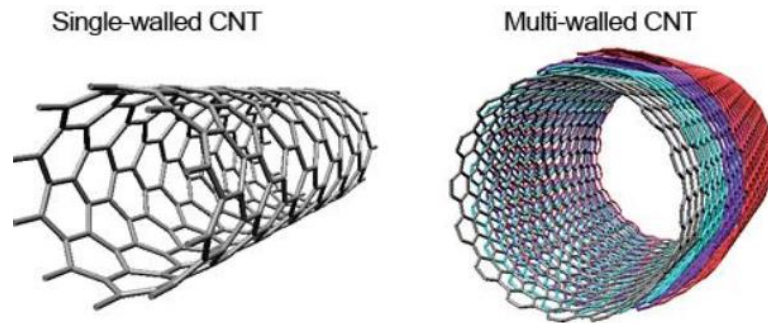


**Figure 2.18 Structures of SWNT and MWNT**

They have high tensile strength (11~63 GPa), extraordinary thermal conductivity (1750-5800 W/mK), large aspect ratio (>1000), high electrical conductivity and low thermal expansion coefficient [4]. Such a combination of these properties makes them pioneer. The Table 2.2 below compares some mechanical properties of CNTs with other materials. CNTs can be used in different applications in different ways as shown in Figure 2.19 below.

Table 2.2 Comparison of some mechanical properties of CNTs with various materials [4]

Material	Young's modulus (GPa)	Tensile Strength (GPa)	Density (g/cm <sup>3</sup> )
Single wall nanotube	1054	150	
Multi wall nanotube	1200	150	2.6
Steel	208	0.4	7.8
Epoxy	3.5	0.005	1.25
Wood	16	0.008	0.6

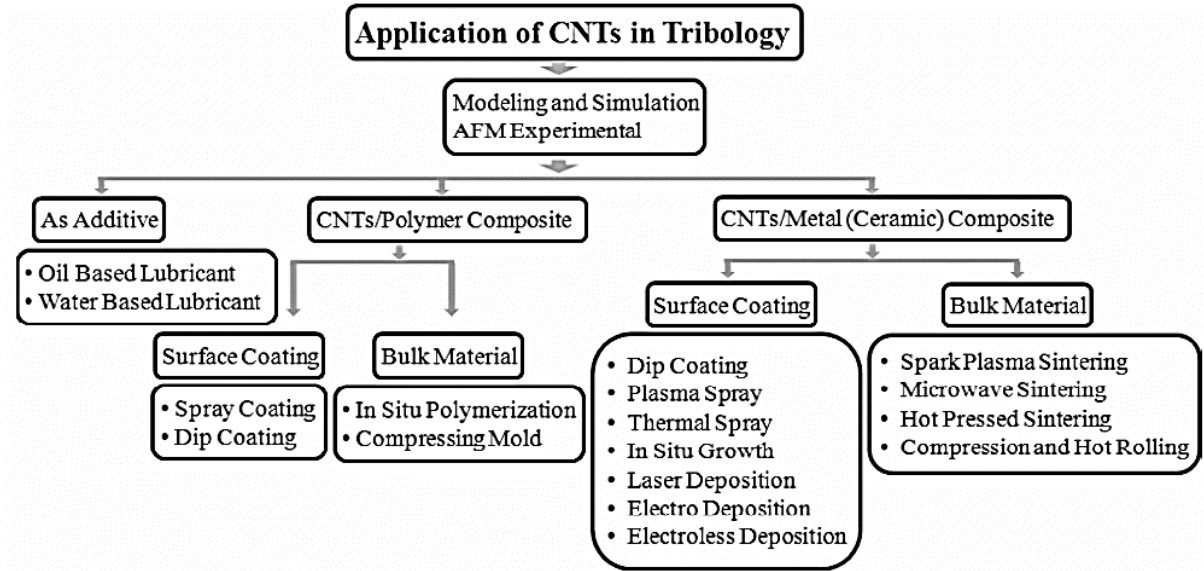


Figure 2.19 Application of CNTs in tribology [88]

Many researchers used CNTs as nanofiller due to its extraordinary properties in the UHMWPE matrix in the form of bulk as well as coating. Xue et al. [89] studied the effect of addition of MWCNTs (functionalized with nitric acid) on creep and wear resistance of UHMWPE/HDPE composite. They proved that by adding MWCNTs from 0.2 to 2 wt% wear resistance of nanocomposite increased. By adding 0.5 wt% MWCNTs to the UHMWPE/HDPE mixture, wear rate was reduced approximately 50%.

Zoo et al. [90] found the effect of CNT addition on the tribological properties of UHMWPE. They found that (Figure 2.20 below) with the addition of CNT from 0 to 0.5 wt%, wear loss reduced from 0.35 to 0.025 mg. One more thing they observed



by adding 0.5 wt% of CNTs was that COF was increased from 0.07 to 0.12 due to extraordinary mechanical properties of CNTs (Figure 2.21 below). The increase or decrease of COF is a complex behavior because it is also found in literature that by adding 5% CNTs in High density Polyethylene (HDPE), COF was decreased up to 12 % [91]. Because it is possible that during plastic deformation, CNTs are detached from composite's surface and these detached debris can behave as solid lubricant particles. But wear rate always decrease by adding CNTs.

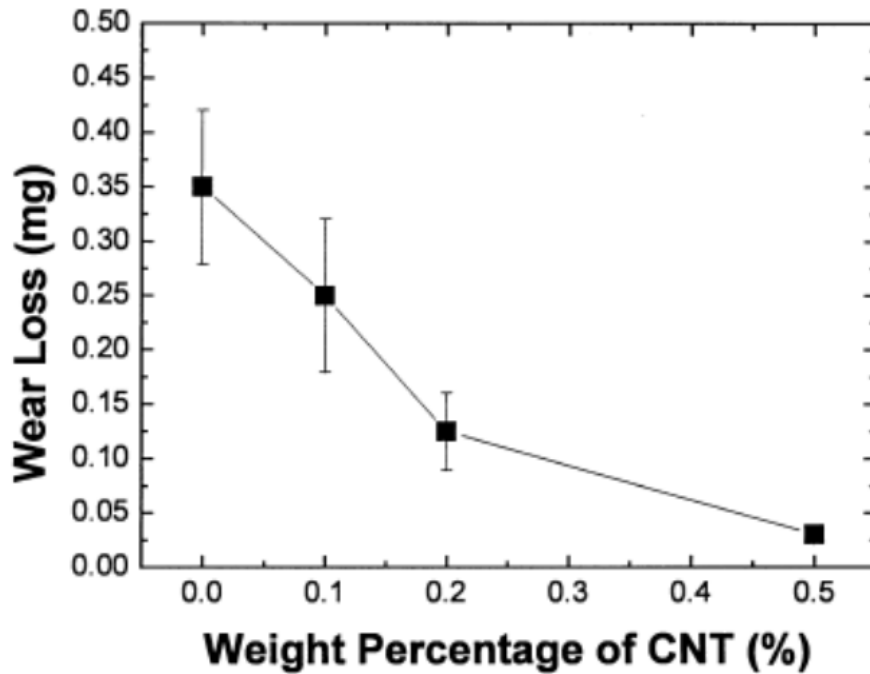


Figure 2.20 Weight loss with respect to CNT contents after wear test [91]

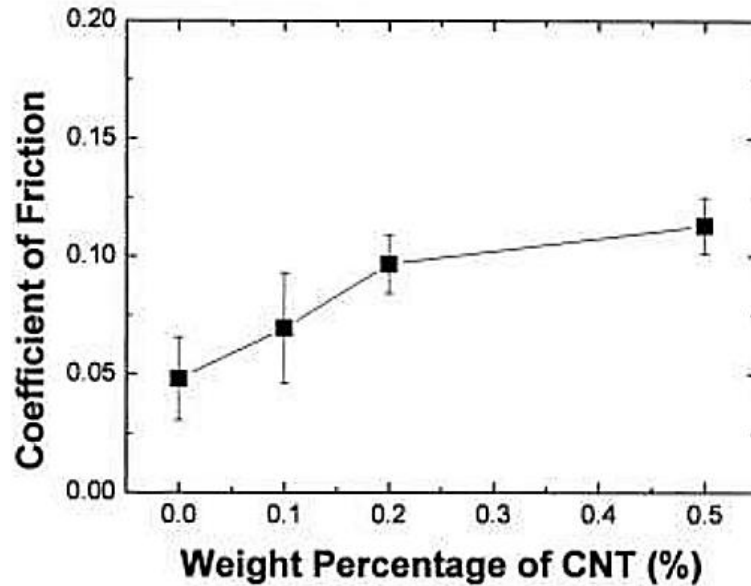


Figure 2.21 COF with respect to CNT contents after wear test [91]

S.R. Bakshi et al [6] deposited 5% MWNT- UHMWPE nanocomposites coating on a steel substrate by using electrostatic spraying process. By making this nanocomposite coating, they enhanced the wear resistance of coating as compared to pristine UHMWPE with slightly increase in COF due to CNTs addition which has high shear strength.

To get benefits from the outstanding properties of CNTs, it is necessary that these reinforcements should be well dispersed in matrix and have good interfacial bonding with matrix. Otherwise due to agglomeration of these fillers, the required properties will be deteriorated. In his studies, Bal et al. [92] found that due to poor dispersion of CNTs tensile strength, electrical conductivity and thermal conductivity of matrix polymer were deteriorated. The graphs in Figure 2.22 below show trend of these above mentioned properties by addition of CNTs in polymer matrix and also show the comparison between the well dispersed and poorly dispersed CNTs. For well dispersion of CNTs various

methods such as ball mill or sonication are used. For good interfacial bonding of CNTs with matrix, functionalization of CNTs by different means has been done.

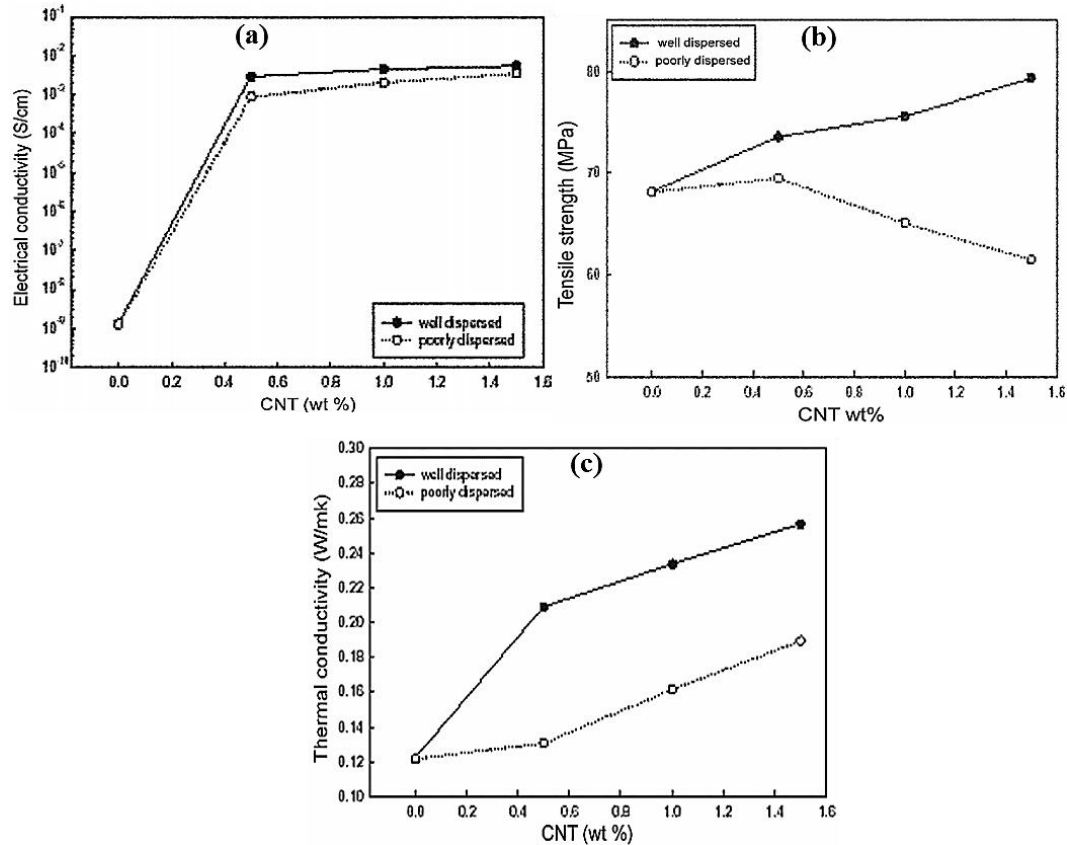


Figure 2.22 Variation of (a) Electrical conductivity (b) Tensile strength (c) Thermal conductivity with addition of CNTs and effect of dispersion [92]

## 2.8 Hybrid nanocomposite coatings

Since from the past few years, a lot of interest has been generated by a new approach namely, development of hybrid nanocomposites in the bulk form or coatings. A hybrid nanocomposite or a hybrid nanocomposite coating is a new emerging approach of reinforcing any parent matrix with two or more nanofillers to mainly take advantage of the individual properties of each of the nanofiller into one product.

Hence efforts are being made to develop polymer based hybrid nanocomposite coatings and films to obtain synergic benefits in various fields such as in thermal, optical, anti-corrosion and electronic applications. In the field of tribology, various researchers developed bulk hybrid nanocomposites for better tribological properties [93, 94]. However, no effort was made to develop a hybrid nanocomposite coating by adding “two different nanofillers” for the improvement in the tribological properties so that these coatings can be used in different environments.

## **2.9 Summary**

In view of the extensive literature review presented above it can be noted that there is still a lot of scope to further improve the properties of these polymer nanocomposites and their coatings so that they can be used in varying environments. Hence, there is an urgent need to further enhance the properties of these coatings so that they will be able to function and protect the sliding components against wear and tear, irrespective of the environment they are exposed to.

Thus we were motivated to explore a novel approach of developing a hybrid nanocomposite coating to solve this problem. For this purpose, it is very essential that the developed hybrid nanocomposite coating should have a low COF, high wear resistance, high load bearing capacity and high resistance to water absorption.

As can be seen from the literature, UHMWPE is one of the most suitable polymer among all other polymers which can be used for coating purposes in tribological applications because of its unique properties such as low COF, high abrasion resistance, self-lubricity, high durability and high impact resistance. However, it has some limitations such as low

thermal properties, load bearing capacity and low Young's modulus. To overcome these limitations two nanofillers CNTs and nanoclays are used individually due to their unique properties as discussed above.

Hence in view of the above justification, we defined the main objective of our study to be as follows: *To develop and characterize the tribological performance of a novel hybrid nanocomposite coating of UHMWPE reinforced with carbon nanotubes (CNTs) and nanoclay (C15A) under dry and water lubricated (with/without abrasives) conditions for mechanical bearing applications.* CNTs shall be added to improve the load bearing capacity of the coating and nanoclay will be added to improve the resistance to water absorption along with mechanical properties.

## CHAPTER 3

### Experimental Work

The details of the materials, experimental procedure for the development of nanocomposite coatings and the characterization techniques used for evaluation of these coatings will be described in this chapter.

#### 3.1 Materials

##### 3.1.1 UHMWPE powder

UHMWPE powder was provided by Good Fellow Corp (Cambridge, UK) with following specifications; average particle size = 80 to 90  $\mu\text{m}$  and density = 0.94  $\text{g}/\text{cm}^3$ . Figure 3.1 is the SEM image of UHMWPE powder.

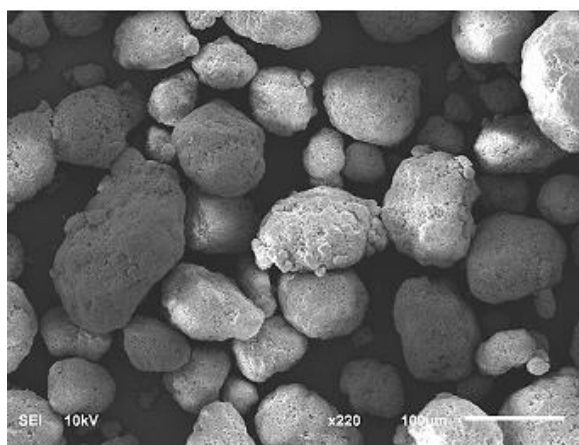


Figure 3.1 SEM image of UHMWPE powder

### 3.1.2 Nano Clay

Organically modified Montmorillonite, Cloisite (C15A) clay modified with quaternary dimethyl dihydrogenated ammonium was used which was provided by Southern Clay Product, USA. Its specific gravity was in the range of 1.7- 1.9. Figure 3.2 is the SEM image of nanoclay sheets in the form of clusters. The composition of nanoclay was as follow; C = 39.3 wt%, O = 38.5 wt%, Mg = 0.6 wt%, Al = 5.6 wt%, Si = 14.2 wt% and Fe = 1.9 wt%.

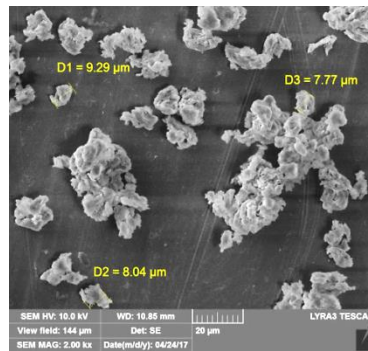


Figure 3.2 SEM image of C15A nanoclay

### 3.1.3 Carbon Nanotubes

Functionalized multi-walled carbon nanotubes (MWCNTs) were provided by Chemical laboratory, KFUPM having an average diameter of  $23 \pm 3$  nm. Figure 3.3 is the SEM image of CNTs.

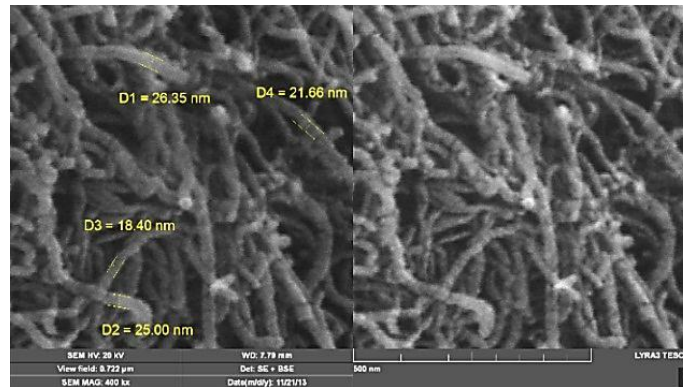


Figure 3.3 SEM image of CNTs

### 3.1.4 Silicon carbide (SiC) abrasives

Hard SiC particles with particle size of  $6\ \mu\text{m} \pm 0.2$  were used as an abrasive media during sliding tests with abrasives. Figure 3.4 is the SEM image of SiC abrasives.

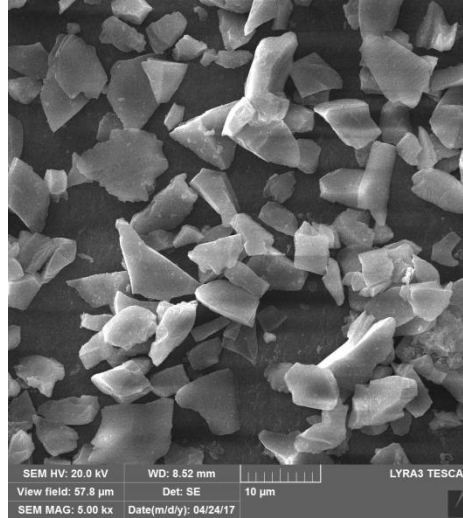


Figure 3.4 SEM image of SiC abrasives

## 3.2 Preparation of nanocomposite powders for coating

Figure 3.5 below shows the nanocomposite powder preparation setup. Nanocomposite powders were prepared by using sonication method coupled with magnetic stirring. Weighted amount of required filler(s) was sonicated for 10 min by using probe sonicator in ethanol solvent (50 ml) with an on/off time cycle of 20/5 s and an amplitude of 30% to disperse them uniformly. The sonication time was selected to be 10 minutes because in studies it was found that beyond 12 minutes, the shortening of nanotubes took place which deteriorated their properties [95]. The mixture of filler (s) and ethanol was stirred at 1000 rpm for 2 min using magnetic stirrers to further disperse the fillers uniformly. Then weighted amount of UHMWPE powder was added slowly in this mixture and this



nanocomposite mixture was left for magnetic stirring for 1 h. Finally, this nanocomposite powder was placed in a furnace to evaporate ethanol at 80 °C for 24 h.

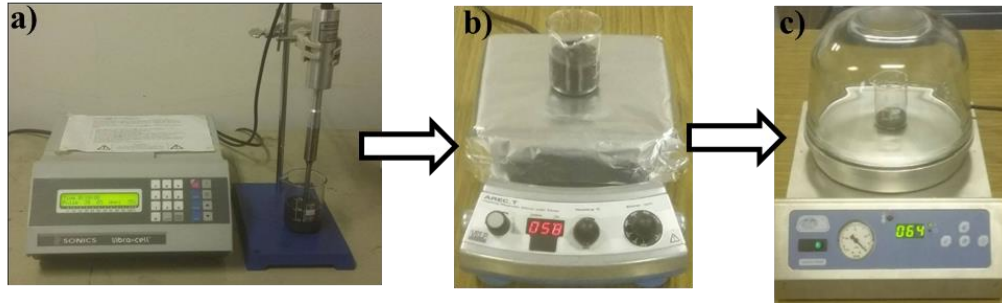


**Figure 3.5 Nanocomposite powder preparation setup (a) Probe sonication of filler material (b) Mixing of filler and polymer matrix by magnetic stirring (c) Drying of nanocomposite powder**

### **3.3 Substrate preparation before coating**

#### **3.3.1 Grinding**

Aluminum alloy (Fe = 0.15%, Si = 0.17%, Mn = 0.5%, Mg = 0.6%, Cr = 0.1%, Ni = 0.3 and the rest = Al) was used as substrate with samples size of 25 x 25 x 6 mm. Aluminum is selected as a substrate because of its light weight and high strength to weight ratio due to which it is replacing other metals in most of the tribological applications. Before coating, the substrate was grinded properly by using two different grit size papers (120 and 240) to obtain a final roughness of  $0.4 \pm 0.05 \mu\text{m}$ .



**Figure 3.6 Grinding machine**

### **3.3.2 Ultrasonic cleaning and drying**

After grinding, samples were cleaned with acetone by using ultrasonic cleaning method for 15 minutes. Benefit of ultrasonic cleaning is that sound waves hit the sample and remove the attached debris particle which is necessary prior to coating. After cleaning, samples were dried using an air blower. Figure 3.7 below is the ultrasonic bath cleaner used for cleaning purpose.



**Figure 3.7 Ultrasonic cleaner.**

### 3.3.3 Plasma treatment

To obtain a good bonding between the coating and the substrate, it is essential that the surface of the substrate is free of any impurities such as hydrocarbons and should have a higher surface free energy. Plasma treatment is one such process that helps in cleaning the surface (carbon cleaning effect) and functionalizing the surface by creating carboxyl dangling bonds (oxidation effect) which helps in improving the adhesion between the coating and the substrate [63]. There are other chemical treatments such as Piranha treatment [63] to increase surface energy but they are toxic due to Hazardous chemicals (e.g.  $\text{H}_2\text{O}_2$ ,  $\text{H}_2\text{SO}_4$ ). But plasma treatment is most favorable due to some advantages such as environmental friendly, cost effective, easily adaptable to industrial applications, no hazardous chemicals used, and less time consuming.

After drying the samples, the plasma treatment was performed on samples using Harrick Plasma equipment (Figure 3.8) for 10 min using a radio-frequency power of 30 W.

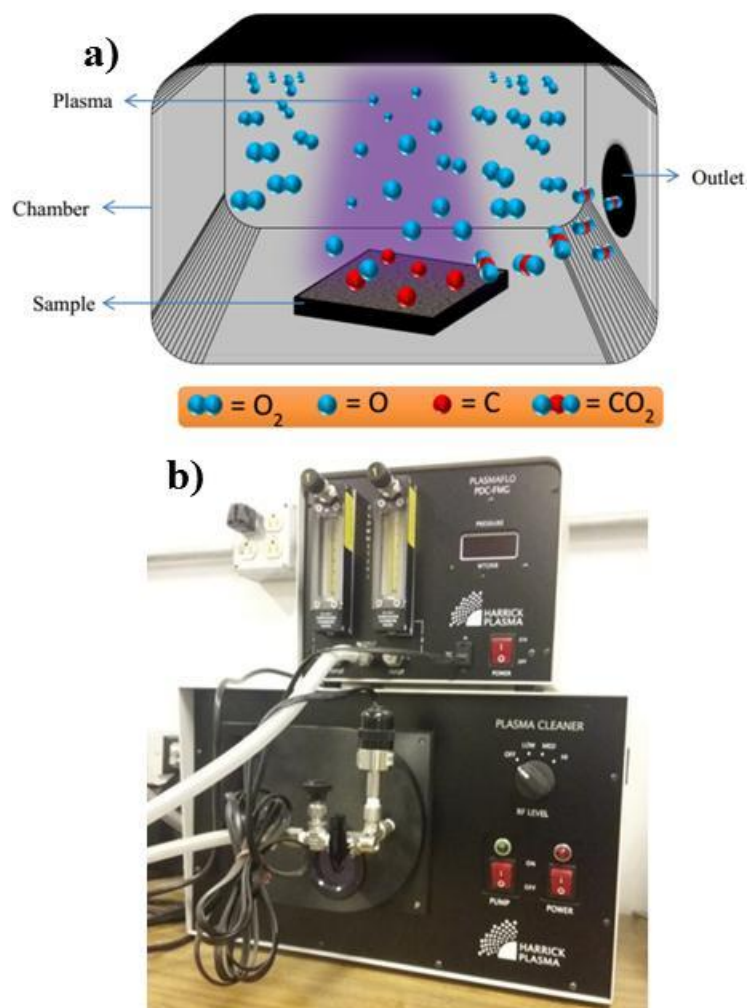


Figure 3.8 (a) Schematic diagram of plasma treatment showing the carbon cleaning effect and the oxidation effect (b) Harrick plasma equipment

### 3.4 Coating procedure

Electrostatic spray gun (Model no 17288, Craftsman<sup>®</sup>) was used for depositing the powders on the substrate. The benefits of using the electrostatic powder spray coating method over other conventional methods are as follows; it is quick, easy, has no requirement of different solvents for specific polymer, environment friendly, energy

efficient and results in less wastage of materials. The basic principle of electrostatic spray gun is that negatively charged powder particles are deposited on positively charged sample.

Cleaned and plasma treated substrates were preheated for 5 min at 180 °C and then the powder of required composition was sprayed on the preheated substrates to get a uniform coating of the powder. The powder coated samples were heated on the heating plate at 180° C for 30-35 min and then air cooled for uniform consolidation of the polymer powder.



Figure 3.9 Electrostatic spray gun

### 3.5 Characterization techniques

#### 3.5.1 X-ray diffraction (XRD)

XRD technique was conducted for analysis of the prepared nanocomposite powders by using X-ray machine (Bruker D8, USA). X-ray source was Cu K $\alpha$  radiation having a wavelength of 1.5407 Å. The powdered samples were analyzed from 2° to 70° with a step

size of  $0.02^\circ$ . The intergallery distance (d-spacing) was measured by using Bragg's equation ( $2d\sin\theta=n\lambda$ ) after analyzing characteristic peak of clay at certain angle.

### **3.5.2 Raman spectroscopy**

Raman spectroscopy was performed on CNT-nanocomposite and hybrid nanocomposite powders to analyze the interfacial interaction of CNTs within UHMWPE matrix by using Raman Microscope (DXR<sup>TM</sup>, Thermo Scientific<sup>®</sup>, USA). Following details were used for the analysis; Laser power = 1–2 (mW), Laser wavelength = 455 nm, aperture = 50 mm and spot size = 0.6 mm. On each of the sample, three spectrums were obtained at different locations and typical images are presented

### **3.5.3 Dispersion analysis**

Field emission scanning electron microscope (FE-SEM) assembled with Schottky field emission gun (TESCAN<sup>®</sup>, Czech Republic) was used to analyze the typical dispersion of nanofillers in UHMWPE matrix. The analysis was carried out with the help of a secondary electron detector at a voltage of 20 kV at various locations and typical images are presented. Thin gold coating was deposited on each sample, prior to analysis, to make it conductive.

### **3.5.4 Thickness measurements**

FE-SEM was used to measure coating thicknesses by analyzing cross sectional area of coated samples with the help of FE-SEM. The analysis was carried out with the help of a secondary electron detector and at a voltage of 20 kV. Thin gold coating was deposited on each sample, prior to analysis, to make it conductive. Three readings for each set of samples were taken and average value of coating thickness was reported.

### **3.5.5 Hardness measurements**

Micro indentation equipment provided by CSM instruments® was used to measure hardness. A normal load of 0.2 N was applied for 10 s with a constant loading and unloading rate of 0.4 N/min with the help of a pyramidal shaped diamond indenter. Ten readings on each sample at various locations were recorded and average value is reported. To avoid the substrate effect, it was made sure that penetration depth was less than 10% [96] of the coating thickness (directly calculated by machine) during indentation. Based on this observation, a normal load of 0.2 N was selected after optimization during hardness measurements on all the coatings.

### **3.5.6 Tribological testing**

Ball-on-disk configuration was used to conduct friction and wear tests on coated samples by using a tribometer (UMT-3, USA) under dry and water lubrication. Stainless steel ball of Grade 440C ( $\phi = 6.3\text{mm}$ , hardness = 62 RC) was used as a counterface at room temperature with a relative humidity of  $55 \pm 6\%$ . The counterface ball was cleaned well with acetone before every test. For wear tests under water lubrication, 45 ml of deionized water (DI water) was used. For abrasive testing, 1 g of SiC was added in 45 ml of DI water. Due to the long duration of the tests the lubricant container was refilled with DI water after every 4 hours to maintain the water level constant (up to 45 ml) because of the evaporation of water. After every test, the counterface ball was examined under an optical microscope (MT7000, Meiji, Japan) to analyze the transfer film phenomenon before and after cleaning of the ball. Three tests were performed for each set of samples and the average value of wear life and COF are reported.



Figure 3.10 Tribometer used in current study

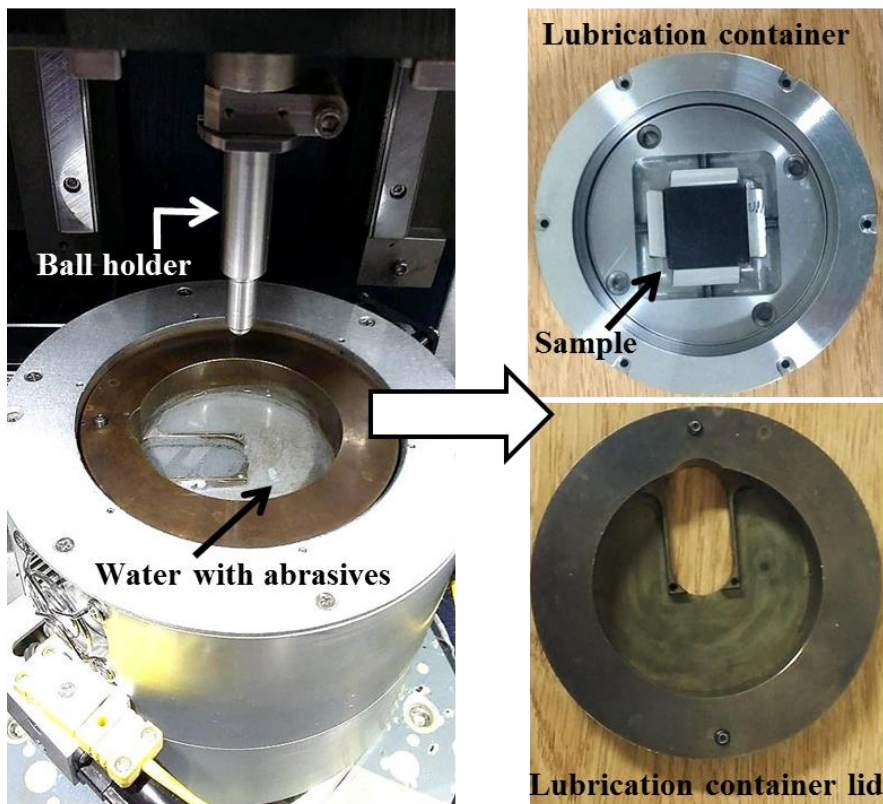


Figure 3.11 Lubrication assembly setup used in tribometer for current study



### **3.5.7 Wear morphology analysis and surface characterization**

FE-SEM was used for wear track analysis to figure out the wear morphology and type of wear mechanisms involved. EDS was carried out for confirmation of coating failures by analyzing the composition of coatings inside and outside of wear tracks. Thin gold coating was deposited on each sample prior to SEM analysis to avoid charging effect on surface of polymer coatings. Moreover, 2D and 3D wear profiles were recorded to measure the wear track profile depth (Z) with the help of optical profilometer (GTK-A, Bruker, USA). Surface roughness of pristine and all type of coatings reinforced with different loadings of nanofillers were analyzed by using optical profilometer.

## **CHAPTER 4**

### **RESULTS AND DISCUSSION**

#### **Phase 1 - Development and characterization of nanocomposite and hybrid nanocomposite coatings under dry conditions**

In the first phase, optimization of nanofiller loadings was carried out through tribological characterization under dry conditions. Phase 1 is further divided into three sections (4.1, 4.2 & 4.3) where different combination of nanofillers were optimized as described below.

##### **4.1 Development and characterization of C15A/UHMWPE nanocomposite coatings**

In this section, our findings from the tribological characterization and analysis of pristine UHMWPE and UHMWPE nanocomposite coatings reinforced with three different nanoclay loadings (0.5, 1.5, 3 wt%), deposited onto aluminum substrate under dry conditions, are discussed. XRD and SEM analysis were used for structural characterization of nanocomposite coatings. Then thickness and hardness measurements were conducted. Later, tribological evaluation of coatings, coupled with SEM analysis and optical profilometry to study wear mechanism involved, was carried out. Similar type of methodology was adopted in other phases as well. The results are presented below.

#### 4.1.1 Structural analysis by XRD

On the basis of degree of dispersion of clay platelets in the polymer matrix, different structures such as intercalated, phase separated and exfoliated can be formed. These different dispersion levels can be characterized qualitatively by using XRD analysis in terms of absence or shifting of signature peaks. No shifting of the characteristic peaks in the XRD pattern indicates the formation of phase separated morphology, because of the presence of clay aggregates. In case of intercalated morphology, shifting of characteristic peak towards lower angle in the XRD pattern is observed because of partial entering of the polymer chains into the intergallery distance between the layered silicates. In case of exfoliated morphology, no characteristic peak is observed in XRD pattern because of complete entering of the polymer chains into the intergallery distance between the layered silicates which separate the clay platelets. In consequence of exfoliation of clay platelets, uniform dispersion of these platelets is obtained which is most desirable morphology among all of them [97].

Figure 4.1 shows the characteristic peaks for pristine UHMWPE at  $21.66^\circ$  and  $24.16^\circ$  corresponding to (110) and (200) planes respectively [98]. The peaks of C15A are observed at  $3^\circ$ ,  $7.4^\circ$  and  $20.3^\circ$  corresponding to an intergallery distance (d-spacing) of 2.94 nm, 1.2 nm and 0.44 nm respectively as also observed in literature [99]. In case of nanocomposites, characteristic peaks of clay are missing except for 3 wt% C15A/UHMWPE which showed a distinct peak which shifted towards the lower angle of  $4^\circ$  corresponding to an intergallery distance of 2.2 nm. The increase in intergallery distance from 1.2 nm to 2.2 nm suggests the possibility of the formation of intercalated morphology in which polymer chains have been entering in intergallery spacing. Similar kind of peak shifting was also observed by

Marija et al. where they reinforced poly ( $\epsilon$ -caprolactone) matrix with different loadings of C15A [100]. However, in case of 0.5 wt% and 1.5 wt% nanoclay composites, no distinct peak is observed at this particular angle which suggests the possibility of formation of exfoliated morphology.

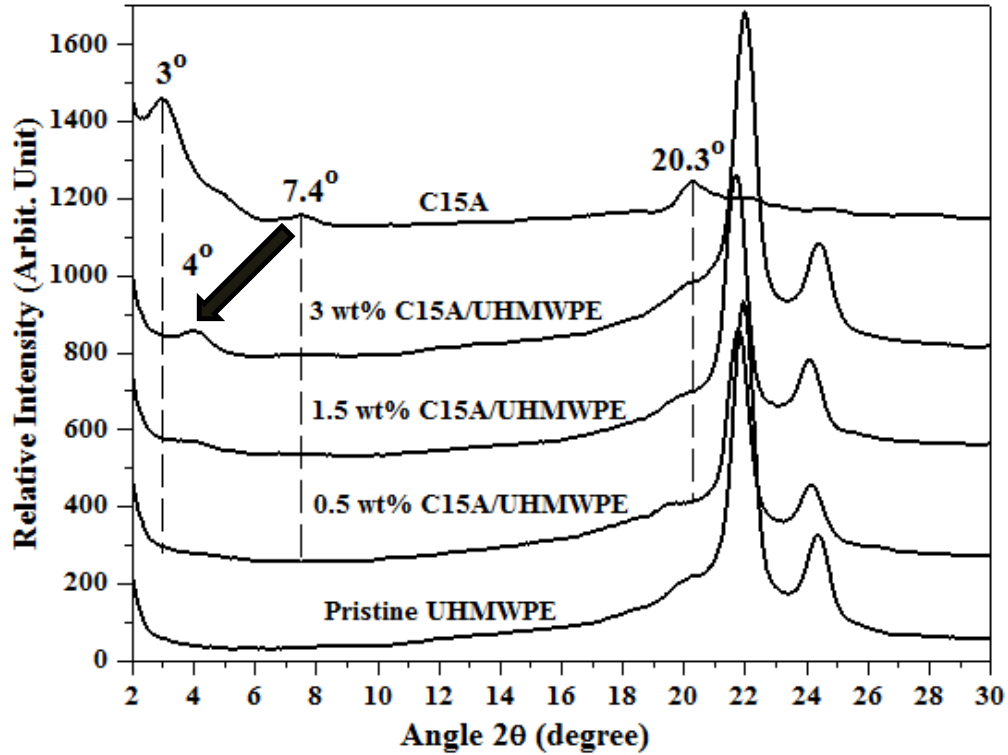


Figure 4.1 XRD patterns of pristine UHMWPE, C15A organoclay and C15A reinforced UHMWPE nanocomposites with different loadings of clay

#### 4.1.2 Dispersion analysis

Figure 4.2 represents the cross sectional FE-SEM images of nanocomposite coatings with different clay loadings at magnification of 50000x. No or negligible agglomeration of nanoclay was observed in case of 0.5 wt% and 1.5 wt% nanoclay loadings as seen in Figure 4.2(a) and (b) but in 3 wt% loading, agglomeration occurred as highlighted in Figure 4.2(c). Moreover, EDS-elemental dot maps of nanocomposite powders were

recorded to further analyze the dispersion of nanoclay in UHMWPE matrix. Figure 4.3 shows dot maps of silicon (Si) and carbon (C) exhibiting nanoclay (layered silicates) and UHMWPE respectively. By analyzing the distribution of Si in elemental dot maps, the dispersion of nanoclays can be observed. It can be concluded from Si dot maps as shown in Figure 4.3 that in case of 0.5 and 1.5 wt% nanoclay loadings there was no or negligible signs of nanoclay agglomerates. However, 3 wt% nanoclay loading exhibited agglomerates in UHMWPE matrix indicating ineffective dispersion and bonding between polymer and clay platelets. Similar kind of dispersion analysis techniques for nanoclays in different polymer nanocomposites were used by various researchers in their studies [101–103].

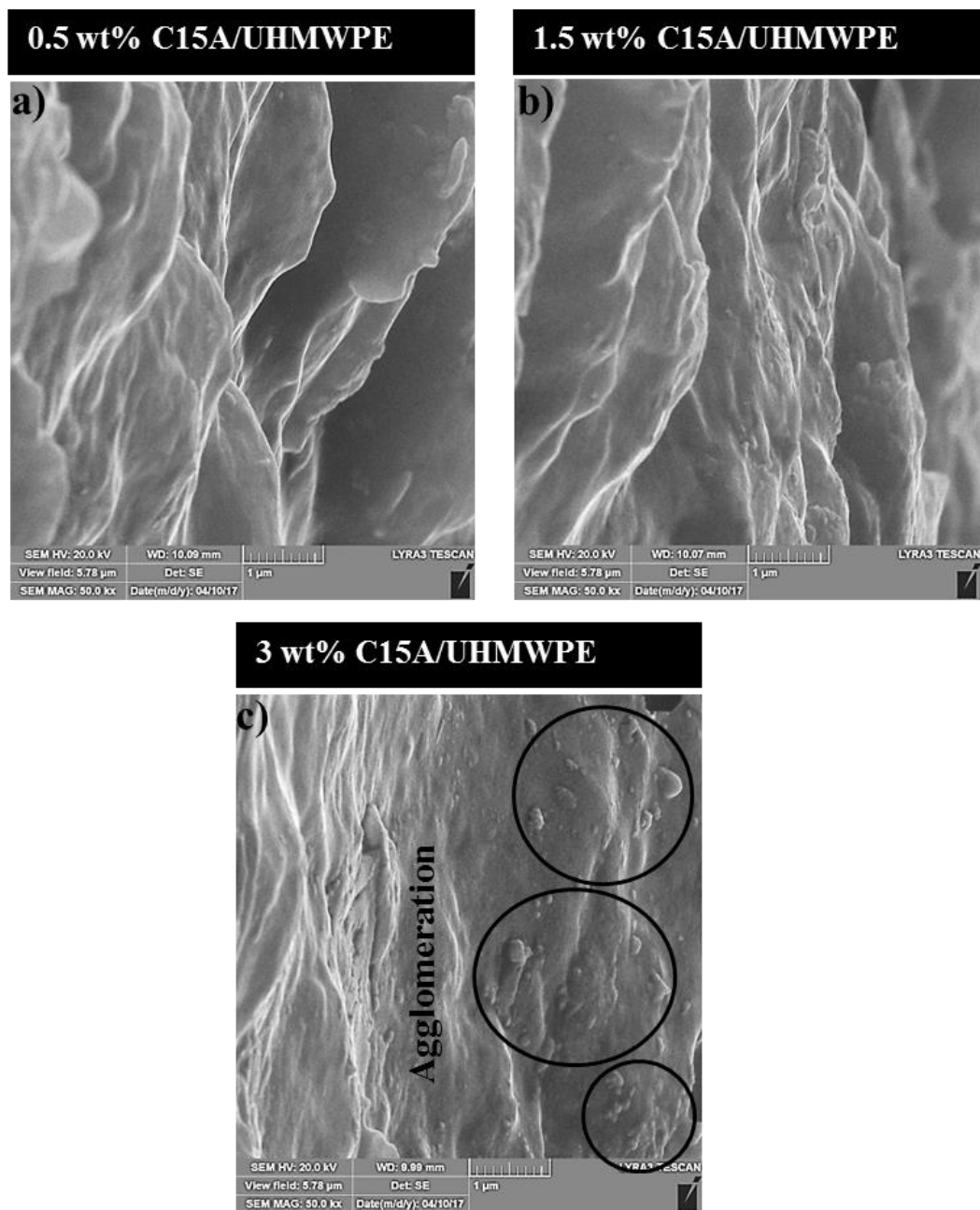


Figure 4.2 FE-SEM images of C15A/UHMWPE nanocomposite coatings with different loadings of C15A

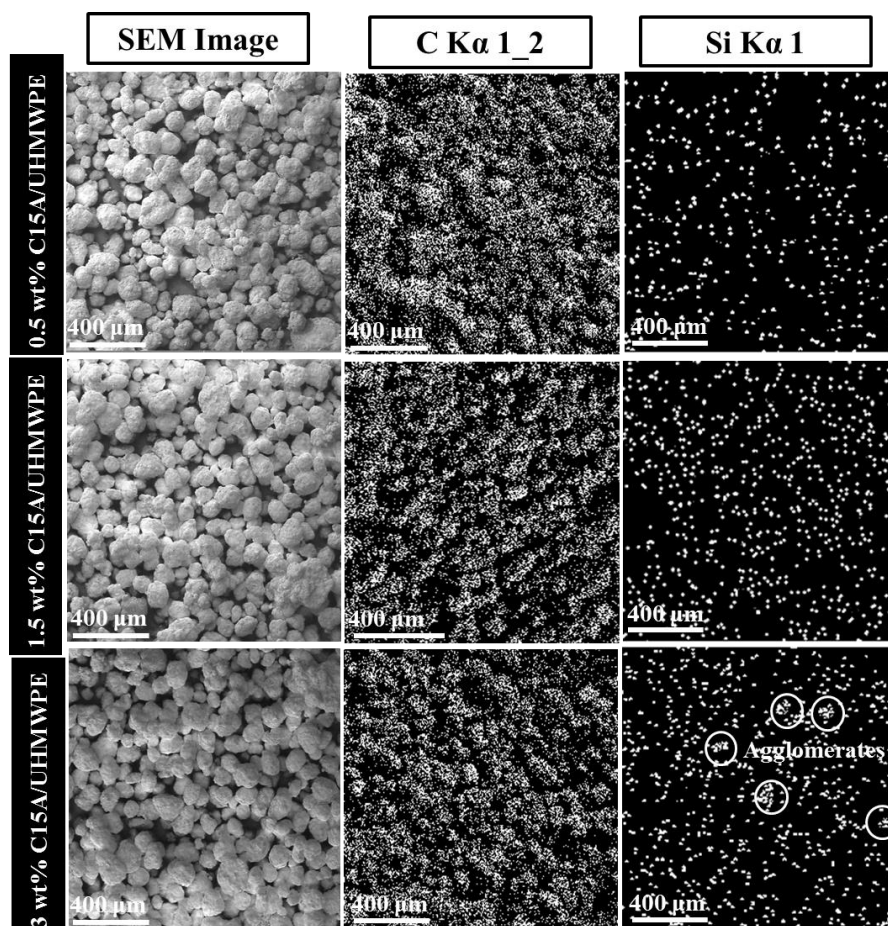
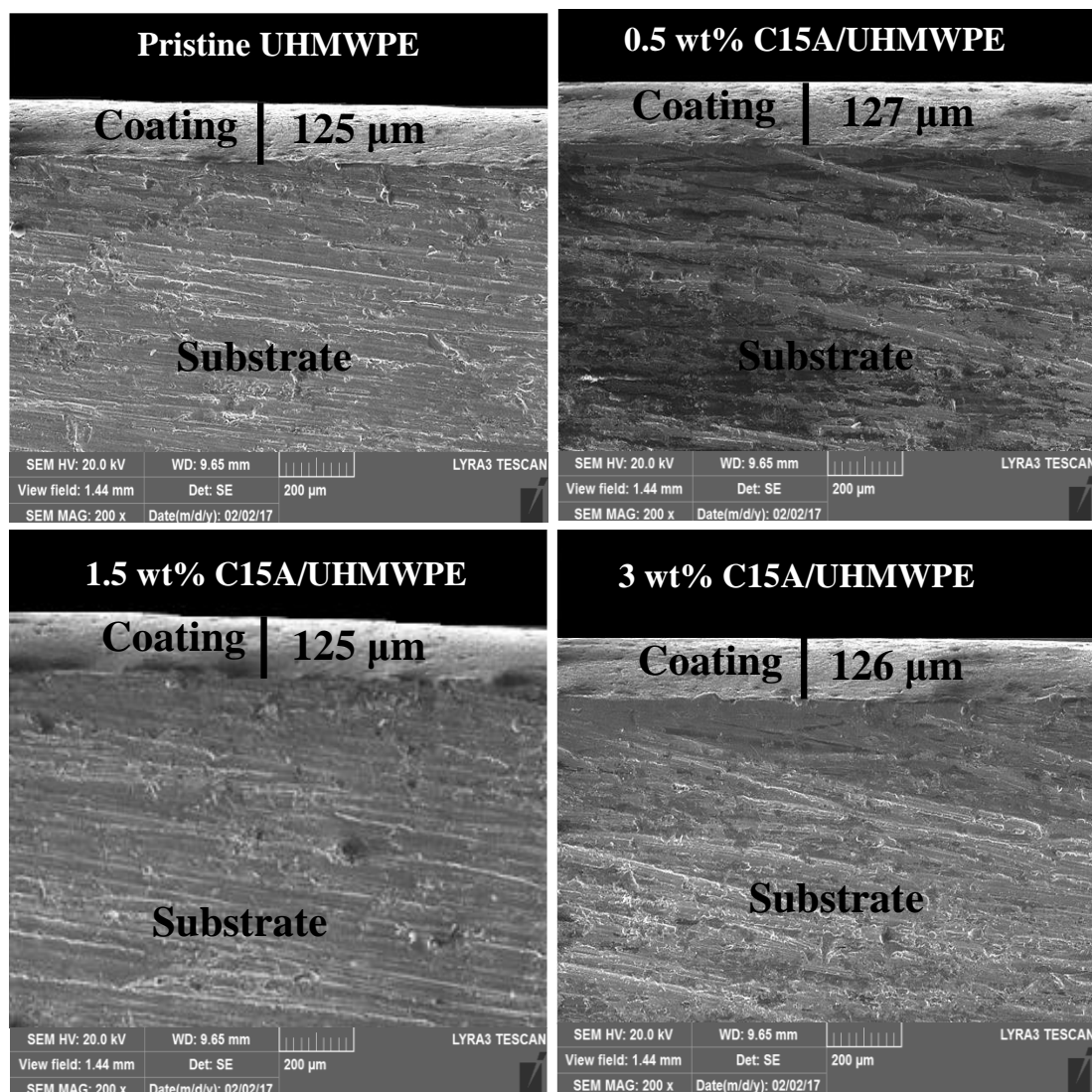


Figure 4.3 SEM-EDS elemental map images of C15A/UHMWPE nanocomposite powders with different loadings of C15A for carbon (C) and Silicon (Si)

### 4.1.3 Thickness measurement results

Figure 4.4 shows the thickness measurements of pristine UHMWPE and C15A/UHMWPE nanocomposite coatings. There was no difference in thicknesses values with the addition of nanoclay. The average value for thickness was approximately similar and measured as  $125 \pm 4 \mu\text{m}$ .



**Figure 4.4** Cross sectional images of pristine UHMWPE and C15A/UHMWPE nanocomposite coatings for thickness measurements

#### 4.1.4 Surface characterization of the coatings

Surface roughness ( $R_a$ ) of pristine UHMWPE and nanocomposite coatings are shown in Figure 4.5 showing 3D images of coating's surfaces. There was no appreciable effect on surface roughness of nanocomposite coatings due to addition of nanoclay.



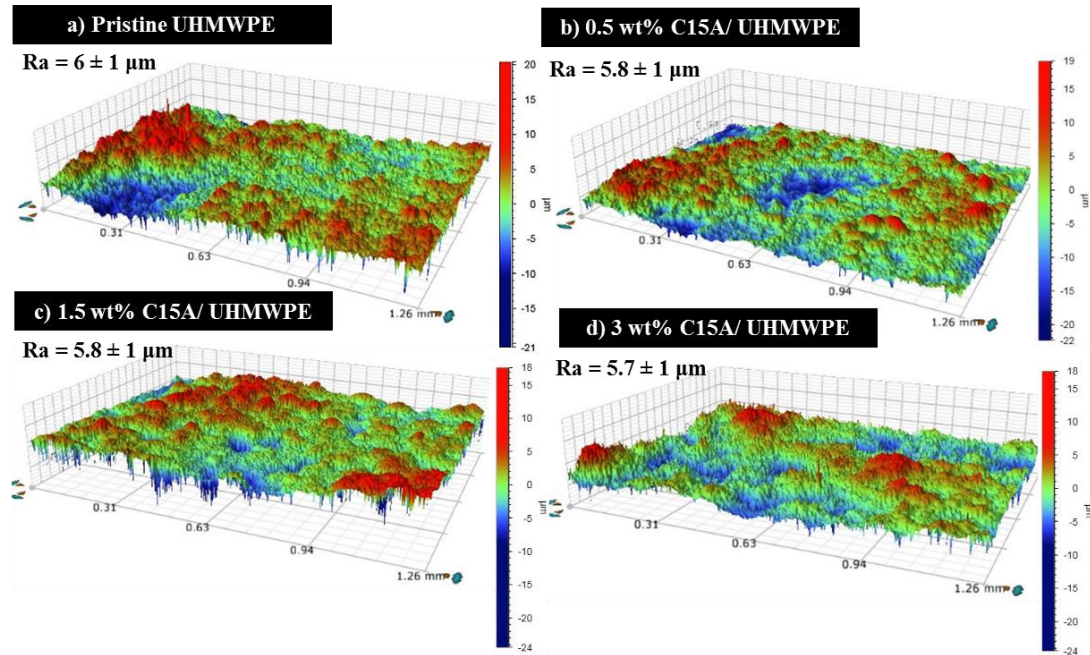


**Figure 4.5** Surface roughness (Ra) of Pristine UHMWPE and C15A/UHMWPE nanocomposite coatings with different loadings of nanoclay

#### 4.1.5 Hardness measurement results

Figure 4.6 represents the variation in hardness with the addition of different loadings of C15A nanoclay in UHMWPE matrix. It can be seen that hardness of nanocomposite coatings was increased with the increase in nanoclay loadings. The increase in the hardness is attributed to the bridging effect provided by the clay platelets in the soft polymer matrix holding the polymer chains together and increasing the resistance to penetration or indentation.

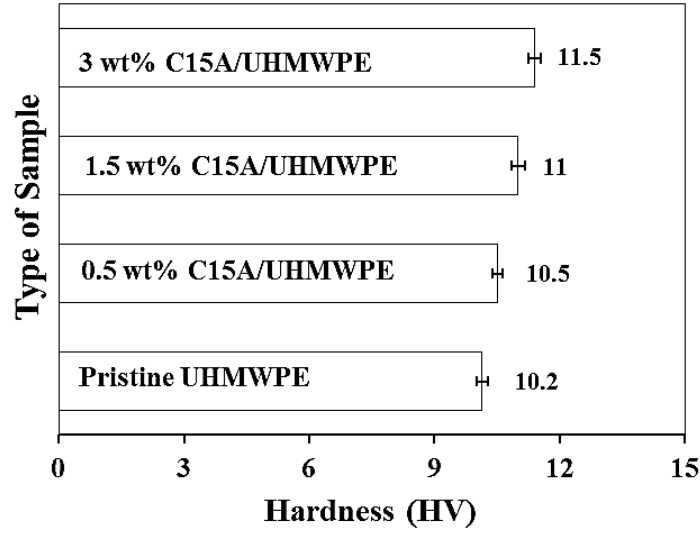


Figure 4.6 Comparison of the hardness of C15A/UHMWPE nanocomposite coatings with different loadings of C15A

#### 4.1.6 Tribological results

Generally the contact pressure in bearings of ship rudders and units of hydraulic turbines is ~50 MPa [104]. Based on this observation, initially, pristine UHMWPE coatings were evaluated for their load bearing capacity at different normal loads (5N, 7N and 9N) at a linear sliding speed of 0.1m/s (480 rpm) and a wear track radius of 2 mm for 10,000 cycles (sliding distance = 125 m). The wear tests were stopped in case of large values/ fluctuations in COF (beyond 0.3) as observed in the frictional graphs indicating the metal to metal contact due to failure of the coating. Figure 4.8 presents the typical frictional graphs of pristine UHMWPE coatings at three different loads (5, 7 and 9 N). From these graphs, it can be clearly seen that these coatings did not fail until 10,000 cycles at normal load of 5 and 7 N. However, there was a complete failure of the coating at a normal load of 9 N just after ~5200 cycles. The exposed substrate in the photograph of the wear track and scar mark on the corresponding counterface (after cleaning) as shown in Figure 4.8 clearly

indicated the failure of coating at 9 N. However, these signs of failure were not observed in case of coatings tested at 5 and 7 N.

Later, C15A/UHMWPE nanocomposite coatings with three different clay loadings (0.5, 1.5 and 3 by wt%) were developed and tested at higher normal loads of 9 and 12 N for 10,000 cycles, at a wear track radius of 2 mm and a linear sliding speed of 0.1 m/s (480 rpm) to evaluate the improvement in tribological performance.

Figure 4.9 compares the average wear life of pristine UHMWPE and C15A/UHMWPE nanocomposite coatings at a normal load of 9 N and a linear sliding speed of 0.1 m/s. It is clear from Figure 4.9 that only 1.5 wt% C15A/UHMWPE nanocomposite coating completed its wear life up to 10,000 and test was stopped while 0.5 wt% C15A/UHMWPE and 3 wt% C15A/UHMWPE nanocomposite coatings failed just after ~5500 and ~8000 cycles respectively. SEM images along with the corresponding EDS spectrums showing Al peak at 1.49 keV and scar mark on counterface ball as shown in Figure 4.10 confirmed the failure of 0.5 wt% C15A/UHMWPE and 3 wt% C15A/UHMWPE nanocomposite coatings. However, EDS spectrum in case of 1.5 wt% C15A/UHMWPE nanocomposite coating showed no Al peak and the wear mechanism was only plastic deformation.

The optimum performance of 1.5 wt% C15A/UHMWPE nanocomposite coating is attributed to the exfoliation of the clay platelets in the polymer matrix that provides bridging effect and holds the polymer chains together as confirmed from XRD results (Figure 4.1), SEM images (Figure 4.2) and EDS-elemental map images (Figure 4.3). However, 0.5 wt% C15A/UHMWPE nanocomposite coating failed which can be attributed to the insufficient bridging effect due to the lower amount of the nanoclay while 3 wt%

C15A/UHMWPE nanocomposite coating failure can be attributed to the agglomeration of nanoclay or possible formation of two phase structures; softer phase (polymer matrix alone) and harder phase (clay platelets because of their high surface energy) causing poor bonding and insufficient bridging effect between polymer and nanoclay as clearly indicated in XRD results (Figure 4.1), SEM images (Figure 4.2) and EDS-elemental map images (Figure 4.3). The softer phase (polymer matrix alone) may act as weak areas for the initiation of failure/peeling off of the coating. Regarding the coefficient of friction, no appreciable difference was observed in case of pristine as well as nanocomposite coatings as shown in Figure 4.7.

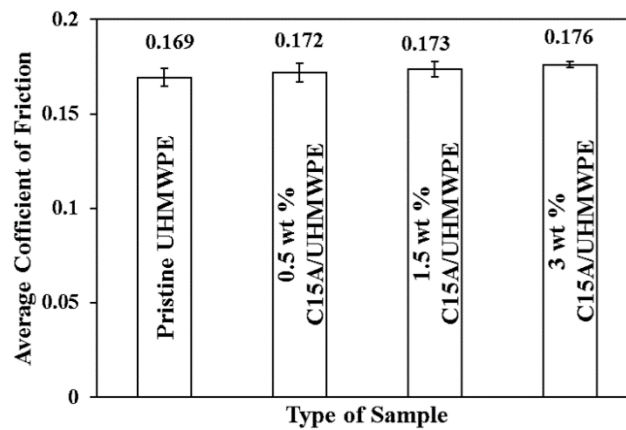


**Figure 4.7 Comparison of average coefficient of friction of pristine and nanoclay/ UHMWPE nanocomposite coatings**

To further evaluate the load bearing capacity of 1.5 wt% C15A/UHMWPE nanocomposite coating, it was tested at a normal load of 12 N for 10,000 cycles with same other parameters (linear speed = 0.1 m/s and rpm = 480). Typical frictional graph in Figure 4.11 shows that coating failed very early (below ~2000 cycles). SEM image as well as corresponding EDS spectrum confirmed the failure of coating at 12 N load.

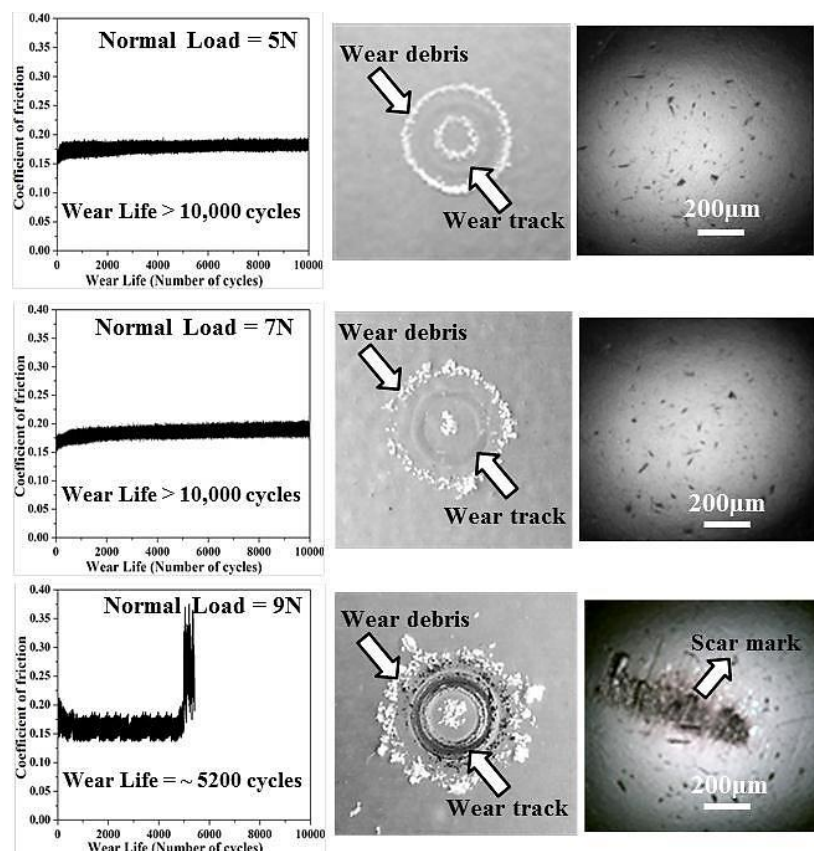


Figure 4.8 Typical frictional graphs (left), photographs of wear tracks (middle) and counterface ball (right) of pristine UHMWPE coatings after the wear tests performed at normal load of 5, 7 and 9 N and a linear sliding speed of 0.1 m/s

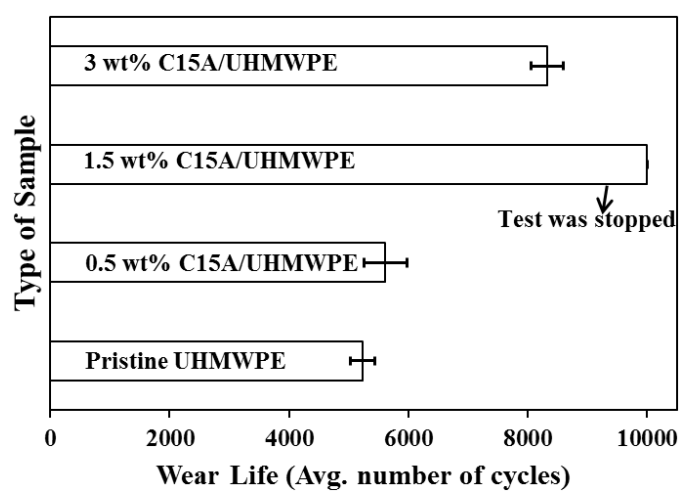


Figure 4.9 Comparison of average wear life of pristine UHMWPE and C15A/UHMWPE nanocomposite coatings at normal load of 9 N and a linear sliding speed of 0.1 m/s

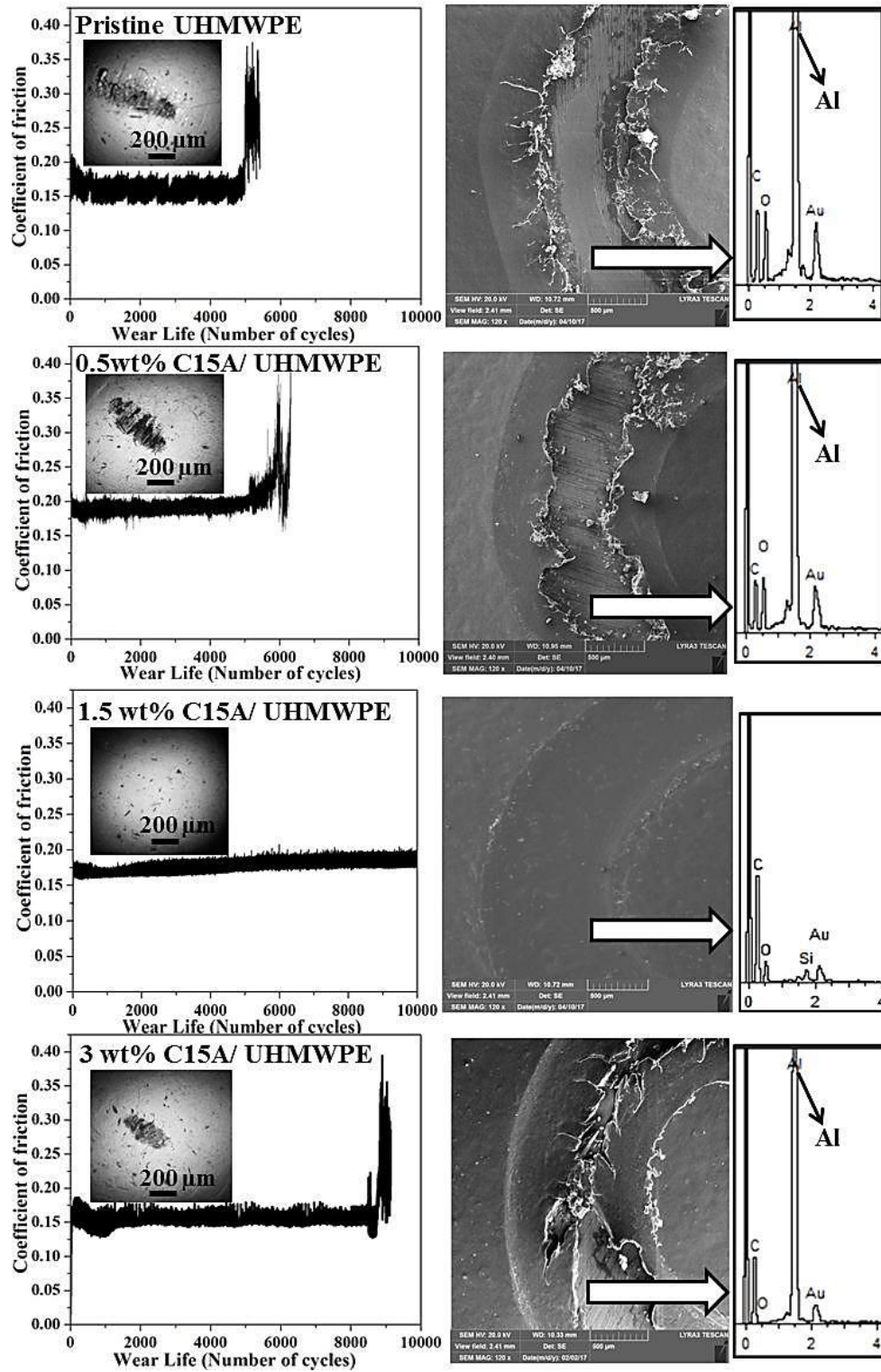


Figure 4.10 Typical frictional graphs of pristine UHMWPE and C15A/UHMWPE nanocomposite coatings along with FE-SEM images (middle) and EDS spectrums (right) after wear tests performed at normal load of 9 N and a linear sliding speed of 0.1 m/s for 10,000 cycles. Inset: Counterface ball images after cleaning with acetone..



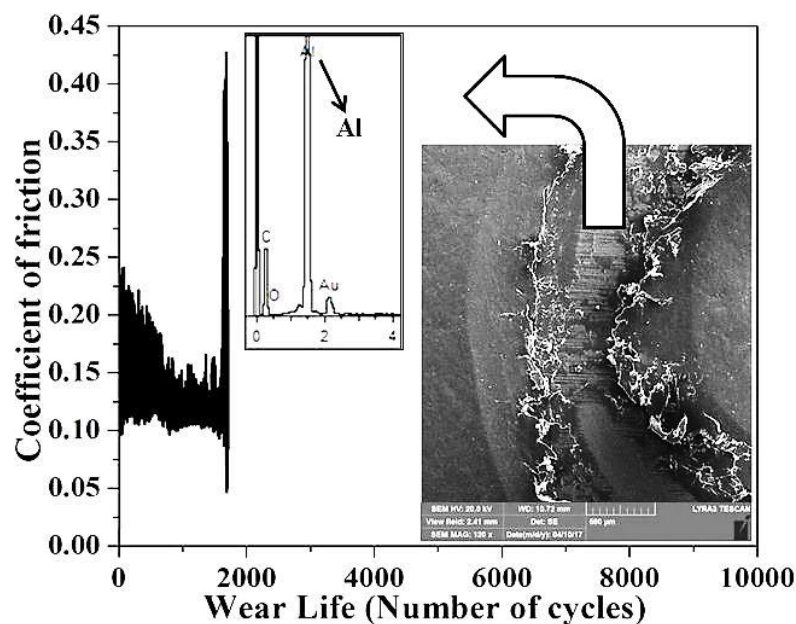


Figure 4.11 Typical frictional graph of 1.5 wt% C15A/UHMWPE nanocomposite coating along with FE-SEM image of wear track and EDS spectrum after wear test conducted at 12 N and a linear sliding speed of 0.1 m/s

#### 4.1.7 Effect of linear sliding speed on tribological performance of 1.5 wt% C15A/UHMWPE nanocomposite coating

After the above screening tests, it was confirmed that only 1.5 wt% C15A/UHMWPE nanocomposite coating did not fail at a normal load of 9 N. In order to further investigate the tribological performance of this nanocomposite coating, wear tests were performed at different linear speeds of 0.1, 0.2 and 0.3 m/s respectively, at a normal load of 9 N for 25,000 cycles (sliding distance = 314 m) and wear track radius of 2 mm. Figure 4.12 shows the typical frictional graphs of 1.5 wt% C15A/UHMWPE nanocomposite coatings (a) to (c), FE-SEM images of wear tracks (d) to (f), 3D optical profile images of wear tracks (g) to (i) and profile depths of wear tracks (j) to (l) after wear tests performed at normal load of 9 N and linear sliding speeds of 0.1, 0.2, 0.3 m/s. It is clear from Figure 4.12 that the nanocomposite coating at a linear speed of 0.1 m/s did not fail even until ~25,000 cycles

as confirmed by the corresponding SEM image showing only plastic deformation as well as wear track profile depth (Z) which was only 30  $\mu\text{m}$  (less than the coating thickness of 125  $\mu\text{m}$ ). However, the nanocomposite coating failed at linear sliding speeds of 0.2 and 0.3 m/s showing a wear life of ~22,500 and ~9,000 cycles respectively. The corresponding SEM images and wear profile depths approaching to the coating's thickness (125  $\mu\text{m}$ ) confirmed the failure of coatings at linear sliding speeds of 0.2 and 0.3 m/s. It is well established that the contact temperature plays a significant role in the wear of polymers. Since UHMWPE polymer starts to lose its dimensional stability at the temperatures above 80 to 90 °C [3], it is possible that with any increase in the linear sliding speed, the localized contact temperature would have been raised beyond 80 to 90 °C which caused the softening of the polymer resulting in the failure of the coatings.



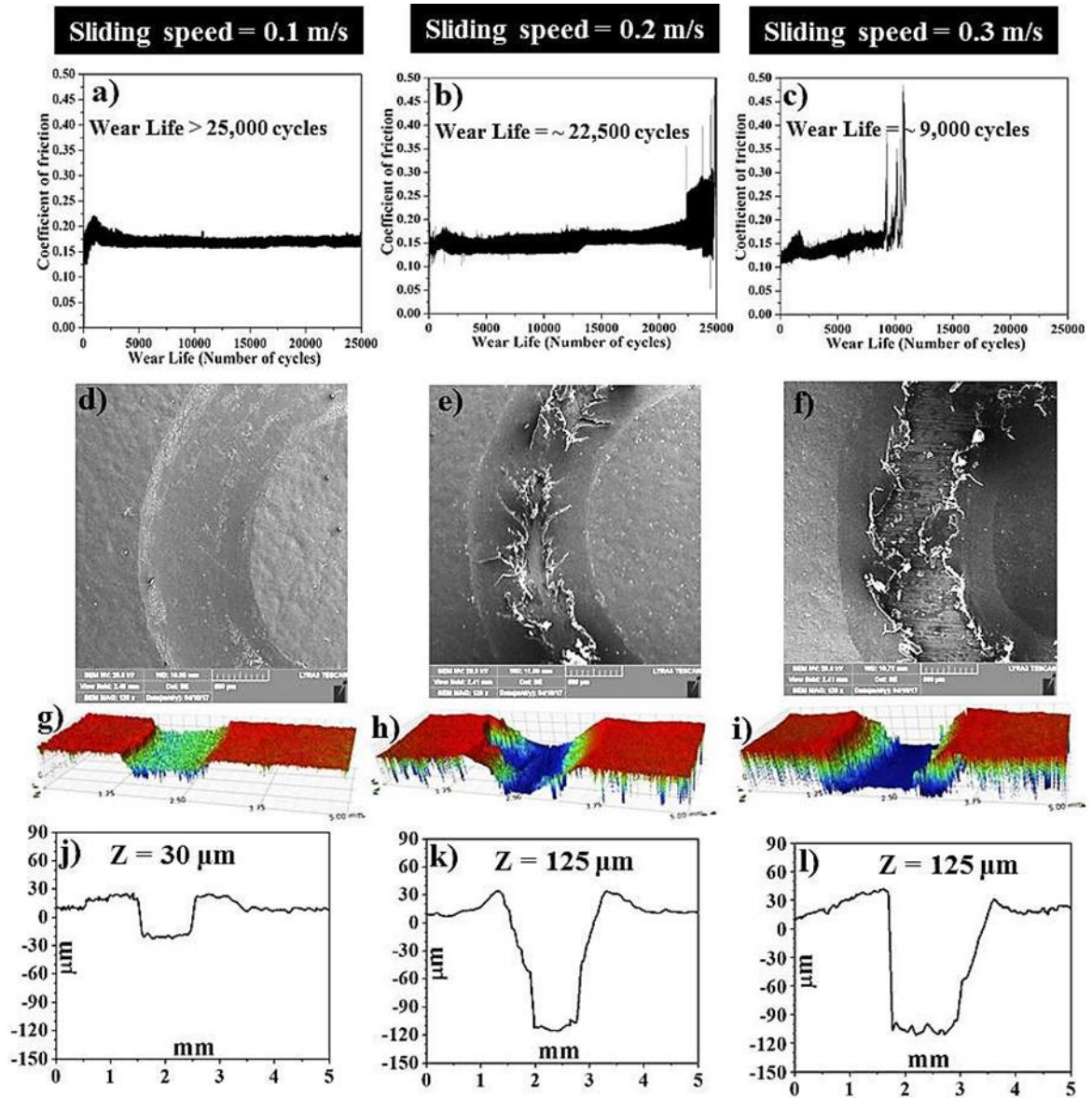
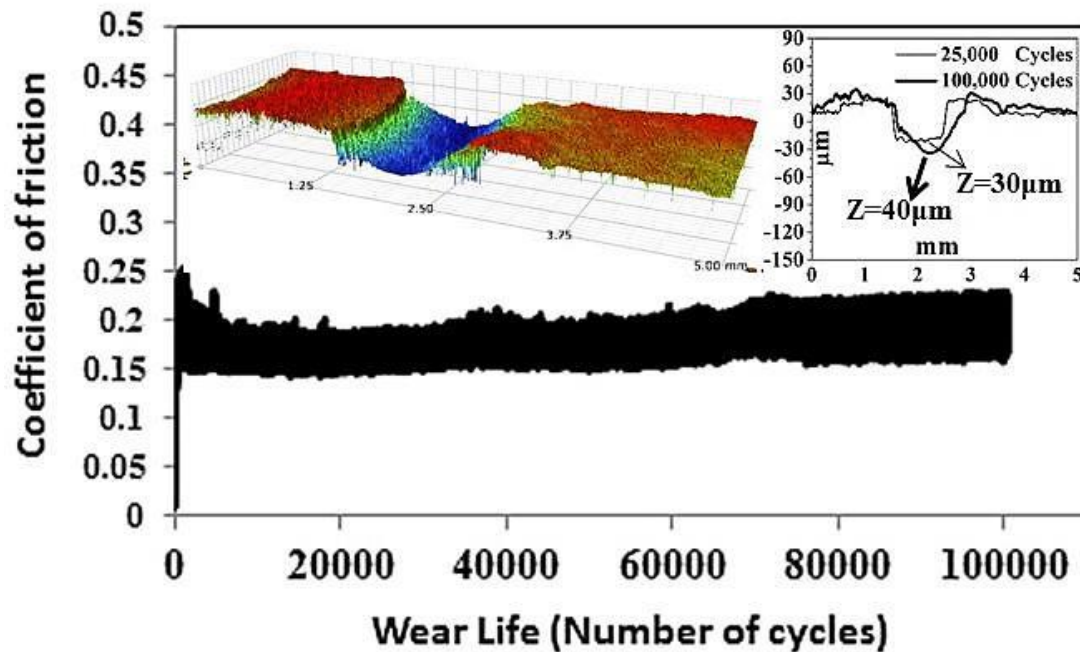


Figure 4.12 Typical frictional graphs of 1.5 wt% C15A/UHMWPE nanocomposite coatings (a) to (c), FE-SEM images of wear tracks (d) to (f), 3D optical profile images of wear tracks (g) to (i) and profile depths of wear tracks (j) to (l) after wear tests conducted at a normal load of 9 N at linear sliding speeds of 0.1, 0.2, 0.3 m/s

#### 4.1.8 Accelerated wear life testing

Long term wear test was performed to confirm the sustainability of 1.5 wt% C15A/UHMWPE nanocomposite coating to protect metallic components at a normal load of 9 N at linear sliding speed of 0.1 m/s for 100,000 cycles (sliding distance = 1.3 km).

Figure 4.13 shows the typical frictional graph showing no failure of the coating even after 100,000 cycles indicating excellent wear resistance of this particular coating to protect the metallic component at a normal load of 9 N. Insets in Figure 11 show the 3D-optical image and a comparison of the 2D-optical wear profiles of wear tracks after the wear test conducted at a normal load of 9 N and linear speed of 0.1 m/s for 25,000 and 100,000 cycles. It can be clearly seen that there was only a difference of about  $\sim 10 \mu\text{m}$  in the profile depth (Z) of the wear tracks due to plastic deformation even after 100,000 cycles as compared to that after 25000 cycles indicating the excellent wear resistance of the coating which can be sustained even beyond 100,000 cycles at a normal load of 9 N and a sliding speed of 0.1 m/s.



**Figure 4.13 Typical frictional graph of 1.5 wt% C15A/UHMWPE nanocomposite coating for a wear test conducted at a normal load of 9 N and a linear sliding speed of 0.1 m/s for 100,000 cycles. Inset (Left): 3D optical image of the wear track. Inset (Right): Comparison of 2D-Optical wear profiles of wear tracks after wear test conducted at normal load of 9 N and a linear speed of 0.1 m/s for 25,000 and 100,000 cycles**

#### **4.1.9 Summary**

From this section, it is found that pristine UHMWPE coating failed at a normal load of 9 N and linear sliding speed of 0.1 m/s just after ~5200 cycles while among the three combinations of C15A/UHMWPE nanocomposite coatings, only 1.5 wt% C15A/UHMWPE nanocomposite coating exhibited excellent wear life as it did not fail even until ~100,000 cycles at a normal load of 9 N and a linear sliding speed of 0.1 m/s due to the exfoliation and uniform distribution of clay platelets in the polymer matrix that provides a bridging effect and holds the polymer chains together instead of being pulled out easily. However, at a normal load of 12 N and a linear speed of 0.1 m/s, 1.5 wt% C15A/UHMWPE nanocomposite coating failed very early (< 2000 cycles) indicating that this coating cannot sustain a load of 12 N.

## 4.2 Development and characterization of CNTs/UHMWPE

### nanocomposite coatings

In our findings presented in section 4.1, we concluded that 1.5 wt% C15A/UHMWPE nanocomposite coating (optimized) failed earlier at a normal load of 12 N. Hence to increase the wear life and the load bearing capacity of the pristine UHMWPE coating under dry conditions, it was reinforced with different loadings (0.5, 1.5 and 3 wt%) of CNTs. In this section, the characterization and analysis of CNT/UHMWPE nanocomposite coating will be discussed. The findings shall suggest how effective CNTs were in the polymer matrix in increasing the load bearing capacity. Table 4.1 below shows compositions of the prepared coatings with their respective designations used in this study.

Table 4.1 Classification and designation of samples in section 4.2

Sample type	Composition	Sample Designation	Group Designation
UHMWPE	Pristine	Pristine UHMWPE	Pristine
CNT/UHMWPE nanocomposite	0.5 wt% CNT/UHMWPE	Sample-A	CNT-nanocomposites
	1.5 wt% CNT/UHMWPE	Sample-B	
	3 wt% CNT/UHMWPE	Sample-C	

#### 4.2.1 XRD analysis of pristine and CNT-nanocomposite powders

Figure 4.14 shows the characteristic peaks for pristine UHMWPE at  $21.66^\circ$  and  $24.16^\circ$  corresponding to (110) and (200) planes respectively [98] and for CNTs at  $25.58^\circ$  corresponding to (002) plane [105]. In case of all CNT-nanocomposites, the characteristic peak of CNT is absent as shown in Figure 4.14 which is an indication of uniform dispersion of CNTs in the polymer matrix. However, the intensity of UHMWPE characteristic peaks in CNT-nanocomposites decreased with the increase in nanofiller concentrations.

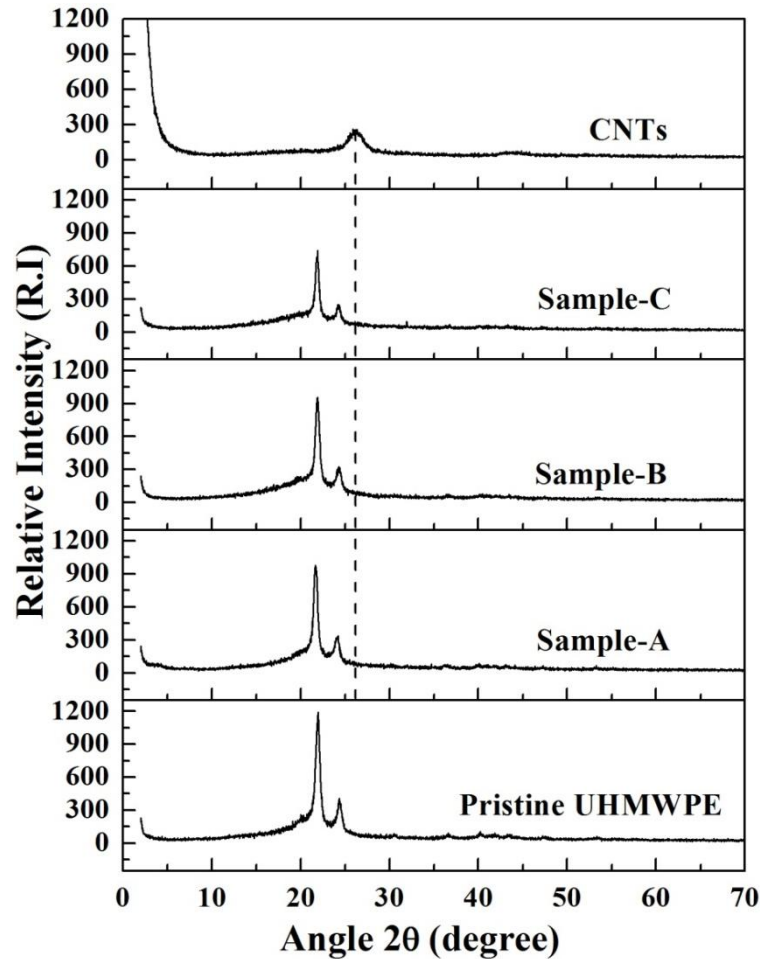


Figure 4.14 XRD patterns of CNT-nanocomposites

#### 4.2.2 Raman spectroscopy of pristine and CNT-nanocomposite powders

Figure 4.15 show the Raman spectra of CNT-nanocomposites along with the spectra of UHMWPE and CNTs in the range of 1000-2000  $\text{cm}^{-1}$ . The characteristic peaks for CNTs, corresponding to D and G bands, are at 1360  $\text{cm}^{-1}$  and 1575  $\text{cm}^{-1}$ . D band delineates disordered graphitic structures whereas G band is due to tangential stretching of C–C bond [106, 107]. Pristine UHMWPE shows its high characteristic peaks at 1064  $\text{cm}^{-1}$ , 1130  $\text{cm}^{-1}$ , 1297  $\text{cm}^{-1}$  and 1440  $\text{cm}^{-1}$ . The characteristic peaks at 1064  $\text{cm}^{-1}$  and 1130  $\text{cm}^{-1}$  represent asymmetric and symmetric stretching modes of C-C bonds [108, 109] whereas peaks at 1297  $\text{cm}^{-1}$  and 1440  $\text{cm}^{-1}$  indicate twisting and bending modes of  $\text{CH}_2$  [110]. Figure 4.15 show that with the addition of CNTs in UHMWPE, G band in all CNT-nanocomposites shifted towards higher frequency of 10  $\text{cm}^{-1}$ . The shifting of the G band towards higher frequencies can be attributed to disentanglement of the CNTs followed by dispersion in the UHMWPE matrix due to penetration of polymer into the CNT bundles. The up-shift also represents strong compressive forces associated with polymer chains on CNTs suggesting good load transfer in the coatings [111].

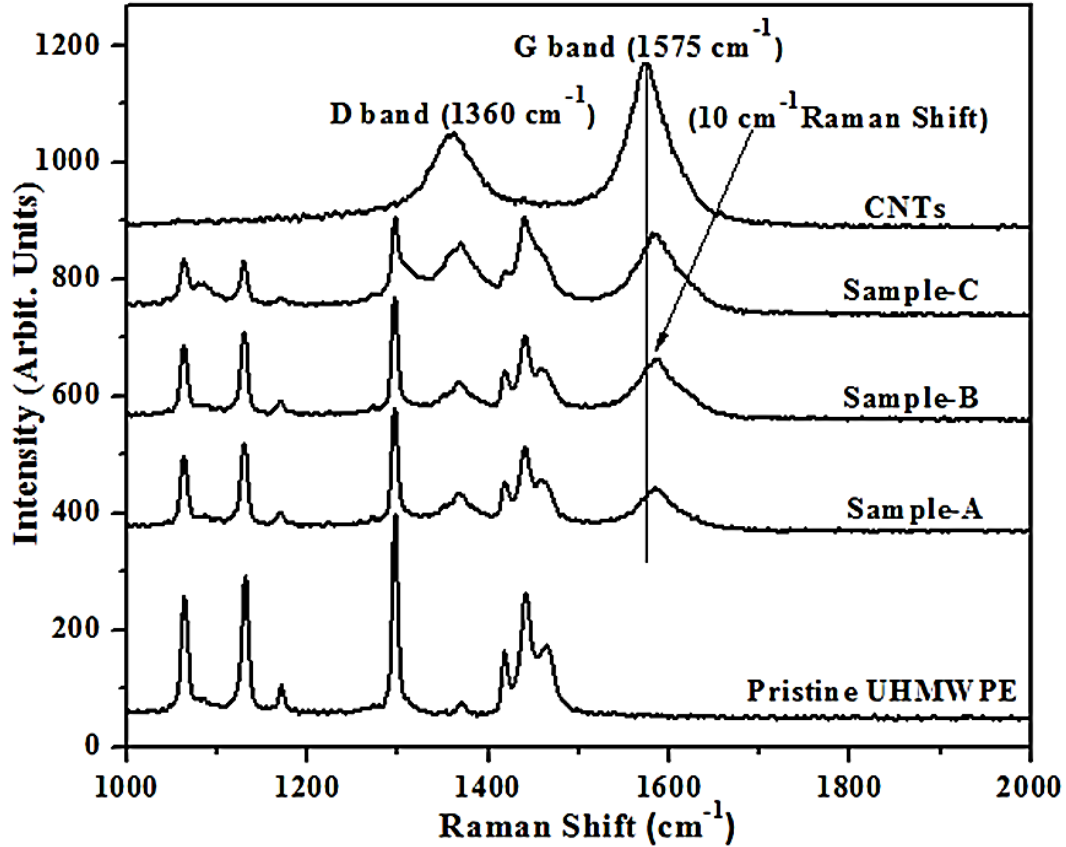


Figure 4.15 Raman spectra for CNT-nanocomposites

#### 4.2.3 Evaluation of the coatings for dispersion of CNTs and thickness measurement

FE-SEM images of the cross section of CNT-nanocomposite coatings were evaluated to conduct the dispersion analysis of CNTs in polymer matrix at magnification of 50,000 x as shown in Figure 4.16. There were no or negligible signs of CNTs agglomeration for Sample-A and B as can be seen in Figure 4.16. But Sample-C showed agglomerates or clusters of CNTs which indicates the ineffective dispersion and bonding between polymer and nanofillers as the CNTs content increased.

In Figure 4.17, thicknesses of coatings are reported which are the average of three readings with a variation of  $\pm 5 \mu\text{m}$ . In case of pristine UHMWPE coating, thickness was found to

be about 125  $\mu\text{m}$ . Whereas, in case of CNT-nanocomposite coatings, approximately similar but higher values ( $\sim 180 \mu\text{m}$ ) as compared to pristine UHMWPE coatings were observed. The reason for this increase in thickness can be attributed to higher thermal conductivity of CNTs which converted the nanocomposite powders into partial molten state more quickly as compared to pristine UHMWPE during the deposition of powders on preheated substrate. In consequence of this early partial melting, more powder particles of nanocomposites were fused or deposited on preheated substrate as compared to that of pristine UHMWPE where more powder particles were scattered or repelled due to similar charge on already deposited powder under the same deposition rate and time of coating.

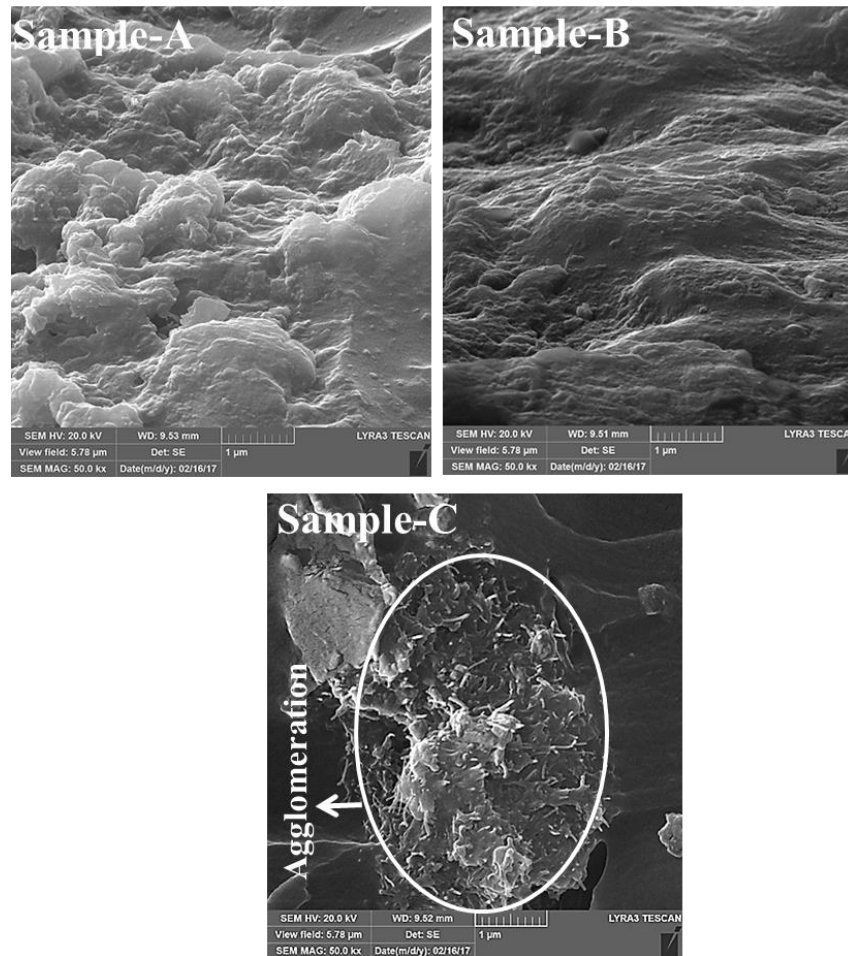


**Figure 4.16 FE-SEM images of CNT-nanocomposite coatings**



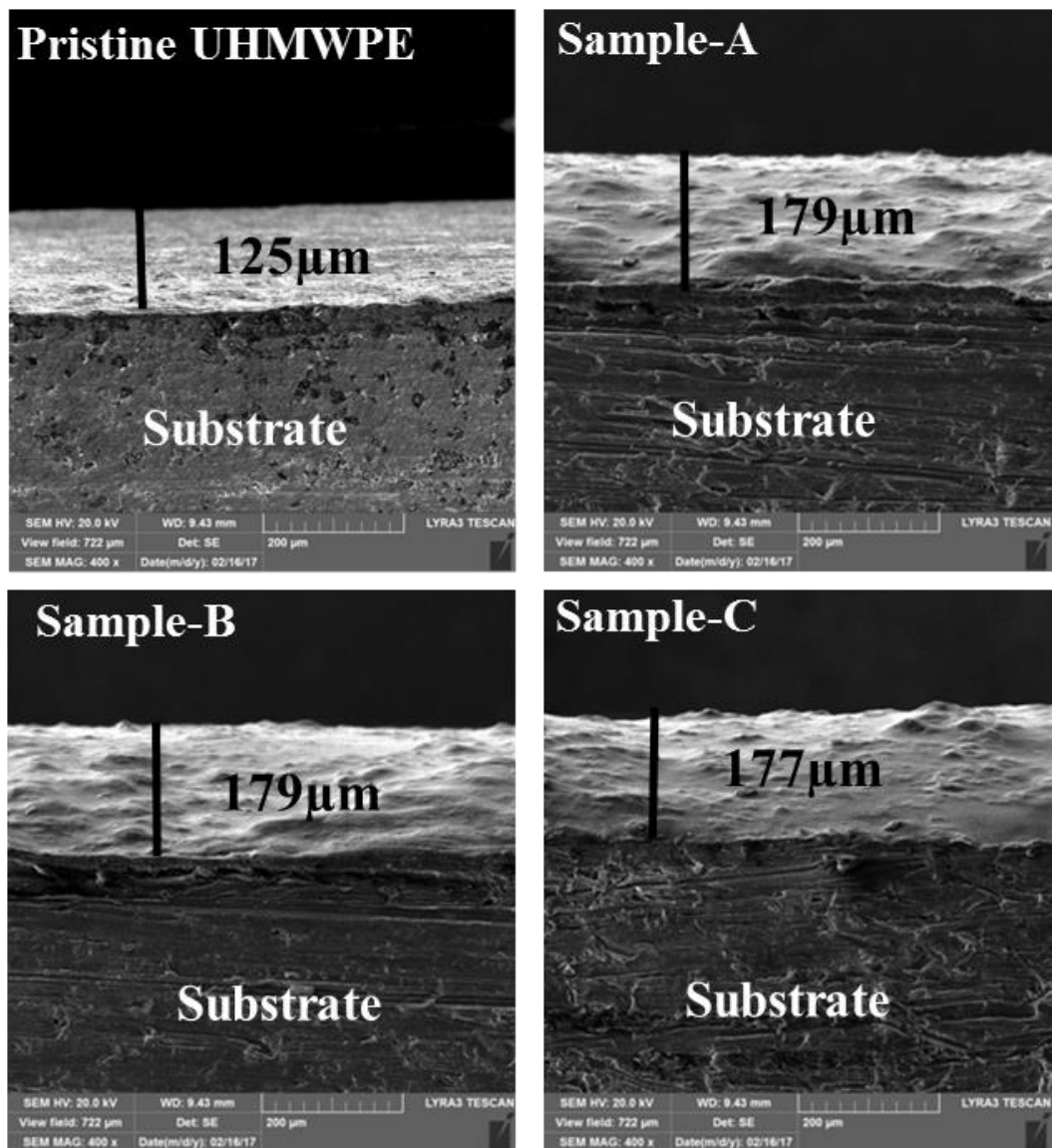


Figure 4.17 FE-SEM images of the cross-section of pristine and CNT-nanocomposite coatings

#### 4.2.4 Surface characterization of the coatings

Surface roughness ( $R_a$ ) of CNT/UHMWPE nanocomposite coatings are shown in Figure 4.18 showing 3D images of coating's surfaces. It can be noticed that there was decrease in roughness of nanocomposite coatings as compared to that of pristine UHMWPE ( $\sim 6 \pm 1 \mu\text{m}$ ) due to the addition of CNT in polymer matrix because of excellent thermal conductivity of CNTs

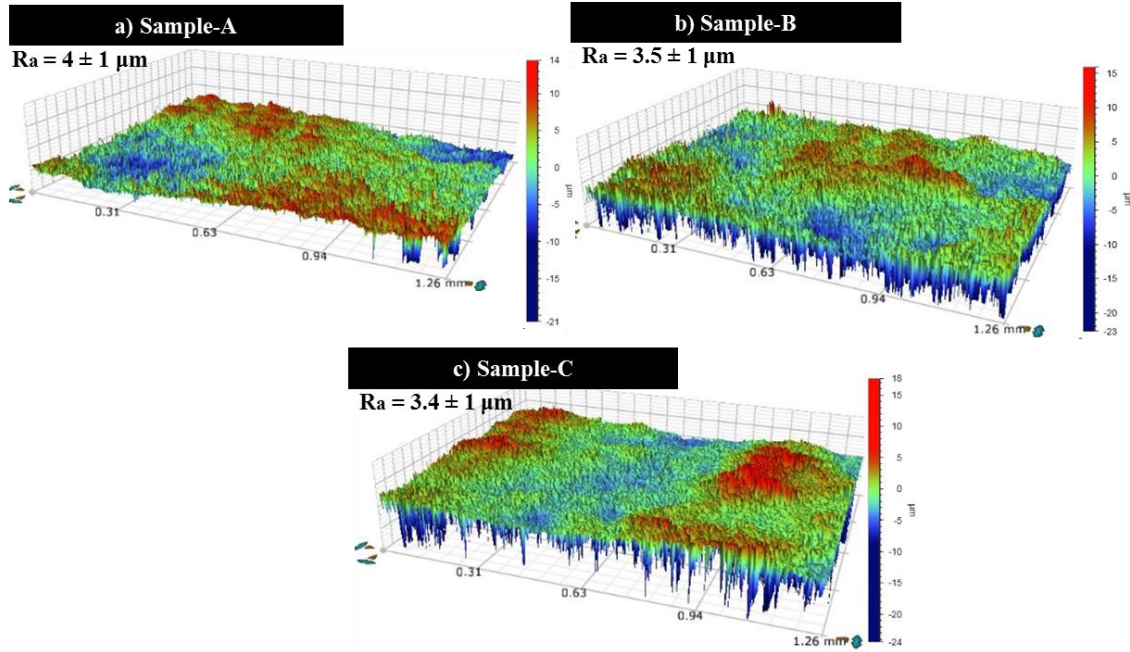


Figure 4.18 Surface roughness (Ra) of CNTs/UHMWPE nanocomposite coatings with different loadings of CNTs

#### 4.2.5 Hardness evaluation of pristine and CNT-nanocomposite coatings

Generally, increase in the hardness was found with the increase of loading of CNTs in polymer matrix. The increase in hardness is attributed to good mechanical properties of CNTs in the soft polymer matrix holding the polymer chains together resulting in greater resistance to penetration or indentation. The maximum hardness was observed for Sample-C (3 wt% CNTs//UHMWPE). Figure 4.19 compares the average hardness values of the coatings.

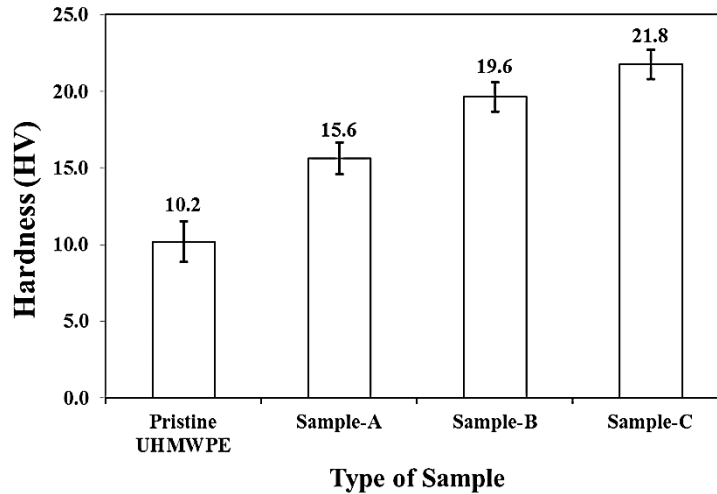
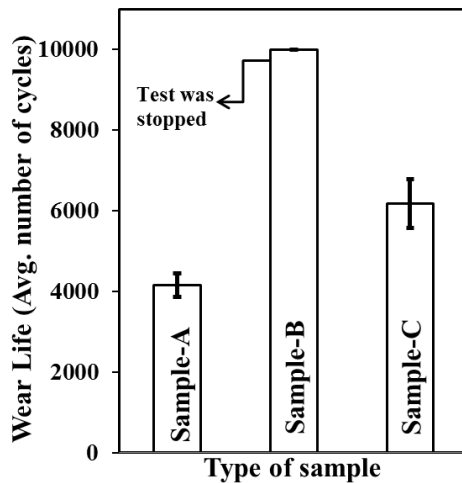


Figure 4.19 Effect of different loading of CNTs on hardness of the coatings

#### 4.2.6 Tribological performance of the CNT-nanocomposite coatings under dry conditions

Since pristine UHMWPE coating was failed at a normal load of 9 N and linear sliding velocity of 0.1 m/s just after ~5200 cycles as reported (in section 4.1.5) earlier. In order to enhance the load bearing capacity of the coating, CNT-nanocomposite coatings of above mentioned compositions as shown in Table 4.1 were developed and evaluated at normal loads of 9, 12 N respectively for screening purposes at a linear sliding speed of 0.1m/s (480 rpm) for 10,000 cycles corresponding to a sliding distance of 125 m. Wear track radius for all tests was kept constant at 2 mm. It is to be noted that the wear tests were stopped in case there was an indication of a large value of COF (beyond 0.3) suggesting a metal to metal contact because of the failure of coating. It was observed that all the nanocomposite coatings did not fail until 10,000 cycles at a normal load of 9 N. However at 12 N the behavior of the nanocomposite coatings was as follows. From Figure 4.20, it can be seen that, only Sample-B (1.5 wt% CNTs/UHMWPE) showed a wear life of 10,000 cycles as compared to 0.5 wt% (Sample-A) and 3 wt% (Sample-C) of CNTs. The better performance

of Sample-B is attributed to the uniform dispersion of CNTs in the UHMWPE polymer matrix as confirmed by the SEM image of nanocomposite coating (Figure 4.16), which helps in anchoring the polymer chains in the matrix and preventing them from being pulled out. However, the failure of Sample-A (0.5 wt%) earlier than 10,000 cycles can be attributed to the insufficient amount of CNTs leading to an ineffective anchoring of the polymer chains of the matrix while the failure of Sample-C (3 wt%) can be attributed to the agglomerations of CNTs or possible formation of two phase structures; softer phase (polymer matrix alone) and harder phase (CNT's agglomerates because of their high surface energy) as indicated in Figure 4.16 causing poor bonding and bridging effect between the polymer matrix and CNTs resulting in an ineffective load sharing by the CNTs during the wear test. The softer phase (polymer matrix alone) may act as weak areas for the initiation of failure/peeling off of the coating. The typical frictional graphs, photographs of the wear track showing the exposed substrate and the scar mark on counterface ball as shown in Figure 4.21 confirmed the failure of all samples except Sample-B.



**Figure 4.20 Comparison of average wear life of CNT-nanocomposite coatings for 10,000 cycles at a normal load of 12 N**

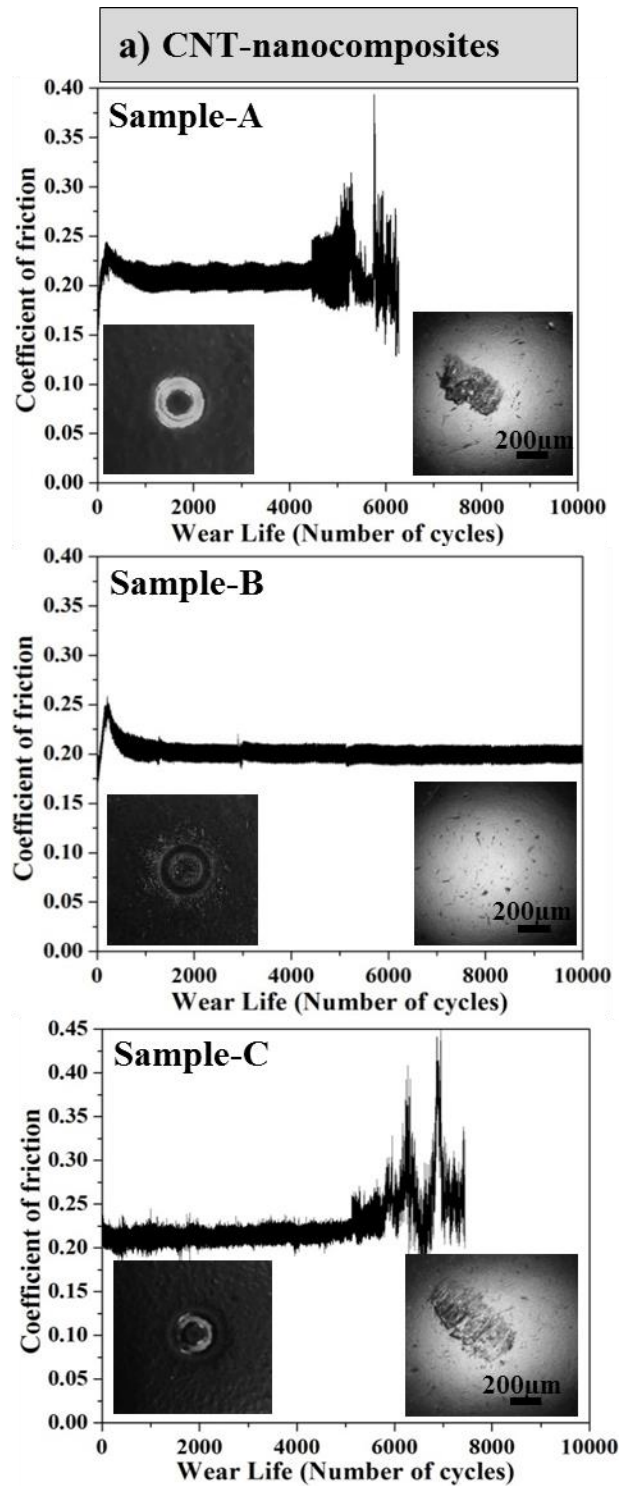


Figure 4.21 Typical frictional graphs of CNT-nanocomposite coatings for 10,000 cycles at a normal load of 12 N. Inset (left): Photographs of wear tracks on samples. Inset (right): Optical images of counterface at 10x (captured after cleaning with acetone) at the end of sliding test

Regarding COF, slight changes were observed as its average value increased from ~0.17 (for pristine UHMWPE) to ~0.2 for CNT-nanocomposite coatings respectively as expected due to the hardness of CNTs. The COF results are presented in Figure 4.22.

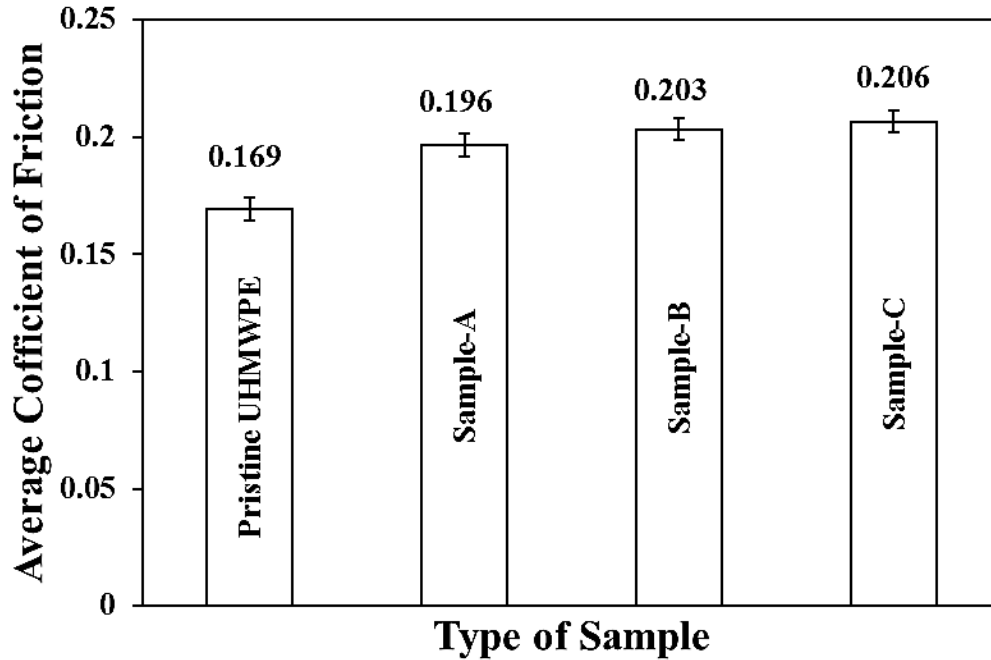
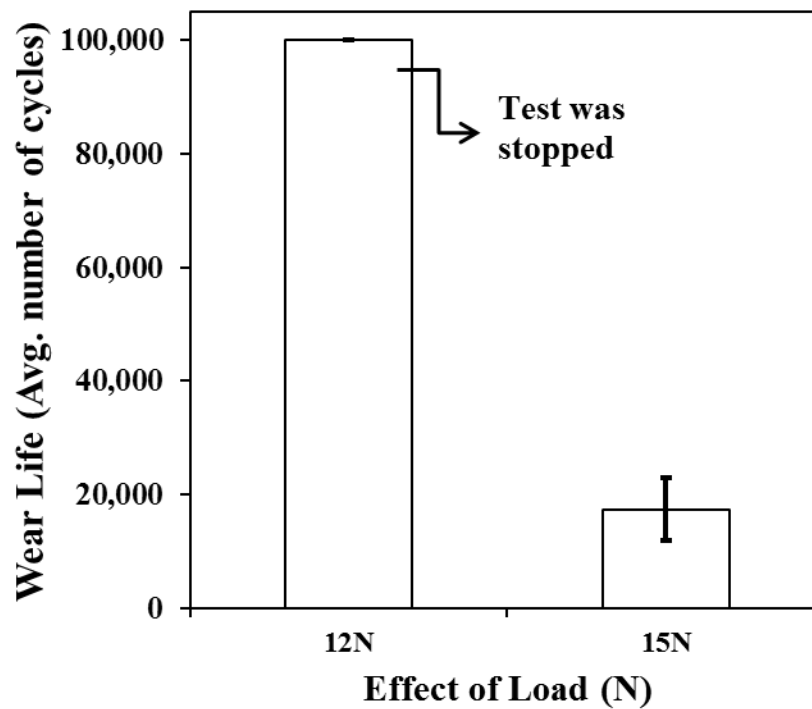


Figure 4.22 Comparison of average coefficient of friction of pristine and CNT/ UHMWPE nanocomposite coatings

After these screening tests, Sample-B was found to be best in terms of wear life which was further tested for longer durations of 100,000 cycles (sliding distance = 1.3 km) at 12 and 15 N respectively with the same linear speed of 0.1 m/s (480 rpm). From Figure 4.23, it can be seen that at 12 N the nanocomposite coating (Sample-B) did not fail until 100,000 cycles while this coating failed very early at 15 N. FE-SEM images of wear tracks of Sample-B (a & b) after sliding tests conducted at normal loads of 12 and 15 N along with their corresponding EDS analysis on the wear track and 2D-Optical wear profiles are shown in Figure 4.24. It is clearly seen that at 15 N there was a complete failure of the coating as EDS confirmed the peaks of bare aluminum substrate (which appears at 1.49

keV) on the wear track and the wear profile depths (Z) reached to  $\sim 180\text{ }\mu\text{m}$  which actually is the thicknesses of the coatings. However, at 12 N, no peak of bare aluminum substrate on the wear track was observed and the wear profile depth (Z) was also less than the coating thicknesses which confirmed that this coating did not fail. The predominant wear mechanism involved in the coating at 12 N was plastic deformation.



**Figure 4.23 Comparison of average wear life of Sample-B (1.5CNT/UHMWPE) at normal loads of 12 and 15 N for 100,000 cycles**

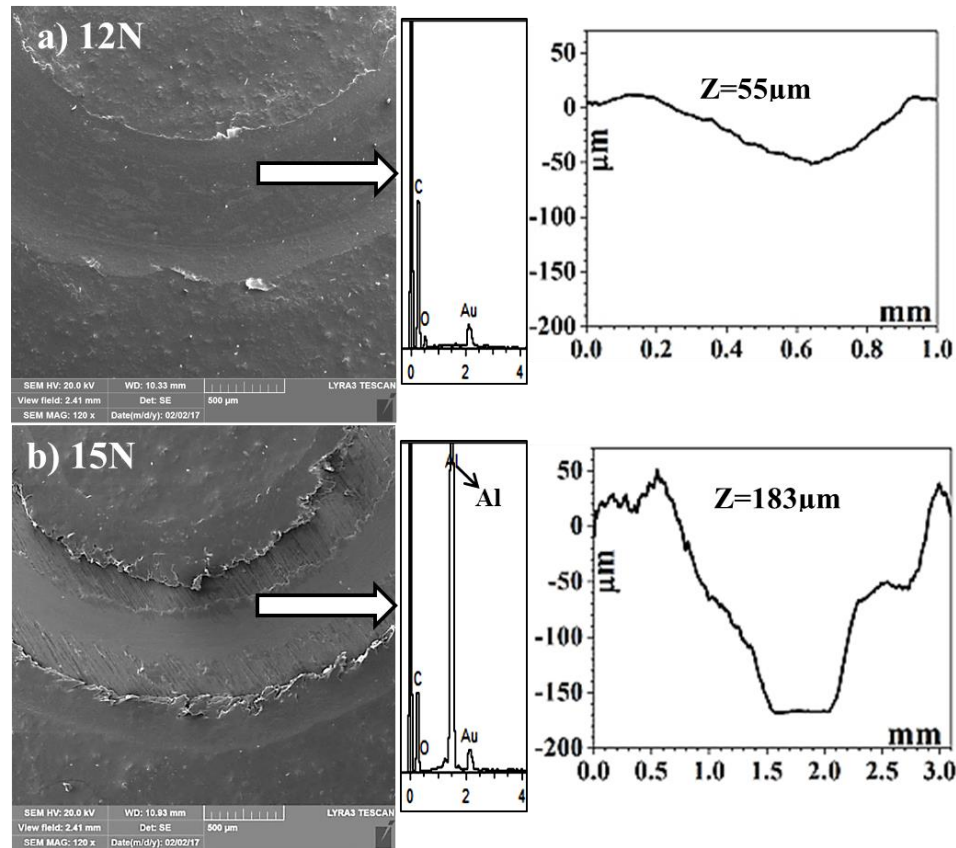


**Figure 4.24** FE-SEM images of wear tracks of Sample-B (a & b) after sliding tests conducted at normal loads of 12 and 15 N for 100,000 cycles. Inset (middle): EDS analysis at wear track. Inset (right): 2D-Optical wear profiles of wear tracks

#### 4.2.7 Summary

From this section, it is found that among the three combinations of CNT/UHMWPE nanocomposite coatings, only 1.5 wt% CNT/UHMWPE nanocomposite coating exhibited excellent wear life as it did not fail even until ~100,000 cycles at a normal load of 12 N and a linear sliding speed of 0.1 m/s. This improvement in the tribological performance is attributed to the uniform dispersion of CNTs in the UHMWPE polymer matrix that provides a bridging effect and holds the polymer chains together instead of being pulled out easily. However, the 1.5wt% CNT/UHMWPE nanocomposite coating failed at a higher load of 15 N.



### **4.3 Development and characterization of CNTs/C15A/UHMWPE**

#### **Hybrid nanocomposite coatings**

From section 4.2, we concluded that 1.5 wt% CNT/UHMWPE nanocomposite coating (optimized coating) showed a wear life of ~ 100,000 cycles at a normal load of 12 N. Hence to further improve the wear resistance of the nanocomposite coating, we took an approach of developing a hybrid nanocomposite coating by reinforcing the polymer matrix by two nano fillers, namely, nanoclay and CNTs. Even though, nanoclays are known for their excellent barrier properties such as improving the resistance to water uptake, they are also known to impart good mechanical properties when used as a reinforcement in polymer matrices [7]. Hence, in this phase we wanted to evaluate the mechanical/tribological properties of the CNT/UHMWPE nanocomposite coating with the addition of 1.5wt% of C15A nanoclay which was the optimum amount obtained from section 4.1 with different loadings (0.5, 1.5 and 3 wt%) of CNTs. This shall help in understanding the interaction effects of each of the nanofillers with each other and with the polymer matrix on the tribological properties of the coating. Table 4.2 shows compositions of samples with their respective designations used in this study.

**Table 4.2 Classification and designation of samples in section 4.3**

Sample type	Composition	Sample Designation	Group Designation
UHMWPE	Pristine	Pristine UHMWPE	Pristine
C15A/CNT/UHMWE Hybrid nanocomposite	0.5 wt% CNT/1.5 wt% C15A/UHMWPE	Sample-D	Hybrid nanocomposites
	1.5 wt % CNT/1.5 wt% C15A/UHMWPE	Sample-E	
	3 wt% CNT/1.5 wt% C15A/UHMWPE	Sample-F	

#### **4.3.1 XRD analysis of pristine and Hybrid nanocomposite powders**

Figure 4.25 shows the characteristic peaks for pristine UHMWPE at  $21.66^\circ$  and  $24.16^\circ$  corresponding to (110) and (200) planes respectively [98], for CNTs at  $25.58^\circ$  corresponding to (002) plane [105], for C15A at  $2.9^\circ$  (typical basal reflection) and at  $19.9^\circ$  [99]. In all hybrid nanocomposites, characteristic peaks of CNT as well as of C15A nanoclay are absent as shown in Figure 4.25 which shows that the nanofillers are dispersed uniformly in the UHMWPE matrix. However, the intensity of UHMWPE characteristic peaks in hybrid nanocomposites decreased with the increase in nanofiller concentrations.

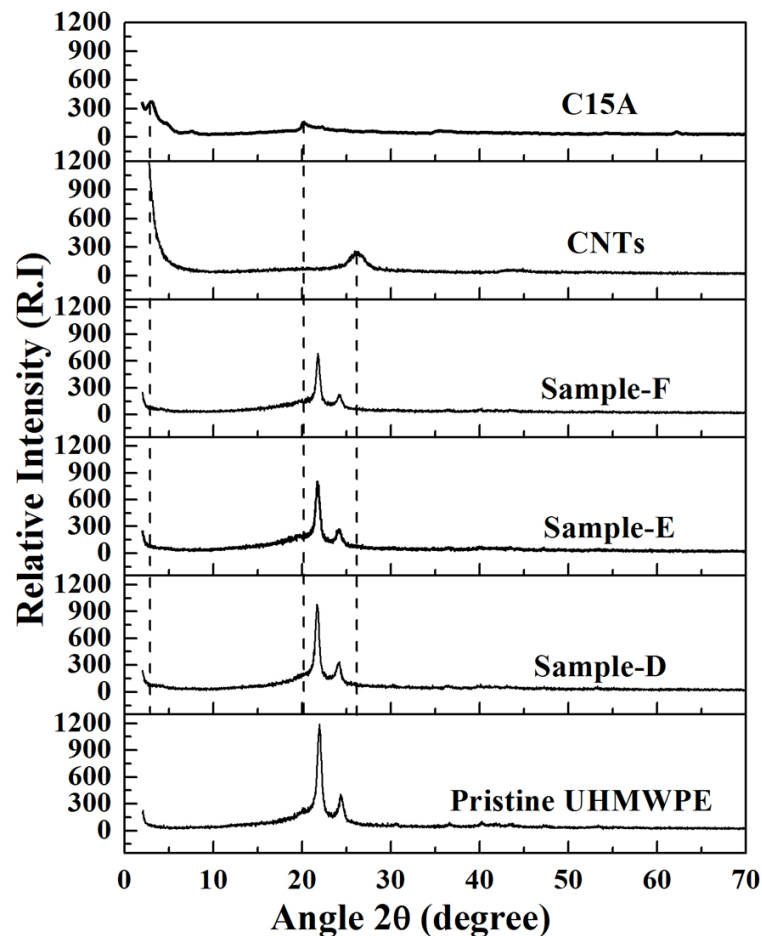


Figure 4.25 XRD patterns of Hybrid nanocomposite powders

### 4.3.2 Raman spectroscopy of pristine and Hybrid nanocomposite powders

Figure 4.26 show the Raman spectra of hybrid nanocomposites along with the spectra of UHMWPE and CNTs in the range of  $1000\text{--}2000\text{ cm}^{-1}$ . Similar to section 4.2.2, it can be seen in Figure 4.26 that with the addition of CNTs in UHMWPE, G band in all hybrid nanocomposites shifted towards higher frequency. However, the maximum shift of  $14\text{ cm}^{-1}$  in G band was observed for Sample-E (1.5% CNTs/1.5% C15A/UHMWPE) showing excellent interaction of nanofillers with the polymer matrix with a good transfer load carried by nanofillers [111] .

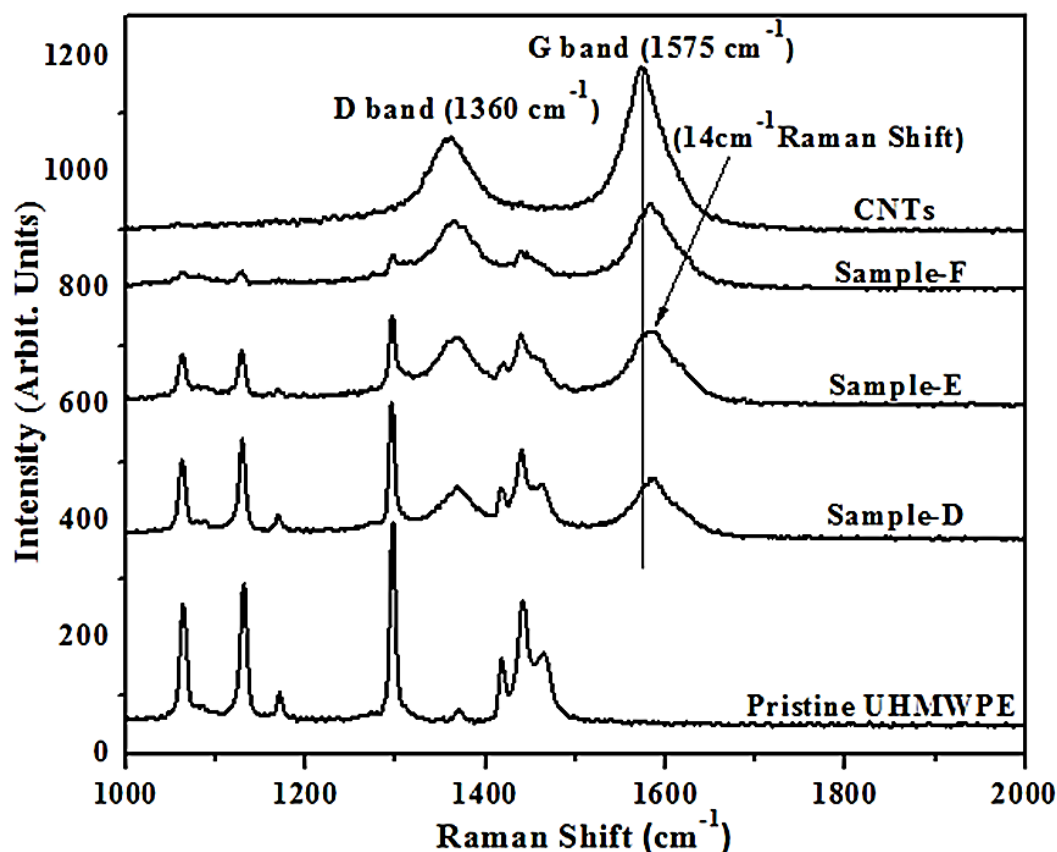


Figure 4.26 Raman spectra for Hybrid nanocomposite powders

### 4.3.3 Evaluation of the coatings for dispersion of nanofillers and thickness measurements

FE-SEM images of the cross section of hybrid nanocomposite coatings were evaluated to conduct the dispersion analysis of nanofillers in polymer matrix at magnification of 50,000 x as shown in Figure 4.27. There were no or negligible signs of CNTs agglomeration for Sample-D and E but Sample-F showed agglomeration of CNTs and nanoclay which indicates the ineffective dispersion and bonding between polymer and nanofillers as the CNTs content increased.

In Figure 4.28, thicknesses of coatings are reported which are the average of three readings with a variation of  $\pm 5\text{ }\mu\text{m}$ . In case of pristine UHMWPE coating, thickness was found to

be about 125  $\mu\text{m}$ . Whereas, in case of hybrid nanocomposite coatings, approximately similar but higher values ( $\sim 180\ \mu\text{m}$ ) as compared to pristine UHMWPE coatings were observed. This trend was found to be similar as in section 4.2.3.

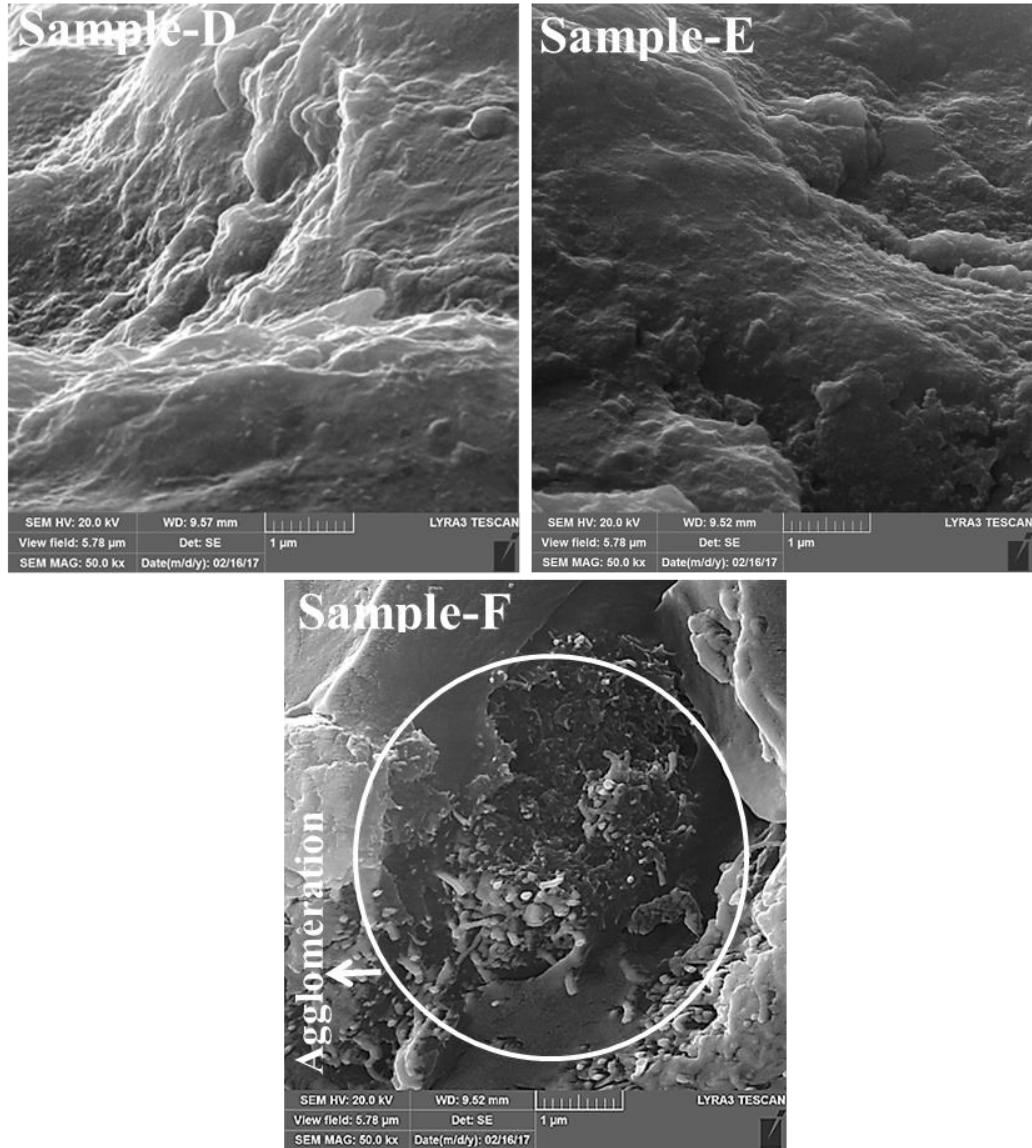


**Figure 4.27** FE-SEM images of Hybrid nanocomposite coatings

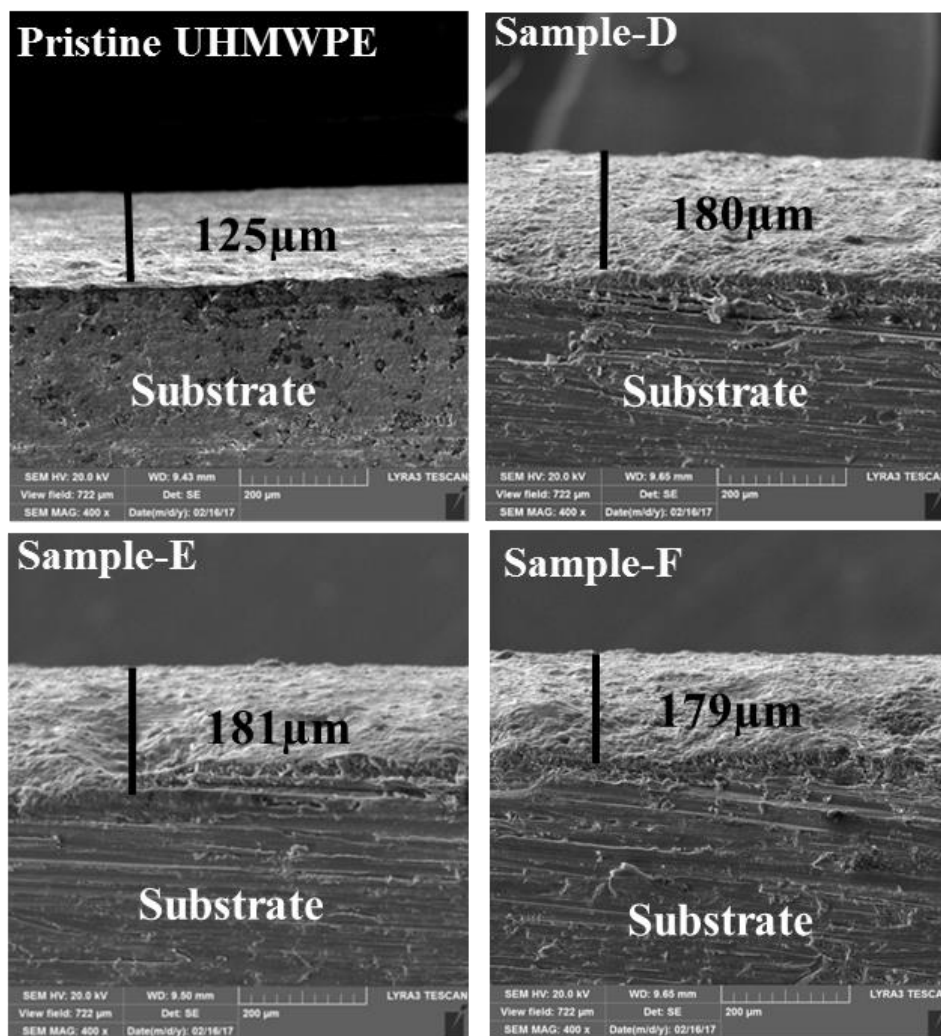


Figure 4.28 FE-SEM images of the cross-section of pristine and Hybrid nanocomposites coatings

#### 4.3.4 Surface characterization of the coatings

Surface roughness ( $R_a$ ) of CNT/C15A/UHMWPE hybrid nanocomposite coatings are shown in Figure 4.29 showing 3D images of coating's surfaces. It can be noticed that there was decrease in roughness of nanocomposite coatings as compared to that of pristine UHMWPE ( $\sim 6 \pm 1 \mu\text{m}$ ) due to the addition of CNT in polymer matrix because of excellent thermal conductivity of CNTs.

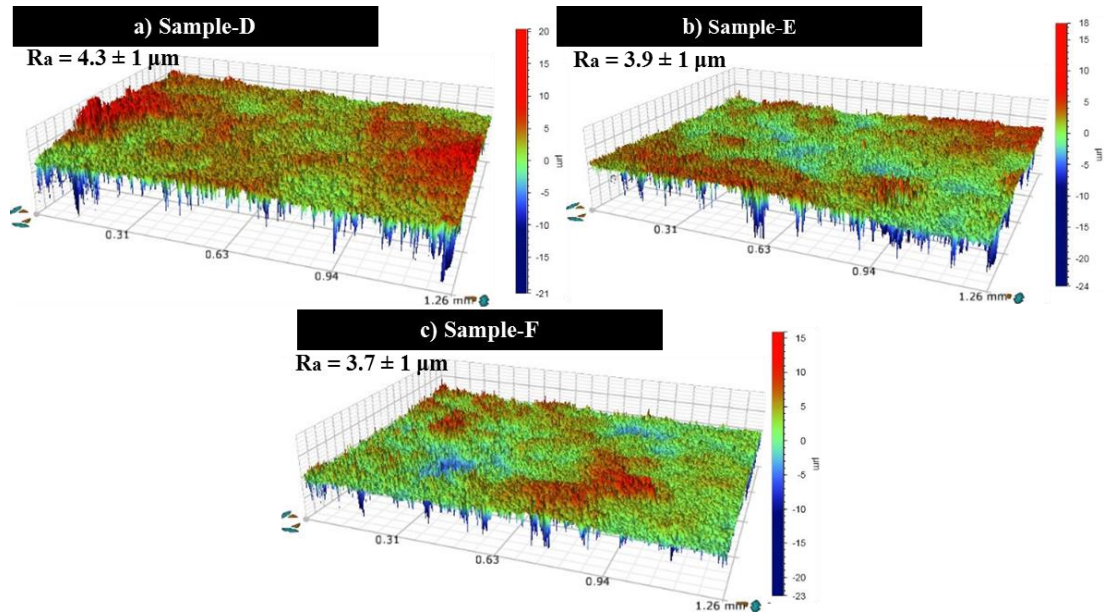


Figure 4.29 Surface roughness (Ra) of Hybrid nanocomposite coatings with different loadings of nanofillers

#### 4.3.5 Hardness evaluation of pristine and Hybrid nanocomposite coatings

Generally, increase in the hardness was found with the increase of loadings of nanofillers (CNTs and nanoclay) in polymer matrix which is attributed to excellent mechanical properties of CNTs in the soft polymer matrix holding the polymer chains together resulting in greater resistance to penetration or indentation. In case of hybrid nanocomposite coatings, clay platelets also participated in anchoring the polymer matrix. Hence maximum hardness was observed for Sample-F (3CNTs/1.5C15A/UHMWPE). Figure 4.30 compares the average hardness values of all types of coatings.

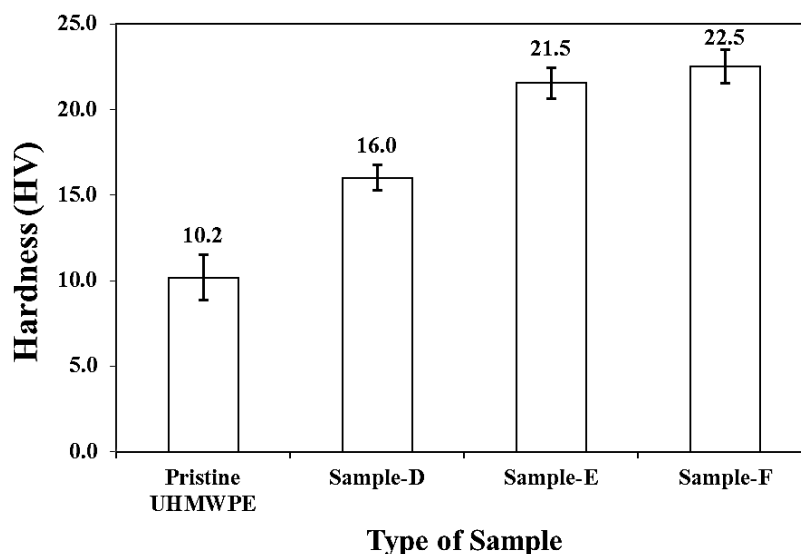


Figure 4.30 Effect of different loadings of CNTs/C15A on hardness of coatings

#### 4.3.6 Tribological performance of the pristine and Hybrid nanocomposite coatings under dry conditions

In order to evaluate the increase in load bearing capacity, hybrid-nanocomposite coatings of above mentioned compositions in Table 4.2 were developed and evaluated at normal loads of 9, 12 N respectively for screening purposes at a linear sliding speed of 0.1m/s (480 rpm) for 10,000 cycles corresponding to a sliding distance of 125 m. Wear track radius for all tests was kept constant at 2 mm. It is to be noted that the wear tests were stopped in case there was an indication of a large value of COF (beyond ~0.3) suggesting a metal to metal contact because of the failure of coating. It was observed that all the hybrid-nanocomposite coatings did not fail until 10,000 cycles at a normal load of 9 N. However, at 12 N the behavior of the hybrid-nanocomposite coatings was as follows. From Figure 4.31, it can be seen that, only Sample-E (1.5wt% CNT/1.5wt% C15A/UHMWPE) did not fail until 10,000 cycles due to an efficient anchoring/bridging effect offered by both the reinforcements, CNTs and C15A nanoclay, respectively in the UHMWPE matrix as



confirmed by the SEM image of nanocomposite coating (Figure 4.27) which helps in anchoring the polymer chains in the matrix and preventing them from being pulled out. However, the failure of Sample-D (0.5 wt% CNTs) earlier than 10,000 cycles can be attributed to the insufficient amount of CNTs leading to an ineffective anchoring of the polymer chains of the matrix while the failure of Sample-F (3 wt% CNTs) can be attributed to the agglomerations of CNTs and nanoclay or possible formation of two phase structures; softer phase (polymer matrix alone) and harder phase (nanofiller's agglomerates because of their high surface energy) as indicated in Figure 4.27 causing poor bonding and inefficient bridging effect between the polymer matrix and CNTs resulting in an ineffective load sharing by the CNTs as well as nanoclay during the wear test. The softer phase (polymer matrix alone) may act as weak areas for the initiation of failure/peeling off of the coating. The typical frictional graphs, photographs of the wear track showing the exposed substrate and the scar mark on counterface ball as shown in Figure 4.32 confirmed the failure of all samples except Sample-E.

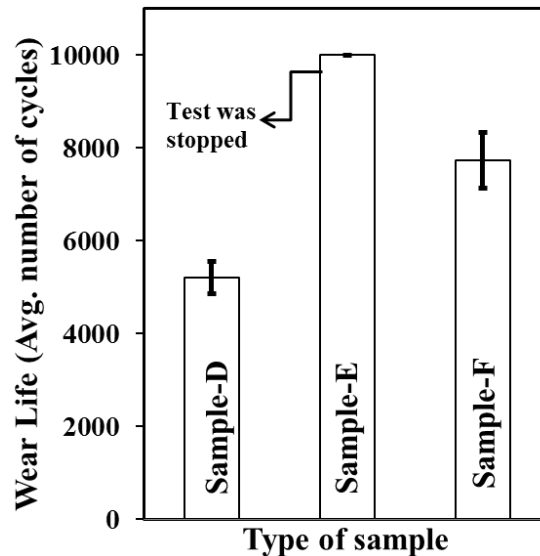


Figure 4.31 Comparison of average wear life of Hybrid nanocomposite coatings for 10,000 cycles at a normal load of 12N

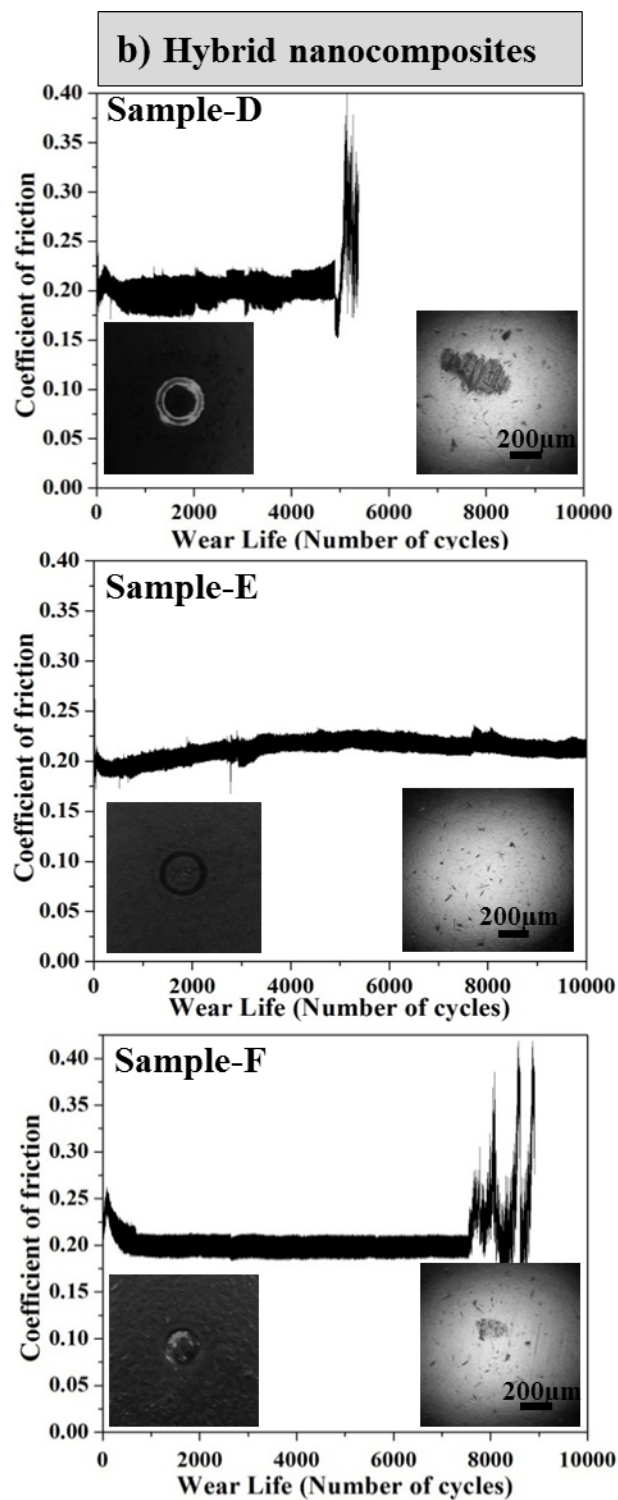
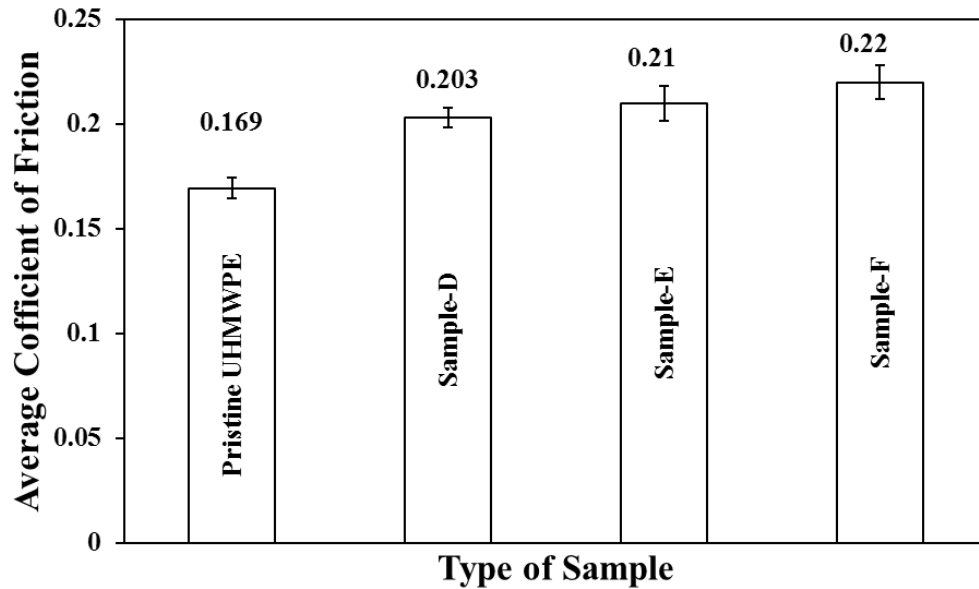


Figure 4.32 Typical frictional graphs of Hybrid nanocomposite coatings for 10,000 cycles at a normal load of 12 N. Inset (left): Photographs of wear tracks on samples. Inset (right): Optical images of counterface at 10x (captured after cleaning with acetone) at the end of sliding test

Regarding COF, slight changes were observed as its average value increased from ~0.17 (for pristine UHMWPE) to ~0.21 for hybrid-nanocomposite coatings respectively as expected due to the hardness of CNTs. The COF friction results are presented in Figure 4.33.



**Figure 4.33 Comparison of average coefficient of friction of pristine and CNT/C15A/ UHMWPE hybrid nanocomposite coatings**

After these screening tests, Sample-E was found to be best in terms of wear life which was further tested for longer durations of 100,000 cycles (sliding distance = 1.3 km) at 12 and 15 N respectively with the same linear speed of 0.1 m/s (480 rpm). From Figure 4.34, it can be seen that at 12 N the nanocomposite coating (Sample-E) did not fail until 100,000 cycles while this coating failed very early at 15 N. FE-SEM images of wear tracks of Sample-E (a & b) after sliding tests conducted at normal loads of 12 and 15 N along with their corresponding EDS analysis on the wear track and 2D-Optical wear profiles are shown in Figure 4.35. It is clearly noticed that at 15 N there was a complete failure of the coating as EDS confirmed the peaks of bare aluminum substrate (which appears at 1.49

keV) on the wear track and the wear profile depths (Z) reached to  $\sim 180\text{ }\mu\text{m}$  which actually is the thicknesses of the coatings. However, at 12 N, no peak of bare aluminum substrate on the wear track was observed and the wear profile depth (Z) was also less than the coating thicknesses which confirmed that this coating did not fail. The predominant wear mechanism involved in the coating at 12 N was plastic deformation.

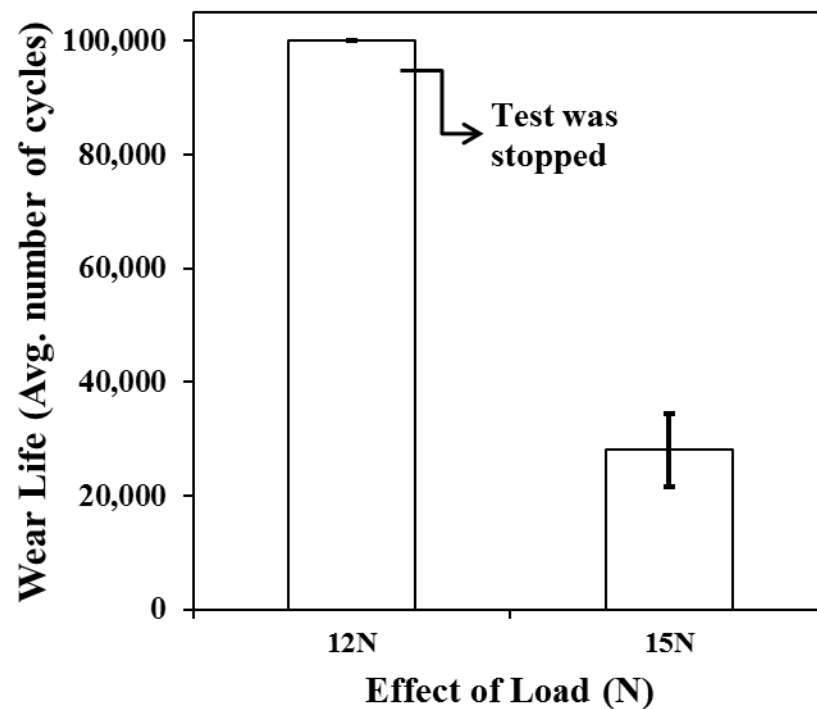
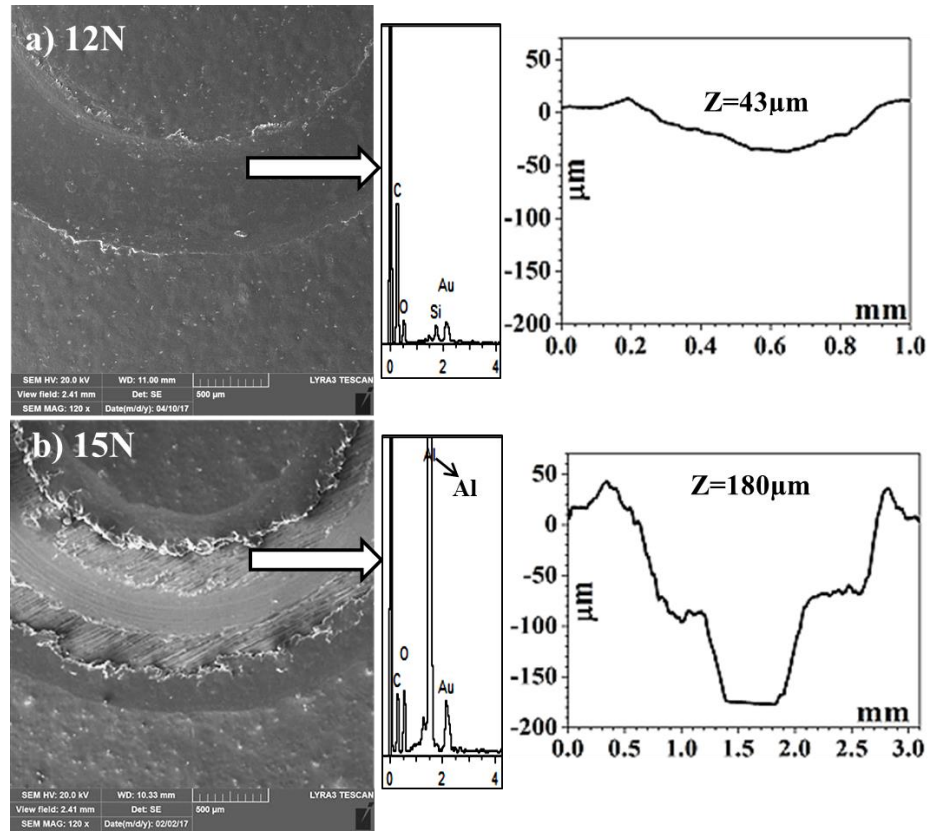


Figure 4.34 Comparison of average wear life of Sample- E (1.5CNT/1.5C15A/UHMWPE) at normal loads of 12 and 15 N for 100,000 cycles



**Figure 4.35 FE-SEM images of wear tracks of Sample-E (a & b) after sliding tests conducted at normal loads of 12 and 15 N for 100,000 cycles. Inset (middle): EDS analysis at wear track. Inset (right): 2D-Optical wear profiles of wear tracks**

In case of hybrid nanocomposite coating (Sample-E), the wear track profile depth ( $Z$ ) was less ( $43\mu\text{m}$ ) as compared to  $55\mu\text{m}$  in case of CNT-nanocomposite coating (Sample-B) as reported in section 4.1.5 earlier indicating the improved wear resistance due to addition of nanoclay into the polymer matrix along with CNTs. Figure 4.36 below shows the comparison of wear track profile depths ( $Z$ ) of both coatings.

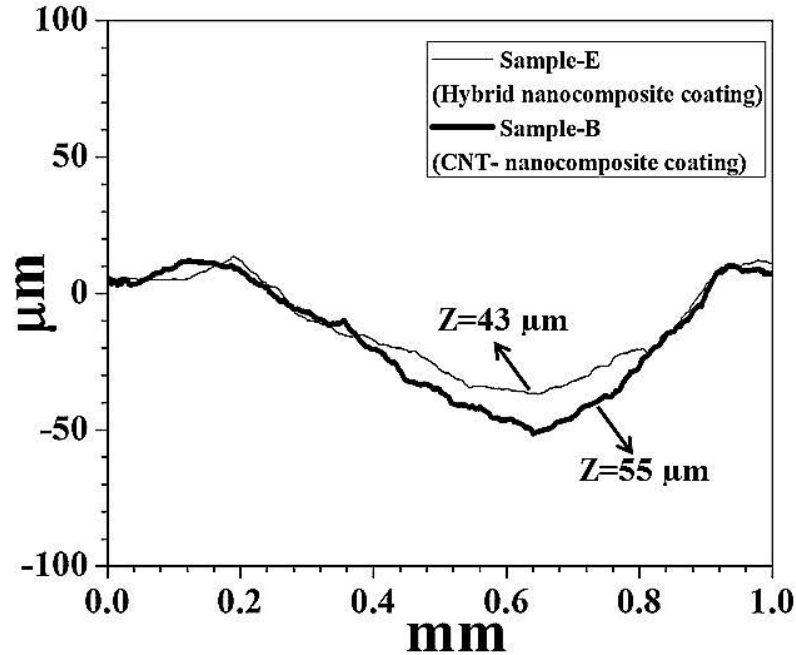


Figure 4.36 Comparison of wear track profile depths (Z) of Sample-E and Sample-B (optimized coatings) after wear test conducted at a normal load of 12 N and linear speed of 0.1 m/s for 100,000 cycles

#### 4.3.7 Effect of linear sliding speed on tribological performance of Sample-E (1.5CNT/1.5 C15A/UHMWPE) hybrid coating

After the above screening tests, it was confirmed that only 1.5 wt% CNT/1.5 wt% C15A/UHMWPE hybrid nanocomposite coating (Sample-E) did not fail at a normal load of 12 N until 100,000 cycles. To further investigate the tribological performance of this particular hybrid coating, wear tests were performed at different linear speeds of 0.1, 0.2 and 0.3 m/s at a normal load of 12 N for 25,000 cycles (sliding distance = 314 m) and wear track radius of 2 mm.

Figure 4.37 shows that hybrid nanocomposite coating at linear speeds of 0.1 and 0.2 m/s did not fail even until ~25,000 cycles as confirmed by the corresponding photograph of wear tracks on samples as well as wear track profile depths (Z) which were only 39  $\mu\text{m}$  and 60  $\mu\text{m}$  (less than the coating thickness of 180  $\mu\text{m}$ ) respectively as shown in Figure 4.38.

However, the coating failed at a linear sliding speed of 0.3 m/s showing an average wear life of ~10,000 cycles. The corresponding photograph of sample showing a peel off of the coating and wear profile depths approaching to the value of the thickness of coating (180  $\mu\text{m}$ ) confirmed the failure of the coating at a linear sliding speed of 0.3 m/s. As explained earlier, the contact temperature plays a significant role in wear of the polymers. Since UHMWPE polymer starts to lose its dimensional stability above 80 to 90  $^{\circ}\text{C}$  [3], it is possible that by increasing the linear sliding speed, the localized contact temperature would have been raised beyond 80 to 90  $^{\circ}\text{C}$  which caused the softening of the polymer resulting in the failure of the coatings at higher linear sliding speeds.

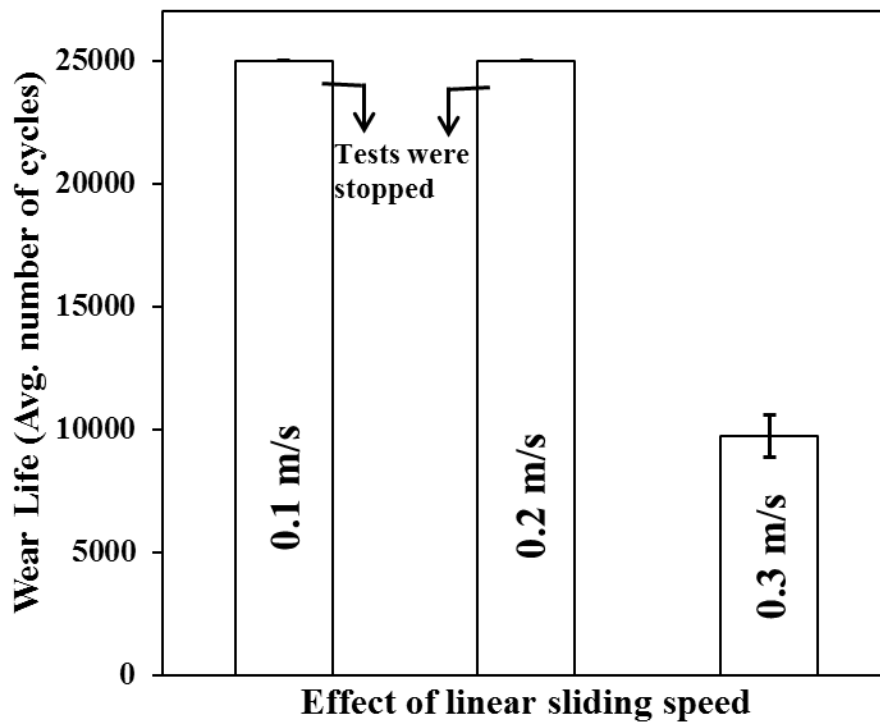


Figure 4.37 Comparison of average wear life of Sample- E (1.5CNT/1.5C15A/UHMWPE) at normal loads of 12N for 25,000 cycles at three different sliding velocities

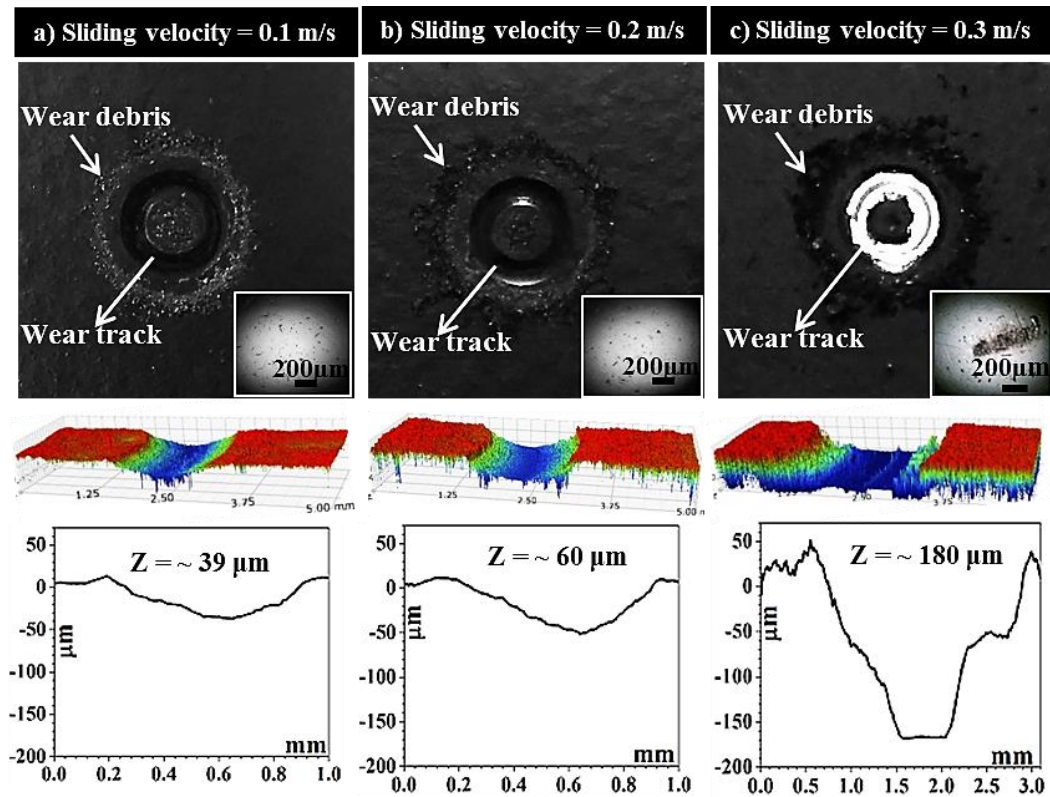


Figure 4.38 Photographs of wear tracks of sample along with their corresponding 3D-optical profile images (middle) and wear track profile depths (Z) (lower) at a normal load of 12 N for 25,000 cycles at three different velocities. Inset: cleaned counterface ball images after the wear tests

However, it is interesting to note the improvement in the wear life of the hybrid coatings as compared to that of the 1.5wt% C15A/UHMWPE coating (as obtained in section 4.1) with the addition of CNTs. It can be recollected from the results of section 4.1 that the 1.5wt% C15A/UHMWPE coating failed earlier than 25000 cycles at a load of 9N and a linear sliding speed of 0.2 m/s. However, the 1.5 wt% CNT/1.5 wt% C15A/UHMWPE hybrid nanocomposite coating did not fail until 25000 cycles at a higher load of 12 N and a linear sliding speed of 0.2 m/s. This improvement can be attributed to the addition of CNTs which are effective in increasing the load bearing capacity of the coating due to their inherent excellent mechanical properties and also to their higher thermal conductivity which helps in dissipating of the local heat generated from the contact region at higher



speeds, thus preventing the softening of the polymer leading to less wear. However, the hybrid nanocomposite coating failed at higher sliding speeds of 0.3 m/s, suggesting that it can withstand a maximum velocity of 0.2 m/s.

#### **4.3.8 Summary**

From the results of this section, we observed that of all the combinations of nanoclay and CNTs tested, the 1.5 wt% C15A/1.5 wt% CNT/UHMWPE hybrid nanocomposite coating showed the best wear resistance. Moreover, it is also noted that the wear resistance of the 1.5 wt% C15A/1.5 wt% CNT/UHMWPE was better than the wear resistance of the 1.5 wt% CNT/UHMWPE nanocomposite coating under dry conditions. This improvement in the wear resistance is attributed to the addition of nanoclay which imparts better bridging/anchoring effect to the polymer matrix preventing the easy pull out of the polymer chains.

#### **4.3.9 Summary of Phase 1 showing the performance of the coatings under dry conditions**

Following are the overall results obtained from sections 4.1 (nanoclay/UHMWPE), 4.2 (CNT/UHMWPE) and 4.3 (CNT/C15A/UHMWPE) which are compiled in figures below to compare the improvement in mechanical and tribological performance of all the nanocomposite and hybrid nanocomposite coatings (developed in current study) with pristine UHMWPE coating.

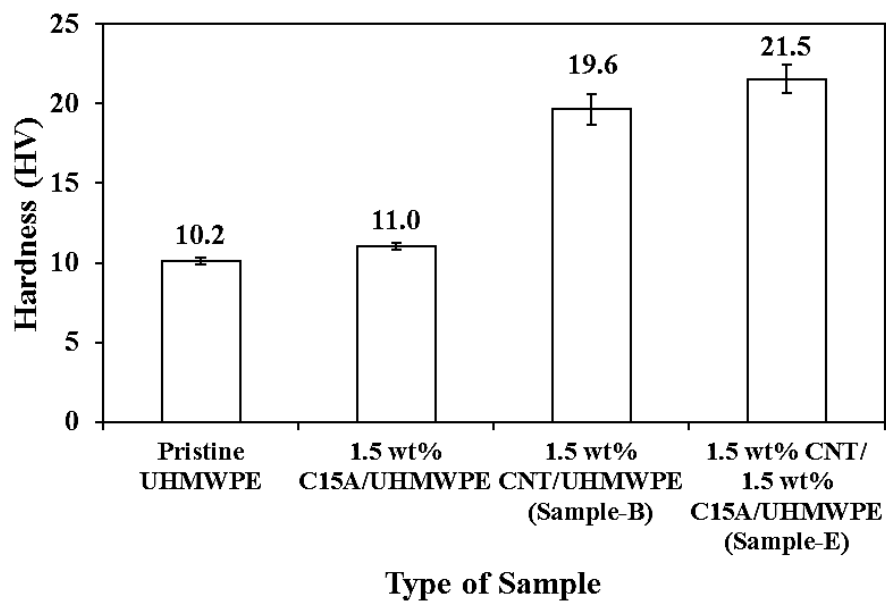


Figure 4.39 Comparison of the hardness of the coatings

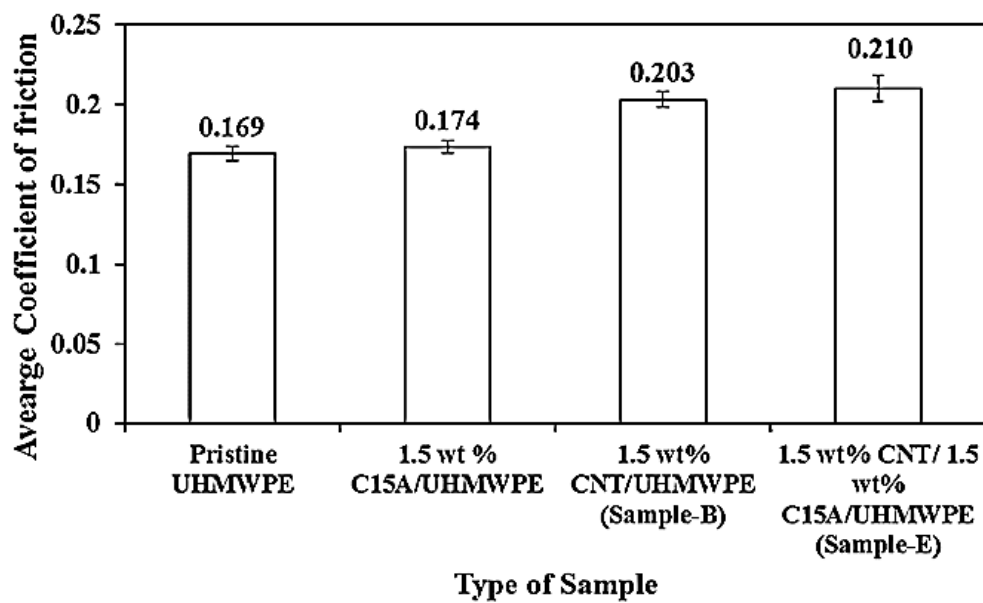


Figure 4.40 Comparison of the average COF of the coatings

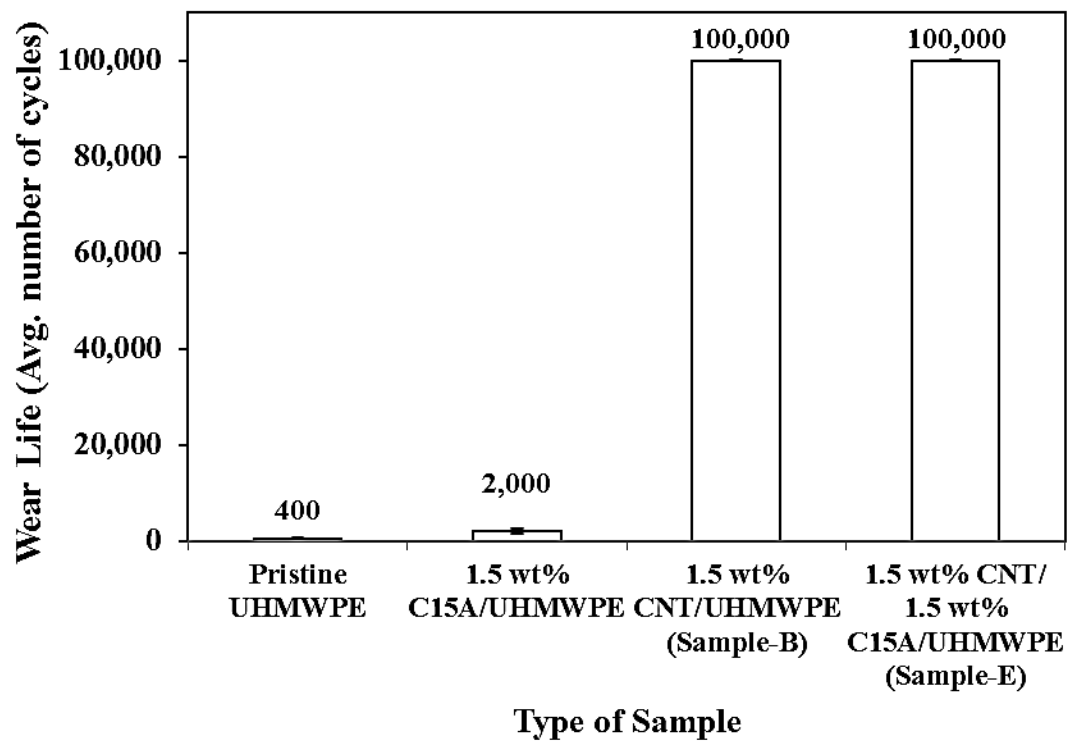


Figure 4.41 Comparison of the average wear life of coatings at a normal load of 12 N and a sliding speed of 0.1 m/s for 100,000 cycles

## **Phase 2 - Tribological characterization of the hybrid nanocomposite coatings under water lubrication with/without abrasives**

In this phase, tribological characterization of the hybrid nanocomposite coatings under water lubrication was evaluated which will be described on section 4.4. Later the tribological performance of the optimized hybrid nanocomposite coating was evaluated under water lubrication in the presence of abrasives which will be described on section 4.5.

### **4.4 Tribological characterization of the hybrid nanocomposite and the optimized CNT nanocomposite coatings under water lubrication**

The evaluation of tribological performance of polymer coatings under aqueous environment becomes important because sometimes water is entrained into sliding components of machineries which are being used in different fields such as food and chemical industries; either accidentally (through any leakage), deliberately (as a coolant or lubricant) or as a contaminant (as humidity or rain) etc. In these conditions, different factors such as the surface wettability, interaction of polymer with water and formation of transfer film on counterface etc., significantly affect the tribological behavior of polymers [28]. Water can deteriorate the properties of polymers because polymers get swelled after absorbing water resulting in reduction in their hardness and strength [27].

The objective of this phase was to evaluate the tribological performance of the hybrid nanocomposite coatings under water lubrication. However, since the testing environment is changed from dry to water lubrication conditions, we proceeded to optimize the loadings of the nanoclay and the CNTs in the new conditions.

#### **4.4.1 Evaluation of tribological performance of the coatings under water lubrication**

Tribological performance of hybrid nanocomposite coatings with different loadings of nanofillers as described in Table 4.2 were evaluated under water lubrication at a normal load of 12 N for 150,000 cycles (Sliding distance = 1.9 km) at a sliding speed of 0.1 m/s (480 rpm) and radius 2 mm. It is to be noted that for screening test under water lubrication, higher number of cycles (150,000) were selected as compared to that of under dry conditions where only 10,000 cycles were selected. This is done because polymers exhibit a change in their mechanical and tribological properties usually on prolonged exposure to water. It can be seen from Figure 4.42 that Sample-E (1.5 wt% CNT/ 1.5 wt% C15A/ UHMWPE) showed increased wear life as it did not fail even until 150,000 cycles. This can be attributed to the efficient anchoring/bridging effect offered by both the reinforcements, CNTs and C15A nanoclay, respectively in the UHMWPE matrix in addition to the improvement in the resistance to water uptake offered by the platelet like structure of the nanoclay which offers a torturous path to the diffusion of the water molecule into the polymer matrix. However, Sample-D (0.5 wt% CNT/ 1.5 wt% C15A/ UHMWPE) and Sample-F (3 wt% CNT/ 1.5 wt% C15A/ UHMWPE) failed earlier because of inefficient bridging effect and agglomeration of the nanofillers respectively as described earlier in above phases as well. The corresponding photographs of the wear track showing the exposed substrate as shown in Figure 4.42 confirmed the failure of Sample-D and F.

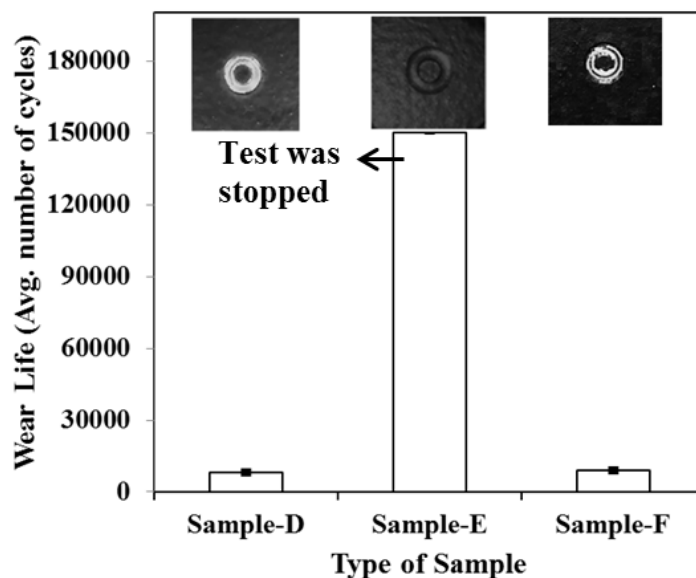


**Figure 4.42** Comparison of the average wear life of Hybrid nanocomposite coatings at normal loads of 12 N and a linear speed of 0.1 m/s for 150,000 cycles under water lubrication. Inset: Photographs of wear tracks on samples.

Furthermore, the most wear resistant coatings such as Sample-B (1.5 wt% CNT/UHMWPE) as obtained in Phase 1 (section 4.2) under dry condition and Sample-E (1.5 wt% CNT/1.5 wt% C15A/UHMWPE) were evaluated for their tribological performance under water lubrication at a normal load of 12 N for a longer duration of 300,000 cycles (Sliding distance = 3.8 km) at a linear speed of 0.1 m/s (480 rpm) and radius 2 mm. Under water lubrication, Sample-E (Hybrid nanocomposite coating) showed increased wear life as it did not fail even until 300,000 cycles after which the test was stopped due to the time constraint (10 h). However, Sample-B (CNT-nanocomposite coating) failed at about ~170,000 cycles as shown in Figure 4.43. The photographs of the wear tracks of the tested samples in inset of Figure 4.43 with the substrate completely exposed confirmed that Sample-B could not survive under water lubrication as the coating completely peeled off from the wear track. This can be attributed to the swelling of the polymer due to the water absorption resulting in the deterioration of the properties. However, Sample-E (hybrid nanocomposite coating) survived until 300,000 cycles as

confirmed by EDS analysis on the wear track as shown in Figure 4.44 where no peak of bare aluminum was observed and wear profile depth ( $112\text{ }\mu\text{m}$ ) was also much less than the coating thickness. The major wear mechanism involved in this particular coating was plastic deformation by ploughing. This improvement in wear life is attributed to the addition of CNTs which helps in improving the load bearing capacity and C15A nanoclay which provides a torturous path for the diffusion of water molecules in the polymer matrix due to its platelet like structure resulting in a significant reduction in the water uptake and hence leading to an improvement in wear resistance. Similar kind of trend was observed in previous study where Samad et al. [74] investigated the effect of water uptake on tribological performance of C15A nanoclay/UHMWPE bulk nanocomposite and found that nanoclay reduced the water absorption upto  $\sim 21\%$  by reinforcing UHMWPE matrix with nanoclay.

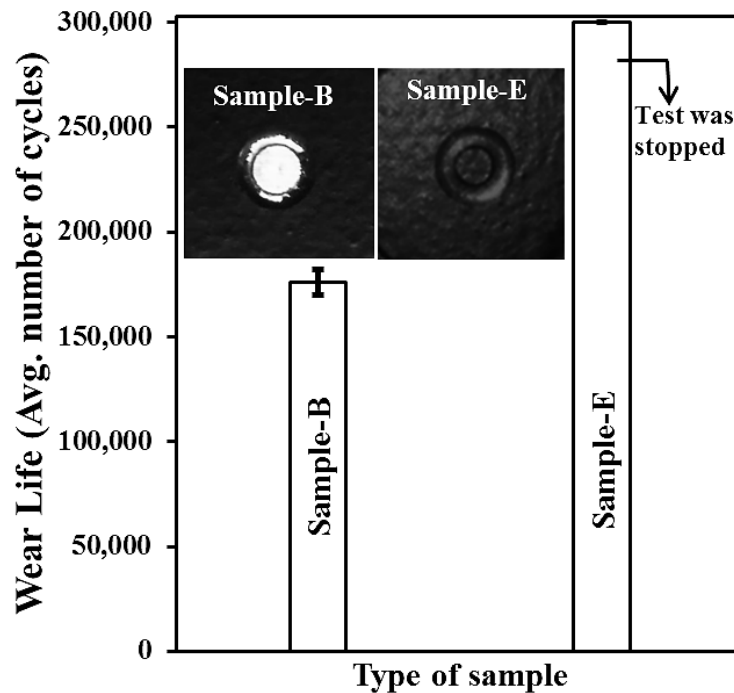


**Figure 4.43 Comparison of the average wear life of Sample (B and E) at normal loads of 12 N for 300,000 cycles under water lubrication. Inset: Photographs of wear tracks on samples.**

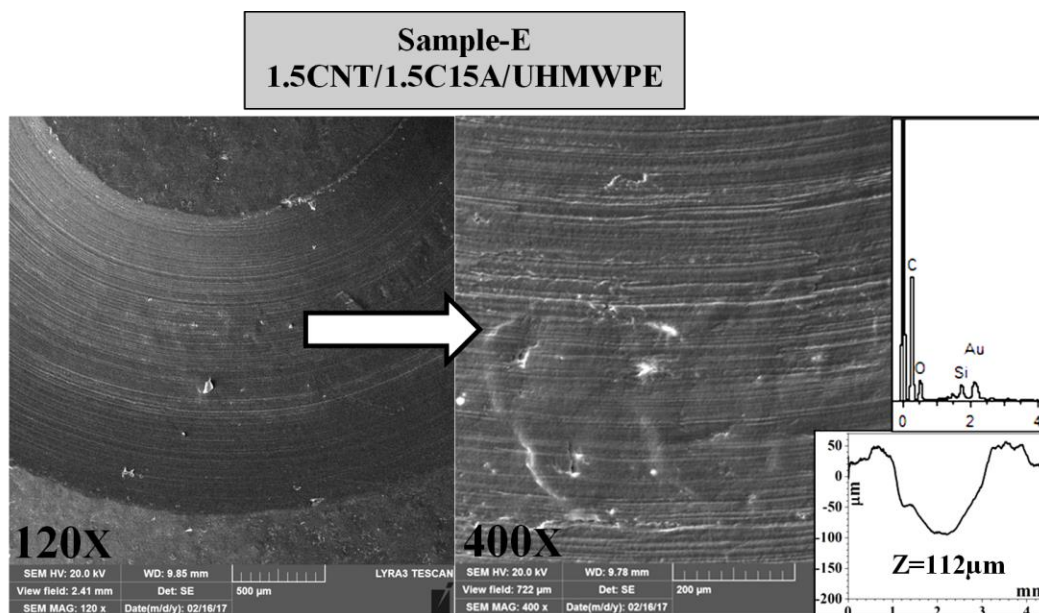


**Figure 4.44 FE-SEM images of wear track of Sample-E at lower and higher magnifications after sliding tests conducted at normal load of 12 N for 300,000 cycles. Inset: EDS analysis and 2D-Optical wear profiles of the wear track**

Figure 4.45 shows the two wear profile depths of the hybrid nanocomposite coating after the wear tests until 150,000 and 300,000 cycles respectively. It can be observed that even though the number of wear cycles doubled, there is hardly any difference between the depth of the wear track showing a significant improvement in the wear resistance of the hybrid nanocomposite coating and indicating that the wear life of the hybrid coating can go beyond 300,000 cycles at a normal load of 12 N. This is primarily attributed to the addition of CNTs which help in improving the load bearing capacity of the coating because of their inherent excellent mechanical properties and secondly to the addition of nanoclays which also contribute to the improvement in the load bearing capacity by increasing the resistance to water uptake.



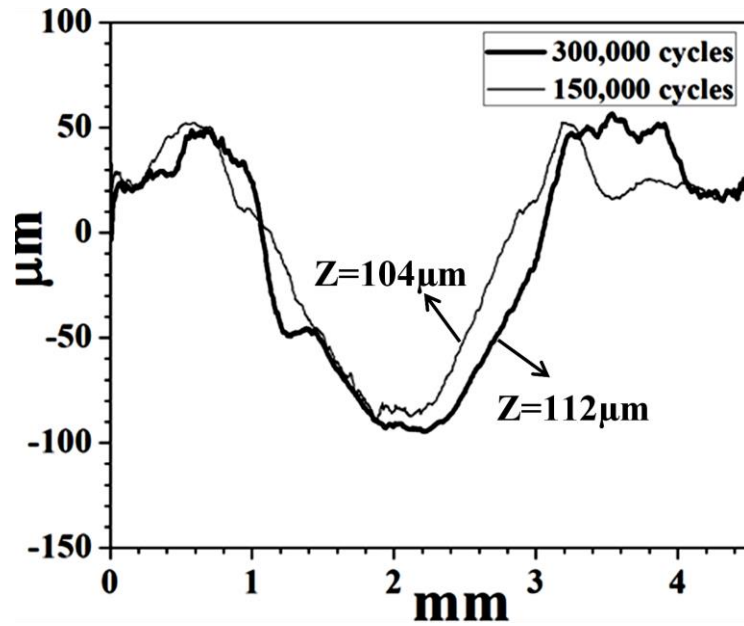


**Figure 4.45 Comparisons of 2D-Optical wear profiles of wear track of Sample-E after sliding tests conducted under water lubrication for 150,000 and 300,000 cycles at normal load of 12 N**

The significant decrease in COF was observed under water lubrication as shown in Figure 4.46 because water can act as a lubricant as also found in many studies [23–25] where similar trend in COF was observed. The COF was found to be ~0.14 under water lubrication. Figure 4.46 shows the comparison of COF of Sample-E after sliding test under dry and water lubrication at a normal load of 12 N and sliding velocity of 0.1 m/s.

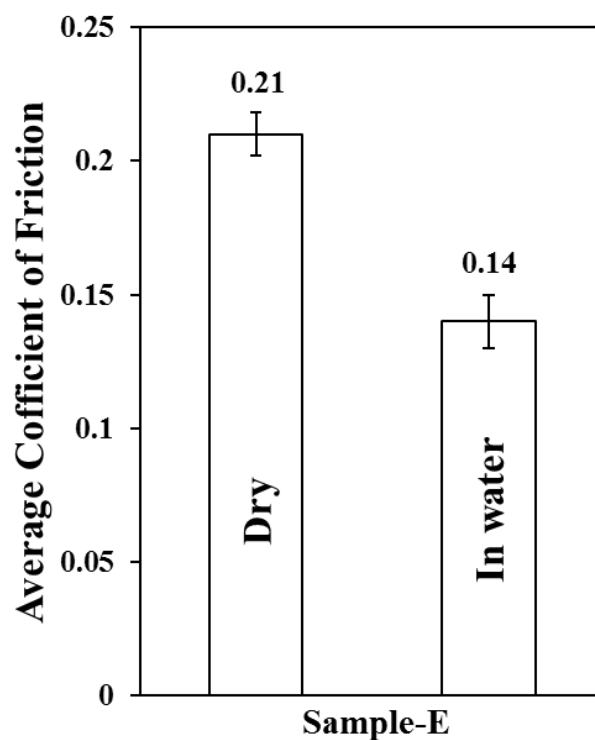


**Figure 4.46 Comparison of COF of Sample-E after sliding test under dry and water lubrication**

To evaluate the possible effect of water interaction on hardness of Sample-E, hardness measurements were carried out before and after the sliding test under water lubrication for 300,000 cycles. Figure 4.47 indicates that there was hardly any change in hardness after the water lubricated test, indicating that the interaction of water with this particular coating did not deteriorate its mechanical properties leading to a significant improvement in its wear resistance. This again is attributed to the addition of nanoclays which help in increasing the resistance to water absorption.

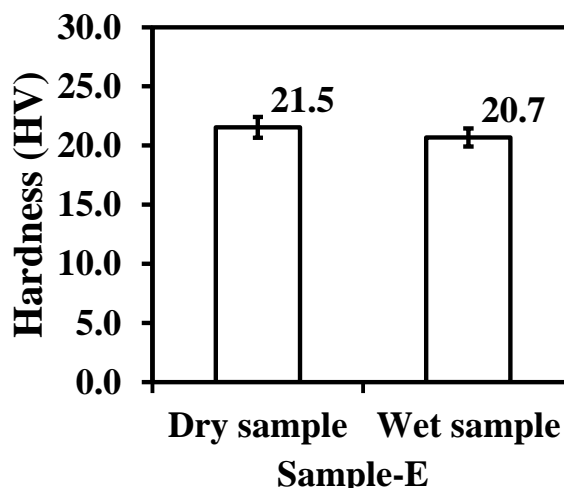


**Figure 4.47** Comparison of hardness of 1.5CNTs/1.5C15A/UHMWPE hybrid nanocomposite coating (Sample-E) before and after conducting the sliding test under water lubrication for 300,000 cycles

#### 4.4.2 Summary

From this section, it is found that among the three combinations of (0.5, 1.5 and 3 wt%) CNT/ 1.5wt%C15A/UHMWPE hybrid nanocomposite coatings, only 1.5 wt% CNT/ 1.5 wt% C15A/ UHMWPE hybrid coating exhibited excellent wear life as it did not fail even until ~300,000 cycles at a normal load of 12 N and a linear sliding speed of 0.1 m/s under water lubrication. This is attributed to the uniform dispersion of CNTs and nanoclays in the polymer matrix that provides an improved bridging effect and holds the polymer chains together instead of being pulled out easily leading to an increase in the load bearing capacity and also to the improvement in the resistance to water absorption due to the addition of nanoclay which provides a torturous path for the diffusion of water molecules in polymer chains resulting in less polymer softening and significantly less wear..

## **4.5 Tribological characterization of Hybrid nanocomposite coating under water lubrication in the presence of abrasive particles**

The evaluation of tribological performance of polymer coatings under aqueous environment in presence of abrasive particles becomes important because sometimes, in some particular cases, there are chances of contamination of water with sand particles due to sandstorm, dusty condition or rain especially in desert environment. These sand particles can either act as third body particles which can abrade the polymer and increase the wear rate [42] or they can be embedded in polymer resulting in reduced wear rate [43]. In this section, the tribological performance of the most wear resistant coating; Sample-E (1.5 wt% CNT/1.5 wt% C15A/UHMWPE) as optimized under water lubrication in section 4.4 above, was evaluated for its tribological performance under water lubrication in the presence of abrasive particles (SiC) at a normal load of 12 N for a duration of 150,000 cycles (Sliding distance = 1.9 km) at a linear speed of 0.1 m/s (480 rpm) and wear track radius of 2 mm.

### **4.5.1 Effect of abrasives on tribological performance of Hybrid nanocomposite coating**

Figure 4.48 compares the typical frictional graphs of 1.5 wt% CNT/1.5 wt% C15A/UHMWPE hybrid nanocomposite coating (a) & (b), FE-SEM images of wear tracks at lower (120 x) and higher (400 x) magnifications (c) & (d), 3D optical profile images of wear tracks (e) & (f) and profile depths of wear tracks (g) & (h) after wear tests performed at normal load of 12 N and linear sliding speeds of 0.1 m/s for 150,000 cycles under water lubricated conditions with/ without abrasive particles.

It is clearly observed from Figure 4.48, the hybrid nanocomposite coating in both the cases (with/ without abrasives), survived until 150,000 cycles as confirmed by EDS analysis on the wear track as shown in insets of Figure 4.48 (c) and (d) where no peak of aluminum was observed. The wear profile depths in both the cases were also much less than the total coating thickness of 180  $\mu\text{m}$ . However, it is interesting to note that the wear profile depth of the hybrid nanocomposite coating was less (80  $\mu\text{m}$ ) in case of the sliding test in the presence of abrasives as compared to that in the absence of abrasives where the wear profile depth was found to be  $\sim 104$   $\mu\text{m}$ . This can be attributed to the embedment of the hard SiC abrasive particles in the softer polymer matrix as indicated by the silicon (Si) peak (appearing at 1.49 keV) in the EDS spectrum on the wear track, which helps in providing with an enhanced anchoring effect of the polymer chains leading to an improvement in the resistance to their easy pull-out. A similar observation was made by [44] wherein the wear rate of a polymer coating reduced in the presence of abrasives. Figure 4.49 shows a schematic of the abrasive particles embedded in softer polymer coating which may have contributed in the improvement in the wear resistance. However, it is to be noted that the hybrid nanocomposite coating is developed for the protection of both the surfaces in a tribo pair against wear and tear. It can be observed from the optical images of the counterface ball with/without as shown in the insets of Figure 4.37 (g) and (h) that the ball got severely abraded when sliding against the hybrid nanocomposite coating in the presence of abrasives as compared to when sliding against the coating in the absence of the abrasives.

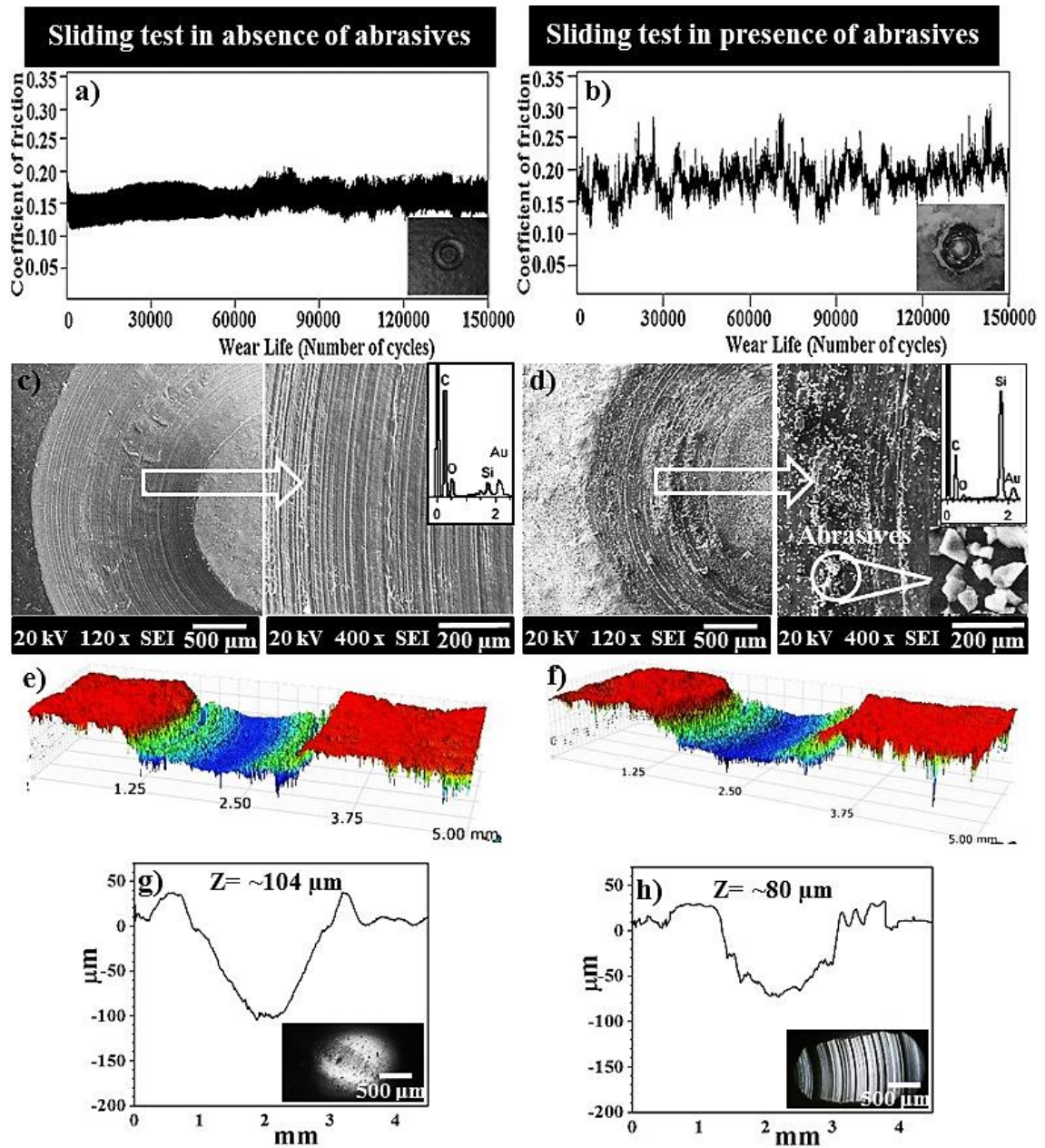
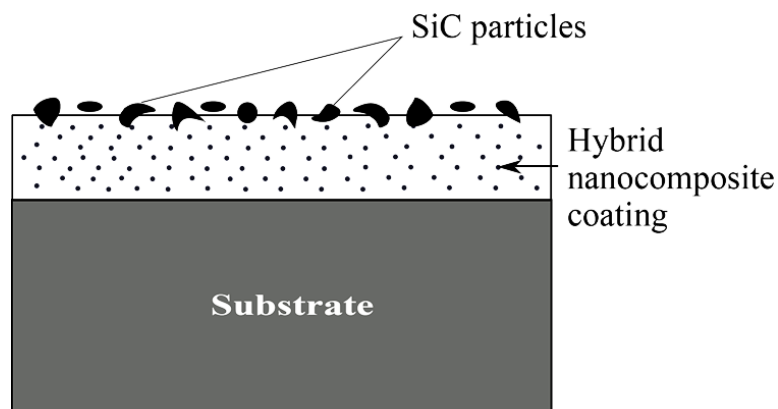


Figure 4.48 Comparison of typical frictional graphs of 1.5 wt% CNT/1.5 wt% C15A/UHMWPE Hybrid nanocomposite coating (a) & (b), FE-SEM images of wear tracks at lower (120 x) and higher (400 x) magnifications (c) & (d), 3D optical profile images of wear tracks (e) & (f) and profile depths of wear tracks (g) & (h) after wear tests performed at normal load of 12 N and linear sliding speeds of 0.1 m/s under water lubricated conditions with/ without the presence of abrasive particles, Counterface ball images (i) & (j) after cleaning with acetone. Insets in (a) & (b) show the wear track on coated sample.



**Figure 4.49** Schematic diagram of abrasive particles embedded in softer polymer coating

## 4.5.2 Summary

In this section, the tribological performance of the hybrid nanocomposite coating (1.5wt% CNT/1.5wt% C15A/UHMWPE) was evaluated in the presence of abrasives at a normal load of 12 N and sliding speed of 0.1 m/s for 150,000 cycles. It was observed that the hybrid nanocomposite coating did not fail even until 150,000 cycles in the presence of abrasives and infact showed better wear resistance due to the embedment of the abrasive particles in the softer polymer matrix which helps in providing with an enhanced anchoring effect of the polymer chains leading to an improvement in the resistance to their easy pull-out. However, the counterface ball showed severe wear in this case.

## **CHAPTER 5**

### **CONCLUSIONS AND RECOMMEDATIONS**

#### **5.1 Conclusions**

In this work, tribological performance of pristine UHMWPE coating was enhanced by reinforcing it with individual nanofillers such as nanoclay, CNTs and their combinations under dry and water lubricated conditions (with/without abrasives). Effect of normal load and linear sliding speed was evaluated on the developed nanocomposite coatings. Following conclusions can be deduced from this study which are summarized below. The conclusions are presented for each phase of the project:

##### **PHASE 1**

Pristine UHMWPE coating failed at a normal load of 9 N and linear sliding speed of 0.1 m/s just after ~5200 cycles. To enhance the tribological properties of pristine UHMWPE coating, initially it was reinforced with C15A nanoclay. C15A/UHMWPE nanocomposite coatings with different loadings (0.5, 1.5, 3 wt%) were developed and evaluated under dry conditions. The conclusions for this part of study are:

- The hardness of C15A/UHMWPE nanocomposite coatings increased with an increase in the nanoclay loading which is attributed to the inherent good mechanical properties of nanoclay and the bridging effect offered by the clay platelets in the soft polymer matrix network leading to a resistance to indentation.



- Among the three combinations of C15A/UHMWPE nanocomposite coatings, only 1.5 wt% C15A/UHMWPE nanocomposite coating exhibited excellent wear life as it did not fail even after ~100,000 cycles at a normal load of 9 N and a linear sliding speed of 0.1 m/s.
- The improvement in the performance of 1.5 wt% C15A/UHMWPE nanocomposite coating is attributed to the exfoliation of clay platelets in the polymer matrix that provides a bridging effect and holds the polymer chains together instead of being pulled out easily.
- However, at a normal load of 12 N and a linear speed of 0.1 m/s, 1.5 wt% C15A/UHMWPE nanocomposite coating failed very early (< 2000 cycles).
- No appreciable difference in the coefficient of friction was observed in the pristine as well as C15A/ UHMWPE nanocomposite coatings.

To further enhance the load bearing capacity, pristine UHMWPE coating was reinforced with various loadings of CNTs (0.5, 1.5, 3 wt%) and evaluated under dry conditions. The conclusions for this part of study are:

- By increasing the content of CNTs from 0.5 to 3 wt%, the hardness of the CNT-nanocomposite coatings increased.
- Among all combinations of coatings, 1.5 wt% CNTs/UHMWPE nanocomposite coating showed excellent tribological results as it did not fail upto ~100,000 cycles at normal load of 12 N and linear speed of 0.1 m/s under dry condition.
- The increase in the wear life of this particular coating is attributed to efficient dispersion of CNTs in polymer matrix that anchored the polymer chains in matrix.

- Regarding COF, slight changes were observed as its average value increased from ~0.17 (for pristine UHMWPE) to ~0.20 for CNT-nanocomposite coatings as expected due to the higher hardness of CNTs.

From section 4.2 (CNT/UHMWPE), we concluded that 1.5 wt% CNT/UHMWPE nanocomposite coating (optimized coating) showed a wear life of ~ 100,000 cycles at a normal load of 12 N. Hence to further improve the wear resistance of the nanocomposite coating, we took an approach of developing a hybrid nanocomposite coating by reinforcing the polymer matrix by two nano fillers, namely, nanoclay and CNTs. In this phase we evaluated the mechanical/tribological properties of the CNT/UHMWPE nanocomposite coating with the addition of 1.5 wt% of C15A nanoclay which was the optimum amount obtained from section 4.1 (nanoclay/UHMWPE) with different loadings (0.5, 1.5 and 3 wt%) of CNTs. The conclusions for this part of study are:

- By increasing the content of CNTs from 0.5 to 3 wt%, hardness of the hybrid nanocomposite coatings increased. In case of hybrid nanocomposites coatings, clay platelets further improved the hardness.
- Among all combinations of coatings, 1.5 wt% CNTs/1.5 wt% C15A/UHMWPE hybrid nanocomposite coating showed excellent tribological results as it did not fail until ~100,000 cycles at normal load of 12 N and linear speed of 0.1 m/s under dry condition.
- The increase in the wear life of this particular coating is attributed to efficient dispersion of CNTs and clay platelets in polymer matrix that anchored the polymer chains in matrix.

- In 1.5 wt% CNTs/1.5 wt% C15A/UHMWPE hybrid nanocomposite coating, the wear track profile depth (Z) was found to be less (43  $\mu\text{m}$ ) as compared to 55  $\mu\text{m}$  in case of 1.5 wt% CNT/ UHMWPE nanocomposite coating indicating the improvement in the wear resistance due to addition of nanoclay into the polymer matrix along with CNTs.
- Regarding COF, slight changes were observed as its average value increased from ~0.17 (for pristine UHMWPE) to ~0.21 for hybrid nanocomposite coatings respectively as expected due to the hardness of CNTs as well nanoclay.

## PHASE 2

In this phase, initially, we evaluated the mechanical/tribological properties of the CNT/C15A/UHMWPE hybrid nanocomposite coatings by reinforcing the UHMWPE matrix with 1.5wt% of C15A nanoclay (optimized amount obtained from phase 1) and different loadings (0.5, 1.5 and 3 wt%) of CNTs under water lubricated conditions. Then long term tribological tests were performed on best coatings. The conclusions for this part of study are:

- Among all combinations of coatings, 1.5 wt% CNTs/1.5 wt% C15A/UHMWPE hybrid nanocomposite coating showed excellent tribological results as it was not failed until ~150,000 cycles at normal load of 12 N and linear speed of 0.1 m/s under water lubricated conditions.
- Among two optimized coatings such as 1.5 wt% CNTs/1.5 wt% C15A/UHMWPE hybrid nanocomposite coating and 1.5 wt% CNTs/UHMWPE nanocomposite, hybrid coating performed better under water lubrication at 12 N, as it did not fail

up to ~300,000 cycles whereas 1.5 wt % CNTs/UHMWPE nanocomposite coating failed at ~170,000 cycles.

- The improvement in wear life of this particular hybrid nanocomposite coating is attributed to the addition of nanoclay which provides torturous path for diffusion of water molecules in polymer chains resulting in less water absorption less wear.
- The slight difference between two wear depth profiles of the 1.5 wt% CNTs/1.5 wt% C15A/ UHMWPE hybrid nanocomposite coating after the wear tests at 150,000 and 300,000 cycles respectively showed the improved wear resistance of the hybrid nanocomposite coating and indicating that the wear life of the hybrid nanocomposite coating can go beyond 300,000 cycles at a normal load of 12 N.
- There was hardly any change in hardness of the 1.5 wt% CNTs/1.5 wt% C15A/ UHMWPE hybrid nanocomposite coating UHMWPE hybrid nanocomposite coating before and after the water lubricated test indicating that the interaction of water with this particular coating did not deteriorate its mechanical properties leading to a significant improvement in its wear resistance.

After optimizing the tribological performance of the coatings under water lubrication conditions, the most wear resistant coating such as 1.5 wt% CNT/1.5 wt% C15A/UHMWPE hybrid nanocomposite coating was evaluated for its tribological performance under water lubrication in the presence of abrasive particles (SiC) at a normal load of 12 N for a duration of 150,000 cycles. Following are the conclusions.

- The evaluation of tribological performance of the hybrid nanocomposite coating in both cases (with/ without presence of abrasives) for 150,000 cycles at a normal load

of 12 N and sliding speed of 0.1 m/s showed that the coatings survived until 150,000 cycles.

- However, wear profile depth of the coating was less ( $\sim 80\text{ }\mu\text{m}$ ) in case of sliding testing in presence of abrasive as compare to that in absence of abrasives where wear profile depth was found to be  $\sim 104\text{ }\mu\text{m}$ .
- This is mainly attributed to the embedment of the abrasive particles in the softer polymer matrix which help in providing with an enhanced anchoring effect of the polymer chains leading to an improvement in the resistance to their easy pull-out.
- The counterface ball due to presence of abrasives was worn severely indicating that although coating can behave as wear resistant but the counterface (e.g. some metallic component) can be damaged severely.

## **5.2 Recommendations**

Following are some recommendations to increase the scope of work for some other different applications under different environments

1. Hybrid nanocomposite coating can be tested under different environments
2. The performance of this hybrid coating can be evaluated at elevated temperatures
3. Erosion and corrosion preventions by using this coating can be evaluated to expand its application in various fields.

## References

- [1] B. Bhushan, *Introduction to Tribology*, 1st ed. New York: John Wiley & Sons, 2002.
- [2] B. J. Briscoe and S. K. Sinha, *Chapter 1 – Tribological applications of polymers and their composites – past, present and future prospects*, Second Edition. Elsevier, 2013.
- [3] R. Harvey L. Stein, *Ultra High Molecular Weight Polyethylene ( UHMWPE )*, Ticona LLC. ASM International, 1999.
- [4] R. J. Grow, *Electromechanical properties and applications of carbon nanotubes*. 2006.
- [5] M. A. Samad and S. K. Sinha, “Mechanical, thermal and tribological characterization of a UHMWPE film reinforced with carbon nanotubes coated on steel,” *Tribol. Int.*, vol. 44, no. 12, pp. 1932–1941, 2011.
- [6] S. R. Bakshi, K. Balani, T. Laha, J. Tercero, and A. Agarwal, “The Nanomechanical and Nanoscratch Properties of MWNT- Reinforced Ultrahigh-Molecular- Weight Polyethylene Coatings,” *Compos. Part A Appl. Sci. Manuf.*, vol. 38, pp. 50–53, 2007.
- [7] M. R. Bagherzadeh and F. Mahdavi, “Preparation of epoxy-clay nanocomposite and investigation on its anti-corrosive behavior in epoxy coating,” *Prog. Org. Coatings*, vol. 60, no. 2, pp. 117–120, 2007.
- [8] K. Kowalczyk and T. Szychaj, “Epoxy coatings with modified montmorillonites,” *Prog. Org. Coatings*, vol. 62, no. 4, pp. 425–429, 2008.
- [9] Golgoon, M. Aliofkhazraei, M. Toorani, M. H. Moradi, and a. S. Rouhaghdam, “Corrosion and Wear Properties of Nanoclay- polyester Nanocomposite Coatings Fabricated by Electrostatic Method,” *Procedia Mater. Sci.*, vol. 11, pp. 536–541, 2015.
- [10] J. M. Yeh, S. J. Liou, H. J. Lu, and H. Y. Huang, “Enhancement of Corrosion Protection Effect of Poly(styrene-co- acrylonitrile) by the Incorporation of Nanolayers of Montmorillonite Clay into Copolymer Matrix,” *J. Appl. Polym. Sci.*, vol. 92, no. 4, pp. 2269–2277, 2004.
- [11] S. Vizintin, J., Kalin, M., Dohda, K., Jahanmir, *Tribology of Mechanical Systems: A Guide to Present and Future Technologies*. American Society of Mechanical Engineers, USA, 2004.
- [12] J. Gold, P.W., Loos, “Wear resistance of PVD coatings in roller bearings,” *Wear*, vol. 253, pp. 465–472, 2002.
- [13] a. Erdemir, F. a. Nichols, X. Z. Pan, R. Wei, and P. Wilbur, “Friction and wear

- performance of ion-beam-deposited diamond-like carbon films on steel substrates,” *Diam. Relat. Mater.*, vol. 3, no. 1–2, pp. 119–125, 1994.
- [14] A. Grill, “Tribology of diamondlike carbon and related materials: an updated review,” *Surf. Coatings Technol.*, vol. 94, pp. 507–513, 1997.
  - [15] R. Gåhlin, M. Larsson, and P. Hedenqvist, “ME-C:H coatings in motor vehicles,” *Wear*, vol. 249, no. 3–4, pp. 302–309, 2001.
  - [16] J. H. W. Siu and L. K. Y. Li, “An investigation of the effect of surface roughness and coating thickness on the friction and wear behaviour of a commercial MoS<sub>2</sub> – metal coating on AISI 400C steel,” *Wear*, vol. 237, pp. 283–287, 2000.
  - [17] A. Neville, A. Morina, T. Haque, and M. Voong, “Compatibility between tribological surfaces and lubricant additives-How friction and wear reduction can be controlled by surface/lube synergies,” *Tribol. Int.*, vol. 40, no. 10–12 SPEC. ISS., pp. 1680–1695, 2007.
  - [18] J. Li, T. Ren, H. Liu, D. Wang, and W. Liu, “The tribological study of a tetrazole derivative as additive in liquid paraffin,” *Wear*, vol. 246, no. 1–2, pp. 130–133, 2000.
  - [19] K. Varlot, M. Kasrai, G. M. Bancroft, E. S. Yamaguchi, P. R. Ryason, and J. Igarashi, “X-ray absorption study of antiwear films generated from ZDDP and borate micelles,” *Wear*, vol. 249, no. 12, pp. 1029–1035, 2001.
  - [20] A. E. Jiménez, M. D. Bermúdez, F. J. Carrión, and G. Martínez-Nicolás, “Room temperature ionic liquids as lubricant additives in steel-aluminium contacts: Influence of sliding velocity, normal load and temperature,” *Wear*, vol. 261, no. 3–4, pp. 347–359, 2006.
  - [21] R. P. Glovnea, a. V. Olver, and H. a. Spikes, “Lubrication of Rough Surfaces by a Boundary Film-Forming Viscosity Modifier Additive,” *J. Tribol.*, vol. 127, no. 1, p. 223, 2005.
  - [22] S. Briscoe, B., and Sinha, “Tribology of Polymeric Solids and Their Composites,” in *Wear–Mechanisms, Materials and Practice*, G. W. Stachowiak, Ed. UK: John Wiley & Sons, 2005, pp. 223–268.
  - [23] G. Schmidig, A. Patel, I. Liepins, M. Thakore, and D. C. Markel, “The effects of acetabular shell deformation and liner thickness on frictional torque in ultrahigh-molecular-weight polyethylene acetabular bearings,” *J. Arthroplasty*, vol. 25, no. 4, pp. 644–653, 2010.
  - [24] C. Gao, J. Abeysekera, M. Hirvonen, and R. Grönqvist, “Slip resistant properties of footwear on ice,” *Ergonomics*, vol. 47, no. 6, pp. 710–6, 2004.
  - [25] D. P. Manning and C. Jones, “The superior slip-resistance of footwear soling compound T66/103,” *Saf. Sci.*, vol. 18, no. 1, pp. 45–60, 1994.

- [26] G. Srinath and R. Gnanamoorthy, "Sliding wear performance of polyamide 6-clay nanocomposites in water," *Compos. Sci. Technol.*, vol. 67, no. 3–4, pp. 399–405, 2007.
- [27] Y. Yamamoto and M. Hashimoto, "Friction and wear of water lubricated PEEK and PPS sliding contacts Part 2. Composites with carbon or glass fibre," *Wear*, vol. 257, no. 1–2, pp. 181–189, 2004.
- [28] A. Borruto, G. Crivellone, and F. Marani, "Influence of surface wettability on friction and wear tests," *Wear*, vol. 222, no. 1, pp. 57–65, 1998.
- [29] J. H. Jia, H. D. Zhou, S. Q. Gao, and J. M. Chen, "A comparative investigation of the friction and wear behavior of polyimide composites under dry sliding and water-lubricated condition," *Mater. Sci. Eng. A*, vol. 356, no. 1–2, pp. 48–53, 2003.
- [30] H. Unal and A. Mimaroglu, "Friction and wear behaviour of unfilled engineering thermoplastics," *Mater. Des.*, vol. 24, no. 3, pp. 183–187, 2003.
- [31] Z. RYMUZA, "Tribology of Polymers," *Arch. Civ. Mech. Eng.*, vol. 7, no. 4, pp. 177–184, 2007.
- [32] K.-H. Zum Gahr, "Microstructure and Wear of Materials," Amsterdam: Elsevier, 1987, p. 292.
- [33] K. Friedrich, Z. Lu, and A. M. Häger, "Overview on polymer composites for friction and wear application," *Theor. Appl. Fract. Mech.*, vol. 19, no. 1, pp. 1–11, 1993.
- [34] C. G. Clarke and C. Allen, "The Water Lubricated, Sliding Wear Behavior of Polymeric Materials against Steel," *Tribol. Int.*, vol. 24, no. 2, pp. 109–118, 1991.
- [35] S. Wang, X. Yang, W. Su, and Y. Li, "Fabrication of polyurethane-based composites used in water-lubricated bearings," *Adv. Polym. Technol.*, vol. 33, no. 4, pp. 1–6, 2014.
- [36] H.-J. Song, N. Li, J. Yang, C.-Y. Min, and Z. Zhang, "Preparation and tribological behaviors of poly (ether ether ketone) nanocomposite films containing graphene oxide nanosheets," *J. Nanoparticle Res.*, vol. 15, no. 2, p. 1433, 2013.
- [37] M. Abdul Samad and S. K. Sinha, "Effects of counterface material and UV radiation on the tribological performance of a UHMWPE/CNT nanocomposite coating on steel substrates," *Wear*, vol. 271, no. 11–12, pp. 2759–2765, 2011.
- [38] N. Campo and a. M. Visco, "Properties of Nanocomposites Based on Polyethylene (UHMWPE) and Carbon Nanotubes Mixed by High-Energy Ball Milling and UV-Source Irradiated," *Int. J. Polym. Anal. Charact.*, vol. 17, no. 2, pp. 144–157, 2012.
- [39] T. Q. Nguyen, J. Sukumaran, J. De Pauw, and P. De Baets, "Tribological Behaviour of Polymer Bearings Under Dry and Water Lubrication," *Int. J. Sustain. Constr. Des.*, vol. 4, no. 2, 2013.



- [40] H. Meng, G. X. Sui, G. Y. Xie, and R. Yang, "Friction and wear behavior of carbon nanotubes reinforced polyamide 6 composites under dry sliding and water lubricated condition," *Compos. Sci. Technol.*, vol. 69, no. 5, pp. 606–611, 2009.
- [41] M. A. Samad and S. K. Sinha, "Dry sliding and boundary lubrication performance of a UHMWPE/CNTs nanocomposite coating on steel substrates at elevated temperatures," *Wear*, vol. 270, no. 5–6, pp. 395–402, 2011.
- [42] J. D. Gates, "Two-body and three-body abrasion: a critical discussion," *Wear*, vol. 214, no. 1, pp. 139–146, 1998.
- [43] H. . Pei, X.Q., Wang, Q.H., Wang, "Actuality and prospect in research on fretting of polymers and polymer-based composites," *Mater. Sci. Eng*, vol. 22, pp. 446–451, 2004.
- [44] A. A. Ezzat, M. O. Mousa, and W. Y. Ali, "Influence of Aluminum Oxide Nanofibers Reinforcing Polyethylene Coating on the Abrasive Wear," *Frict. Wear Res.*, vol. 4, pp. 1–13, 2016.
- [45] H. Unal, A. Mimaroglu, U. Kadioglu, and H. Ekiz, "Sliding friction and wear behaviour of polytetrafluoroethylene and its composites under dry conditions," *Mater. Des.*, vol. 25, no. 3, pp. 239–245, 2004.
- [46] J. Y. Lee and D. S. Lim, "Tribological behavior of PTFE film with nanodiamond," *Surf. Coatings Technol.*, vol. 188–189, no. 1–3 SPEC.ISS., pp. 534–538, 2004.
- [47] N. L. McCook, D. L. Burris, G. R. Bourne, J. Steffens, J. R. Hanrahan, and W. G. Sawyer, "Wear resistant solid lubricant coating made from PTFE and epoxy," *Tribol. Lett.*, vol. 18, no. 1, pp. 119–124, 2005.
- [48] M. Hedayati, M. Salehi, R. Bagheri, M. Panjepour, and F. Naeimi, "Tribological and mechanical properties of amorphous and semi-crystalline PEEK/SiO<sub>2</sub> nanocomposite coatings deposited on the plain carbon steel by electrostatic powder spray technique," *Prog. Org. Coatings*, vol. 74, no. 1, pp. 50–58, 2011.
- [49] Y. Li, Y. Ma, B. Xie, S. Cao, and Z. Wu, "Dry friction and wear behavior of flame-sprayed polyamide1010/n-SiO<sub>2</sub> composite coatings," *Wear*, vol. 262, no. 9–10, pp. 1232–1238, 2007.
- [50] J. O. Bello and R. J. K. Wood, "Micro-abrasion of filled and unfilled polyamide 11 coatings," *Wear*, vol. 258, no. 1–4 SPEC. ISS., pp. 294–302, 2005.
- [51] D. Bellisario, F. Quadrini, and L. Santo, "Nano-clay filled polyester coatings," *Prog. Org. Coatings*, vol. 76, no. 12, pp. 1863–1868, 2013.
- [52] D. Zaarei, A. A. Sarabi, F. Sharif, M. M. Gudarzi, and S. M. Kassiriha, "The Impact of Organoclay on the Physical and Mechanical Properties of Epoxy-Clay Nanocomposite Coatings," *J. Macromol. Sci. Part B-Physics*, vol. 49, no. 5, pp. 960–969, 2010.

- [53] R. Gadow and D. Scherer, "Composite coatings with dry lubrication ability on light metal substrates," *Surf. Coatings Technol.*, vol. 151–152, pp. 471–477, 2002.
- [54] R. Subasri and H. Hima, "Investigations on the use of nanoclay for generation of superhydrophobic coatings," *Surf. Coatings Technol.*, vol. 264, pp. 121–126, 2015.
- [55] Z. Z. Wang, P. Gu, and Z. Zhang, "Indentation and scratch behavior of nano-SiO<sub>2</sub>/polycarbonate composite coating at the micro/nano-scale," *Wear*, vol. 269, no. 1–2, pp. 21–25, 2010.
- [56] H. J. Song, Z. Z. Zhang, X. H. Men, and Z. Z. Luo, "A study of the tribological behavior of nano-ZnO-filled polyurethane composite coatings," *Wear*, vol. 269, no. 1–2, pp. 79–85, 2010.
- [57] Y. Wang and S. Lim, "Tribological behavior of nanostructured WC particles/polymer coatings," *Wear*, vol. 262, no. 9–10, pp. 1097–1101, 2007.
- [58] Y. Wang, S. Lim, J. L. Luo, and Z. H. Xu, "Tribological and corrosion behaviors of Al<sub>2</sub>O<sub>3</sub>/polymer nanocomposite coatings," *Wear*, vol. 260, no. 9–10, pp. 976–983, 2006.
- [59] S. K. Sinha, "Wear Failures of Plastics," in *ASM International Handbook*, vol. 11, Ohio, 2002, pp. 1019–1027.
- [60] W. Callister and D. Rethwisch, *Materials science and engineering: an introduction*, vol. 94. 2007.
- [61] N. Satyanarayana, S. K. Sinha, and B. H. Ong, "Tribology of a novel UHMWPE/PFPE dual-film coated onto Si surface," *Sensors Actuators, A Phys.*, vol. 128, no. 1, pp. 98–108, 2006.
- [62] M. Minn and S. K. Sinha, "DLC and UHMWPE as hard/soft composite film on Si for improved tribological performance," *Surf. Coatings Technol.*, vol. 202, no. 15, pp. 3698–3708, 2008.
- [63] M. Abdul Samad, N. Satyanarayana, and S. K. Sinha, "Tribology of UHMWPE film on air-plasma treated tool steel and the effect of PFPE overcoat," *Surf. Coatings Technol.*, vol. 204, no. 9–10, pp. 1330–1338, 2010.
- [64] S. K. Sinha, C. B. Lee, and S. C. Lim, "Tribological performance of UHMWPE and PFPE coated films on aluminium surface," *Tribol. Lett.*, vol. 29, no. 3, pp. 193–199, 2008.
- [65] M. A. Samad, N. Satyanarayana, and S. K. Sinha, "Effect of Air-Plasma Pre-treatment of Si Substrate on Adhesion Strength and Tribological Properties of a UHMWPE Film," *J. Adhes. Sci. Technol.*, vol. 24, no. 15–16, pp. 2557–2570, 2010.
- [66] A. S. Mohammed and M. Irfan Fareed, "Surface Modification of Polyether Ether Ketone (PEEK) with a Thin Coating of UHMWPE for Better Tribological Properties," *Tribol. Trans.*, pp. 1–7, 2016.

- [67] Z. Tai, Y. Chen, Y. An, X. Yan, and Q. Xue, "Tribological behavior of UHMWPE reinforced with graphene oxide nanosheets," *Tribol. Lett.*, vol. 46, no. 1, pp. 55–63, 2012.
- [68] A. S. Mohammed and M. I. Fareed, "Improving the friction and wear of poly-ether-etherketone (PEEK) by using thin nano-composite coatings," *Wear*, vol. 364–365, pp. 154–162, 2016.
- [69] O. K. Kahyaoglu, H. Unal, A. Mimaroglu, and S. H. Yetgin, "Tribological behavior of an ultrahigh molecular weight polyethylene in lubricated environments," *e-Polymers*, vol. 11.1, no. 62, pp. 667–674, 2011.
- [70] Y. An *et al.*, "Friction and wear properties of graphene oxide/ultrahigh-molecular-weight polyethylene composites under the lubrication of deionized water and normal saline solution," *J. Appl. Polym. Sci.*, vol. 131, no. 1, pp. 1–11, 2014.
- [71] X. Dangsheng, "Friction and wear properties of UHMWPE composites reinforced with carbon fiber," *Mater. Lett.*, vol. 59, no. 2–3, pp. 175–179, 2005.
- [72] D. Xiong and S. Ge, "Friction and wear properties of UHMWPE / Al<sub>2</sub>O<sub>3</sub> ceramic under different lubricating conditions," *Wear*, vol. 250, pp. 242–245, 2001.
- [73] A. Golchin, G. F. Simmons, S. B. Glavatskih, and B. Prakash, "Tribological behaviour of polymeric materials in water-lubricated contacts," *Proc. Inst. Mech. Eng. Part J-Journal Eng. Tribol.*, vol. 227, no. 8, pp. 811–825, 2013.
- [74] A. S. Mohammed and A. Bin Ali, "Investigating the Effect of Water Uptake on the Tribological Properties of Organoclay Reinforced UHMWPE Nanocomposites," *Tribol. Lett.*, vol. 62, no. 1, pp. 1–9, 2016.
- [75] M. Abdul Samad and S. K. Sinha, "Nanocomposite UHMWPE-CNT polymer coatings for boundary lubrication on aluminium substrates," *Tribol. Lett.*, vol. 38, no. 3, pp. 301–311, 2010.
- [76] M. Alexandre and P. Dubois, "Polymer-layered silicate nanocomposites: Preparation, properties and uses of a new class of materials," *Mater. Sci. Eng. R Reports*, vol. 28, no. 1, pp. 1–63, 2000.
- [77] G. Beyer, "Nanocomposites: a new class of flame retardants for polymers," *Plast. Addit. Compd.*, vol. 4.10, no. October, pp. 22–28, 2002.
- [78] T. McNally, W. R. Murphy, C. Y. Lew, R. J. Turner, and G. P. Brennan, "Polyamide-12 layered silicate nanocomposites by melt blending," *Polymer (Guildf)*, vol. 44, no. 9, pp. 2761–2772, 2003.
- [79] S. A. Solomon MJ, Almusallam AS, Seefeldt KF, "Rheology of Polypropylene / Clay Hybrid Materials," *Macromolecules*, vol. 34, pp. 1864–1872, 2001.
- [80] E. P. Giannelis, R. Krishnamoorti, and E. Manias, "Polymer-Silicate Nanocomposites: Model Systems for Confined Polymers and Polymer Brushes,"

*Adv. Polym. Sci.*, vol. 138, pp. 107–147, 1999.

- [81] E. P. Giannelis, “Polymer-layered silicate nanocomposites: Synthesis, properties and applications,” *Appl. Organomet. Chem.*, vol. 12, no. 10–11, pp. 675–680, 1998.
- [82] F. Schmidt, H., Mehrotra, V., Okada, A., Mark, J., & Candeanu, “Polymer-Based Molecular Composites,” *Mater. Process. Rep.*, vol. 5.1, pp. 4–6, 1990.
- [83] P. S. Nanocomposites, “Modeling the Barrier Properties of Polymer-Layered Silicate Nanocomposites,” *Macromolecules*, vol. 34, no. 2, pp. 9189–9192, 2001.
- [84] E. P. Messersmith, P. B., & Giannelis, “Synthesis and barrier properties of poly ( $\epsilon$ -caprolactone)-layered silicate nanocomposites,” *J. Polym. Sci. Part A Polym. Chem.*, vol. 33.7, pp. 1047–1057, 1995.
- [85] E. A. S. Kaloshkin, K. Ergin, V. Tcherdyntsev, A. Maksimkin, M. Petrzhik and V. Gerasin, “Structure and properties of ball milled ultrahigh-molecular weight Polyethylene-clay composite,” *Front. Mechanochemistry Mech. Alloy.*, pp. 90–94, 2011.
- [86] A. S. Mohammed and A. Ali, “Evaluation of Tribological Properties of Organoclay Reinforced UHMWPE Nanocomposites,” *J. Tribol.*, vol. 139, no. January, pp. 1–6, 2017.
- [87] W. A. de H. R.H. Baughman, A.A. Zakhidov, “Carbon nanotubes--the route toward applications, Science,” *Science*, vol. 297, no. 5582, pp. 787–792, 2002.
- [88] G. J. M. and C. W. W. W. Zhang, “Anti-friction, wear-proof and self-lubrication application of carbon nanotubes,” *Rev. Adv. Mater. Sci.*, vol. 36, p. 75–88., 2014.
- [89] Y. Xue, W. Wu, O. Jacobs, and B. Schädel, “Tribological behaviour of UHMWPE/HDPE blends reinforced with multi-wall carbon nanotubes,” *Polym. Test.*, vol. 25, no. 2, pp. 221–229, 2006.
- [90] Y. S. Zoo, J. W. An, D. P. Lim, and D. S. Lim, “Effect of carbon nanotube addition on tribological behavior of UHMWPE,” *Tribol. Lett.*, vol. 16, no. 4, pp. 305–310, 2004.
- [91] B. B. Johnson, A. Technologies, C. Road, and M. H. Santare, “Wear behavior of carbon nanotube/high density polyethylene composites,” *Mech Mater*, vol. 41, no. 10, pp. 1108–1115, 2009.
- [92] S. Bal and S. S. Samal, “Carbon nanotube reinforced polymer composites—A state of the art,” *Bull. Mater. Sci.*, vol. 30, no. 4, pp. 379–386, 2007.
- [93] K. Friedrich, Z. Zhang, and A. K. Schlarb, “Effects of various fillers on the sliding wear of polymer composites,” *Compos. Sci. Technol.*, vol. 65, pp. 2329–2343, 2005.
- [94] Yiu-Wing Mai Zhong-Zhen Yu, *Polymer Nanocomposites*, 1st ed. Cambridge: Woodhead Publishing Ltd, 2006.

- [95] J. Hilding *et al.*, “Dispersion of Carbon Nanotubes in Liquids Dispersion of Carbon Nanotubes in Liquids,” *J Disper Sci Technol*, vol. 2691, no. June, 2017.
- [96] G. M. P. W.C. Oliver, “An improved technique for determining hardness and elastic modulus using load and displacement sensing indentation experiments,” *J. Mater. Res.*, vol. 7, no. 6, pp. 1564–1583, 1992.
- [97] V. Mittal, “Polymer layered silicate nanocomposites: A review,” *Materials (Basel)*, vol. 2, no. 3, pp. 992–1057, 2009.
- [98] A. V. Maksimkin, S. D. Kaloshkin, V. V. Tcherdyntsev, D. I. Chukov, and I. V. Shchetinin, “Effect of high-energy ball milling on the structure and mechanical properties of ultra-high molecular weight polyethylene,” *J. Appl. Polym. Sci.*, vol. 130, no. 4, pp. 2971–2977, 2013.
- [99] N. M. Ismail, A. F. Ismail, A. Mustafa, and A. K. Zulhairun, “Enhanced carbon dioxide separation by polyethersulfone ( PES ) mixed matrix membranes deposited with clay,” *J. Polym. Eng.*, vol. 36, no. 1, pp. 65–78, 2015.
- [100] J. D. Marija S. Nikolic, Natasa Dordevic, Jelena Rogan, “Influence of clay organic modifier on the morphology and performance of poly (  $\epsilon$  -caprolactone )/ clay nanocomposites,” *Serb. Chem. Soc.*, vol. 80, no. 4, pp. 529–547, 2015.
- [101] N. M. Annas bin Ali, Abdul Samad Mohammed, “Tribological Investigations of UHMWPE Nanocomposites Reinforced With Three Different Organo-Modified Clays,” *Polym. Compos.*, 2016.
- [102] P. Bhagabati, T. K. Chaki, and D. Khastgir, “Panoptically exfoliated morphology of chlorinated polyethylene (CPE)/ethylene methacrylate copolymer (EMA)/layered silicate nanocomposites by novel in situ covalent modification using poly( $\epsilon$ -caprolactone),” *RSC Adv.*, vol. 5, pp. 38209–38222, 2015.
- [103] N. Gharehbash and A. Shakeri, “Comparison of Physical and Mechanical Behavior of Polypropylene Nanocomposites Reinforced with Different Percentages of Montmorillonite Modified,” *Orient. J. Chem.*, vol. 31, pp. 129–136, 2015.
- [104] B. M. Ginzburg, D. G. Tochil, V. E. Bakhareva, A. V Anisimov, and O. F. Kireenko, “Polymeric Materials for Water-Lubricated Plain Bearings,” *Russ. J. Appl. Chem.*, vol. 79, no. 5, pp. 695–706, 2006.
- [105] A. Cao, C. Xu, J. Liang, D. Wu, and B. Wei, “X-ray diffraction characterization on the alignment degree of carbon nanotubes,” *Chem. Pyhsics Lett.*, vol. 344, no. August, pp. 13–17, 2001.
- [106] R. J. Nemanich and S. A. Solin, “First- and second-order Raman scattering from finite-size crystals of graphite,” *Phys. Rev. B*, vol. 20, no. 2, pp. 392–400.
- [107] M. S. D. R. Saito, G. Dresselhaus, *Physical properties of carbon nanotubes*. World Sci, 1998.

- [108] R. J. M. B.J. Kip, M.C. Van Eijk, "Molecular deformation of high- modulus polyethylene fibers studied by micro-raman spectroscopy," *J. Polym. Sci. Part B Polym. Phys.*, vol. 29, pp. 99–108, 1991.
- [109] C. C. Naylor *et al.*, "Raman Spectroscopy Employed for the Determination of the Intermediate Phase in Polyethylene," *Macromolecules*, vol. 28, no. 8, pp. 2969–2978, 1995.
- [110] S. L. Wunder and S. D. Merajver, "Ultrahigh-molecular-weight polyethylene: Raman spectroscopic study of melt anisotropy," *J. Polym. Sci. Part B Polym. Phys.*, vol. 24, no. 1, pp. 99–110, 1986.
- [111] G. T. McNallya, P. Potschke, P. Halley, M. Murphy, D. Martin, S.E.J. Bell and J. P. Q. P. Brennan, D. Bein, P. Lemoine, "Polyethylene multiwalled carbon nanotube composites," *Polymer.*, vol. 46, pp. 8222–8232, 2005.

## Vitae

**Name** Muhammad Umar Azam

**Nationality** Pakistani

**Date of Birth** 10/26/1989

**Email** umarazam81@yahoo.com

**Address** Lahore, Pakistan

**Academic Background** BSc Metallurgical and Materials Science Engineering

### Achievements

From this thesis work we were able to submit three Journal Papers which shall add value to the field of surface engineering. Following are the two publications which are submitted recently.

- 1) Muhammad Umar Azam, M. Abdul Samad, “A Novel Organoclay reinforced UHMWPE nanocomposite coating for tribological applications”, **submitted to *Progress in Organic Coatings***
- 2) Muhammad Umar Azam, M. Abdul Samad, “UHMWPE Hybrid Nanocomposite Coating Reinforced with Nanoclay and Carbon Nanotubes for Tribological Applications”, **submitted to *Composites Part A: Applied Science and Manufacturing***
- 3) Muhammad Umar Azam, M. Abdul Samad “UHMWPE Hybrid Nanocomposite Coating Reinforced with Nanoclay and Carbon Nanotubes for Tribological Applications under Water Lubrication with/without Abrasives” **submitted to *Wear***